Field Testing of Helical Piles and SPT-based Method for Estimating Axial Capacities in Sand

by

Yiwen Zhang

A thesis submitted in partial fulfillment of the requirements for the degree of

Master of Science

in

Geotechnical Engineering

Department of Civil and Environmental Engineering

University of Alberta

ABSTRACT

Helical piles comprise of at least one helical-shaped bearing plates appended to the square or round shafts. In the past decades, helical piles have gained significant popularity across Canada in various foundation applications such as power transmission towers, bridges, solar farm, and residential and commercial buildings. They provide a few advantages including quick installation, cost effectiveness, low level of noise, minimal vibration and reusability. Estimating the axial capacity is crucial to the helical piling industry. Because the Standard Penetration Test (SPT) is a popular and economical method in subsurface exploration, SPT-based direct method is one of the direct methods commonly used to predict the capacity of piles. The pile shaft friction and end bearing resistance are empirically correlated with the results of SPT for conventional driven piles or cast-in-place piles. Inspired by the methods of conventional piles, the industry of helical piles also needs a direct method that can estimate the pile capacities with the results of SPT to effectively design the piles.

In this study, twelve full-scale load tests of helical piles, including six axial compressive tests and six tensile tests were carried out in a sandy site. Before conducting the load tests, two SPT tests were carried out in test site to investigate soil stratigraphy. The samples were obtained to proceed laboratory testing. Chin's hyperbolic method was applied to the interpretation of the load vs. displacement curves for the piles that exceeded the loading frame capacity before reaching the axial displacement of 10% of the helix diameter *D* according to the industry convention. Chin's method also used to clarify and correct some abnormal observations in regard to curve segments. Results from the present study and the literature were compiled to construct a helical pile load-test

database. The database includes the test results of 47 single-helix piles with various dimensions in sandy soils. From this database, a direct method based on SPT blow count N for estimating the axial capacity of single-helix piles is proposed. The proposed SPT-based method established simple correlations between the average N over the pile shaft length (N_{bar}) and the unit shaft resistance q_s, and between the average N around pile base (N_b) and the unit end bearing resistance q_b. The shaft resistance is taken into account, and this modification is critical for a long pile whose shaft carries a considerable amount of load. The proposed SPT-based method was verified again by back-analyzed results.

ACKNOWLEDGEMENTS

I would like to extend my sincere thanks to Dr. Lijun Deng for his continuous support and wise guidance throughout my research program. His patience and dedication to student success inspired and motivated me to seek my research goals without hesitation.

Secondly, I also truly appreciate Natural Sciences and Engineering Research Council of Canada (CRDPJ 543483 - 19) and Mitacs - Accelerate program (IT20081) for providing funding for this project and myself. Gratitude is also extended to Reaction Piling Inc. for the financial and technical support. Special thanks to Luke Penner, Sergey Shokot and Ron of Reaction Piling for the assistance in performing the field tests.

Next, I would like to thank my friends and colleagues at the university, particularly Weidong Li and Ali Muhammad, for their assistance in field testing and laboratory soil testing.

Special gratitude goes to my parents for their understanding and financial support during the past seven years I have spent overseas on studying.

TABLE OF CONTENTS

LIST OF TABLES

LIST OF FIGURES

1 Introduction

This chapter introduces the background of the present research, problem statement, general objectives, and thesis organization.

1.1 Background and Problem Statement

Helical piles, also known as screw piles or helical anchors, have been used for a wide range of applications such as power transmission towers, bridges, solar farms, and residential and commercial buildings (Elsherbiny and El Naggars 2013). Figure 1-1 shows that some of the representative applications. In general, a helical pile comprises at least one helical-shaped bearing plate appended to the square or round shaft as presented in Figure 1-2. Helical piles can be used as a deep foundation system to support axially compressive, axially tensile, and lateral loadings. Helical piles provide a few advantages, including quick installation, cost-effectiveness, low noise level, and minimal vibration. Helical piles can attain three to five times higher compressive and tensile capacities than traditional driven steel piles with the same shaft diameter and length (Sakr 2009). Moreover, they can be removed after installation and re-used. Helical piles are usually fabricated from steel and occasionally galvanized for extra protection against corrosion. The number and dimensions of helices depend on design; for instance, helical piles with multiple helices and the helices may be of equal diameter or have diameters tapered towards the pile tip. The spacing between helices may be consistent or varied. For single-helix piles, the helix has to be located at the toe of the shaft in order to lead the pile drilling into the ground by applying torque to the pile head.

(a)

(b)

(c)

Figure 1-1: Selected Applications of Helical Piles: (a) Hubbell Project (b) Domaine Kabin Resort (c) Biosar-Aurora Solar, Minneapolis, MN.

Figure 1-2: Sketch of Single-helix and Multi-helix Piles.

The helical pile shaft is turned into the ground by applying a torque using a truck-mounted auger or hydraulic torque motor attached to a hydraulic machine (Perko 2009). Figure 1-3 shows the in-situ installation of a double-helix pile. The pile cap was connected to the hydraulic torque head using steel pins. Then, the pile was lifted to a desired location and rotated to the ground by applying an axial compressive force on the shaft. The installation usually requires only two people on a crew and approximately 30 minutes per pile (Tappenden 2007). In Alberta, helical piles are typically installed to a shallow depth of less than 6.0 m. The recommended penetration rate should be equal to one pitch per revolution to avoid shearing of the soil (Zhang 1999). In addition, the operator records the final depth, torque, and elevation for each installed pile for further interpretation.

Pile capacity estimation is an essential part of pile foundation design. Most of the design methods require site investigation, e.g., Standard Penetration Tests (SPT). The pile capacity can be predicted using in-situ testing results following two methods: indirect method and direct method. For the indirect method, in-situ investigation and (or) laboratory tests are conducted to

evaluate the soil parameters and then applied to analytical formulas to produce the pile capacity; for direct method, the pile capacity is directly related to certain in-situ measurements without evaluating any intermediate soil parameters, which enables quicker design and less uncertainties (Zhang and Chen 2012). In the past few decades, many researchers, i.e., Meyerhof (1976), Shioi and Fukui (1982) and AIJ (2004), have proposed SPT-based direct methods to predict the capacity of conventional straight piles, which can be used as references for direct method of helical piles. The direct methods for conventional straight piles mentioned above may be unsuitable for helical piles because installation methods have a significant effect on the pile behaviour. A typical direct method (torque method) estimates the capacity of helical piles from the installation torque values using an empirical linear correlation, which may change with soil types and pile dimensions. A method based on in-situ soil characterization index, which would be valuable to the practice, is deficient. Such a direct method, based on SPT, would provide a preliminary design of a helical pile before the pile is installed.

Figure 1-3: Installation of a Double-helix Pile

Perko (2009) proposed an empirical correlation for estimating the unit-area end bearing resistance (q_b) of helical piles. Notably, Perko (2009) neglected the shaft resistance in this correlation, whereas a number of studies indicate that the shaft resistance contributes a significant share (up to 30%) to the total axial capacity, e.g., Elsherbiny and El Naggar (2013), Li et al. (2018), and Lanyi-Bennett and Deng (2019). Therefore, Perko's (2009) correlation may need to be modified with evaluation of shaft resistance and improved with expanded database.

1.2 Objective & Methodology

The primary objective of this study was to develop a method to predict the capacity of helical piles using blow counts *N* from SPT. The second objective was to investigate the reliability and accuracy of the proposed SPT-based method.

The methodology of the present study is stated as follows:

- Conduct a series of field axial loading tests of helical piles in sand. The soil stratigraphy was characterized by in-situ SPT and laboratory testing.
- Collect and compile results from the present tests and the literature to construct a helical pile load-test database.
- Analyze the database and propose end bearing coefficient and shaft coefficient for the SPT-based method.
- Back-calculate the bearing resistance and shaft friction with existing methods based on available soil properties in the adopted literature.

1.3 Scope of Work and Contribution

The author conducted a field test program including axially compressive and tensile loading tests on full-scale single-helix and multi-helix piles. A series of field load tests of helical piles were carried at two sites located in Alberta.

Site 1 at the University of Alberta Botanic Garden near Devon, Alberta, is located 2 km east of Highway 60 (Figure 1-4). The soil at Botanic Garden consists of uniformly-graded sand, and Botanic Garden can be treated as cohesionless soil site. Before the tests, a comprehensive site investigation was carried out, including two boreholes drilled to the depth of 8.3 m. Two SPT's were conducted at 1.5 m depth intervals to determine the SPT blow counts N at different depths. Twelve full-scale load tests of helical piles, including six axial compressive tests and six tensile tests, were carried out at Botanic Garden. The pile load capacity is often defined in terms of ultimate load Q_u. According to industry convention, the ultimate pile capacity Q_u is defined as the pile resistance at the axial displacement of 10% of helix diameter D and the value of Q_u is derived based on load-displacement curves. For those piles which reached the loading frame capacity before the ultimate state, Q_u values were extrapolated to the load at 10% of D using Chin's hyperbolic method (Chin 1970). Results from the present tests and the literature were compiled to construct a helical pile load-test database. A direct method based on N for estimating the axial capacity of single-helix piles is proposed. The equation was calibrated using a database implemented with 35 field load tests available in the literature and 12 field load tests accomplished in the present research. Additionally, this thesis investigated the reliability and accuracy of the proposed SPT-based method by back-calculating the capacity using existing methods.

Site 2 at the University Farm is located in central Edmonton, Alberta, Canada. The general soil profile at Site 2 consists of varved silts and clays of approximately 8 m, with pockets of till, sand, or sandy gravel, underlain by dense silty sand and sandy till. Because this thesis focuses on field tests and the SPT-based method in sand, test results at the University Farm, which may be useful in further research, are only presented in Appendix A.

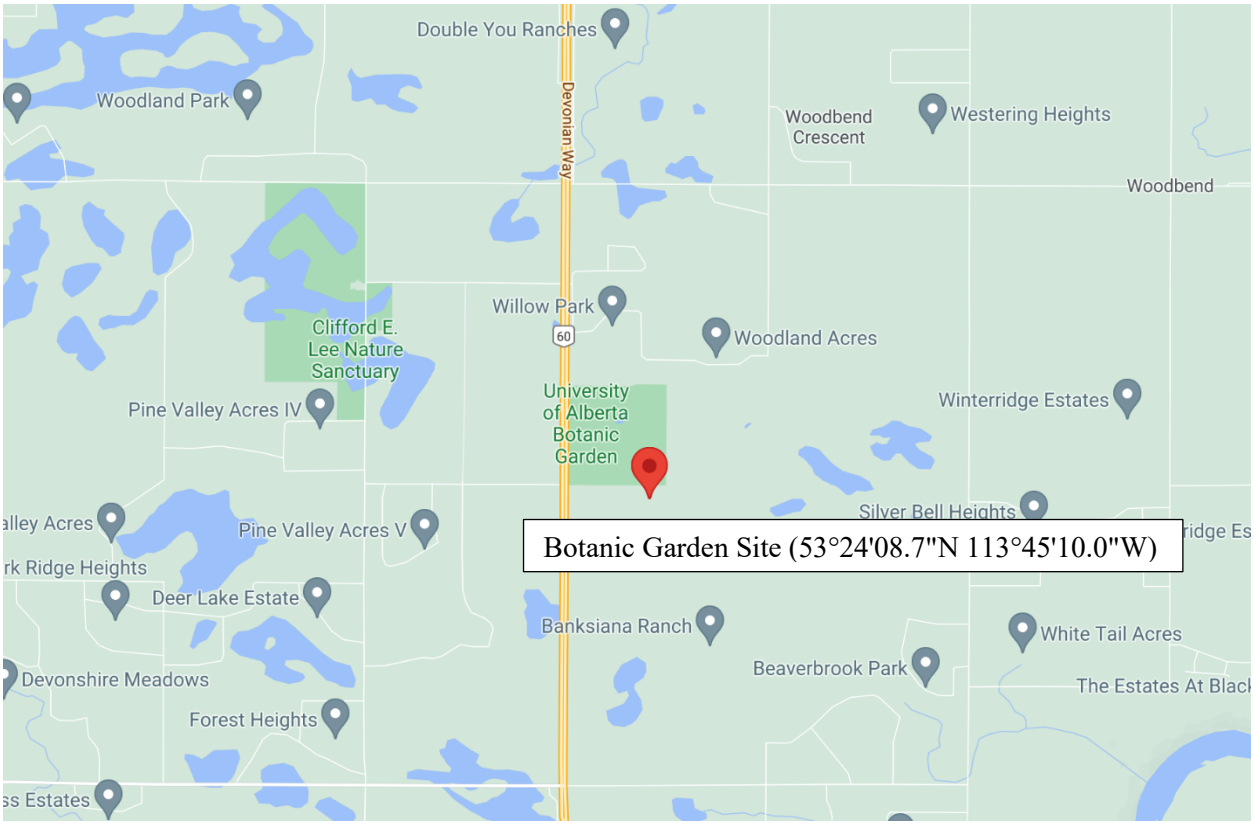

Figure 1-4: Location of University of Alberta Botanic Garden Site

Contributions of the present study are stated as follows. Firstly, this research presented the field test results of helical piles that can offer case studies for further research. Secondly, this research proposed a SPT-based direct method that can be used to guide the helical pile design. Then, the method of estimating the unit end bearing resistance q_b from Perko (2009) was verified by back-calculation. In addition, the direct torque method for estimating helical pile capacities was also verified in this study.

1.4 Thesis Organization

This thesis consists of five chapters. Chapter 1 constitutes the introduction. Chapter 2 is the literature review on the previous studies on helical piles subject to indirect and direct methods to predict helical pile capacity in sand using in-situ soil characterization index. Chapter 3 presents the in-situ SPT, laboratory soil testing and field axial loading tests at Botanic Garden. Chapter 4

describes an SPT-based method for estimating axial capacities of single-helix piles in sand and back-analysis to check the reliability and accuracy of the proposed SPT-based method with existing methods. Chapter 5 summarizes the conclusions, limitations, and recommendations of this research.

Appendix A is the test results at the University Farm. Appendix B is the structural design of the reaction system of the field-testing program.

A part of Chapters 3 and 4 has been published in GeoNiagara 2021 – the annual conference of the Canadian Geotechnical Society. A journal article based on Chapters 3 and 4 is in construction.

2 Literature Review

The purpose of this chapter is to describe a brief history of helical piles, review the Standard penetration test (SPT) and present failure modes of helical piles. In addition, this chapter summarizes the published indirect and direct methods to predict helical pile capacity in sand using site investigation.

2.1 Brief history of helical piles

Helical piles are first proposed by Alexander Mitchell, who is a blind brickmaker and civil engineer. Mitchell patented his invention and named it as “screw pile” in London 1833. The earliest use of screw piles is for ship moorings (Perko 2009). Then, Mitchell used them for the foundation of Maplin Sands Lighthouse at an unstable entrance of the river; the pile layout profile is shown in Figure 2-1. In the following years, Eugenius Birch started to use Mitchell’s screw pile to support seaside piers throughout England. During the expansion of the British Empire, screw piles were widely used to support bridges in many countries and then were soon being applied around the world (Perko 2009, Lutenegger 2003).

The use of helical piles as a kind of deep foundation has considerably increased in recent years. Estimating the axial capacity is crucial to the helical piling industry. Performing pile load tests is a good way to predict capacities; however, such tests are expensive and time-consuming. In recent years, the application of in-situ techniques has increased due to the development of in-situ testing instruments and improved understanding of the behaviour of soils. Supported by in-situ techniques, the helical pile industries prefer to use the direct method to estimate pile capacities. Direct methods allow the geotechnical engineers to obtain raw data in-situ and use it directly into a design without the intermediate step of determining soil parameters. It also can

avoid the misrepresentations which possibly occur in laboratory testing when determining soil parameters.

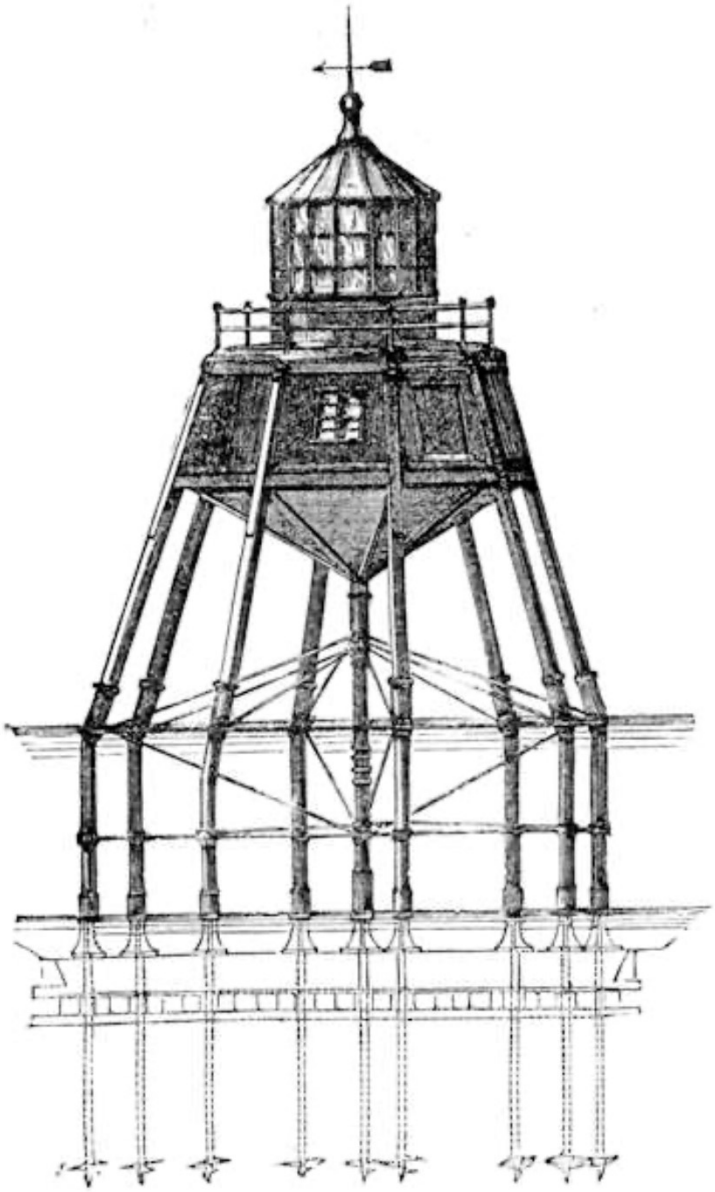

Figure 2-1: Maplin Sands Lighthouse (from internet)

2.2 Overview of Standard Penetration Test (SPT)

The standard penetration test is a common method to use in subsurface exploration. The SPT was introduced in the USA in 1902 by the Raymond Pile Company. The test was not standardized until 1958, and it's currently covered by ASTM D1586-99 (ASTM 2008a).

Boreholes are required to drill before conducting the test. In North America, rotary drilling and augering are the most common drilling methods. After reaching the bottom of the drilled hole, a hollow thick-walled tube into the ground is driven into the subsurface using a calibrated hammer (weights 63.5-kg) which is repeatedly falling from 0.76m (30 inch) to achieve three successive increments of 150-mm each. The SPT entails pushing a hollow, thick-walled tube into the ground and counting how many blows it takes to advance a split-barrel sampler 300 mm vertically (1 ft) (Mayne et al. 2001). The first increment is referred to as a 'seating', and the number of blows required to advance the second and third increments are added together to get the N-values, which are expressed in blows/0.3 m (Mayne et al. 2001). Figure 2-2 shows the sequence of driving split-barrel sampler during the SPT, and Figure 2-3 shows the in-situ drilling equipment. The N-values are usually used to classify soils and determine soil properties.

SPT provides several advantages, such as simple to conduct in practice, low cost, and disturbed soil samples can also be obtained. However, one of the principal issues of the SPT is that the test equipment, drilling techniques, and test procedures have not been entirely standardized on a worldwide premise (Robertson 2006).

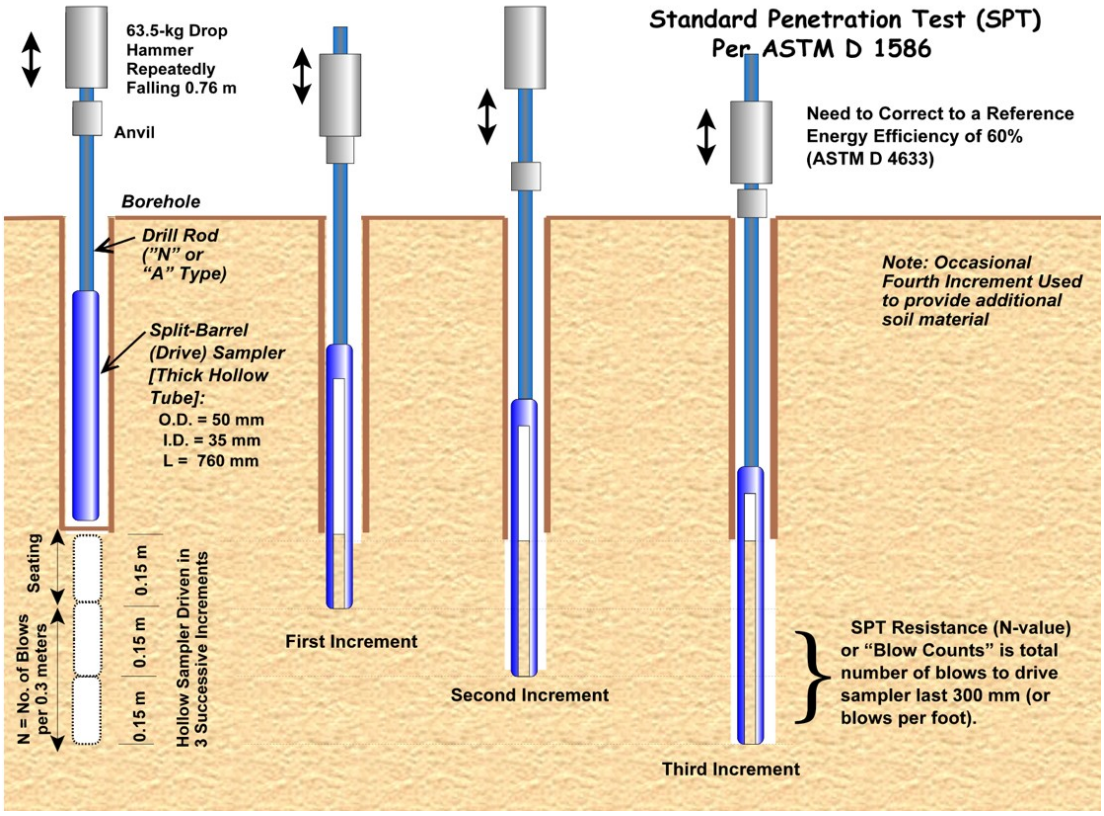

Figure 2-2: Sequence of Driving Split-Barrel Sampler during the Standard Penetration Test (Mayne et al. 2001)

2.2.1 Correction Factors of SPT

In order to eliminate the variability in equipment and test procedures encountered in practice, the raw index N values need to be corrected with the ratio of the measured energy transferred to the rod to 60% of the theoretical potential energy. The corrected N-value (N_{60}) was calculated by Equation [2.1]:

$$N_{60} = \frac{E_m C_B C_S C_R N}{0.60} \qquad [2.1]$$

where

E_m= hammer efficiency,

C_B= borehole diameter correction. C_B increases as borehole diameter increases due to the reduction in confinement, resulting in low blow counts.

C_S= sample correction, referring to the occasional use of a liner sampler without the liner. C_s is taken as 1.0 for the standard sampler or the liner sample with the liner in place; and taken as 1.2 for the liner sampler without a liner. This is because the standard samplers can produce higher blow counts than the sampler without a liner.

C_R= rod length correction. C_R is 0.75 if rod length is less than 4m, 0.85 if rod length is between 4 m and 6 m, 0.95 if rod length is between 6 m to 10 m, and 1 if rod length is larger than 10 m.

Figure 2-3: Photo of SPT Operation

2.2.2 Energy Ratio

It is suggested that SPT *N*-values need to be corrected for hammer efficiency, which is affected by length of drill rod, hammer type, drop height control, borehole diameter, and other factors

(Perko 2009). Bowles (1988) summarized a variety of factors developed by others that can be integrated to correct N for hammer efficiency. The efficiency of the total penetration system is defined by the energy ratio E_r and is calculated as follows:

$$E_r = \frac{\text{Energy delivered to sampler}}{\text{Theoretical input energy}} \times 100 \quad [2.2]$$

The energy ratio is indicated in a subscript to the common abbreviation for blow count. For example, N_{60} indicates the SPT blow count at an energy ratio of 60. In some case, it is valuable to convert blow counts obtained using a certain energy ratio to those based on a different energy ratio (Perko 2009). Bowles (1988) indicated that the product of energy ratio and blow count should be a constant:

$$E_{r1} \times N_1 = E_{r2} \times N_2 \quad [2.3]$$

where N_1 is the blow counts at energy ratio E_{r1}, and N_2 is the blow counts at energy ratio E_{r2}. As a result, Equation [2.3] may be used to convert blow counts across energy systems.

2.3 Failure Modes of Helical Piles

The axial load applied to the head of a single-helix pile is transferred to the soil via soil-shaft shearing and soil-helix normal resistance. As for multi-helix piles, there are two widely recognized axial load transfer mechanisms (ALTM) or failure modes (FM): "individual plate bearing (IPB)" and "cylindrical shear (CS)". Mooney et al. (1985) proposed these two FM's based on their in-situ load tests and scaled model tests of the uplift capacity of horizontal anchors buried in clay and silt. In general, for axially loaded helical piles, the soil between two adjacent helices will evolve into a cylindrical mass if the inter-helix spacing (S) is smaller than a critical value. This critical spacing is usually referred to the ratio of the inter-helix spacing to the helix diameter (D), i.e., S/D. Further observations regarding the FM's were reported by Weikart and Clemence (1987), Hoyt and Clemence (1989), and Narasimha Rao et al. (1991,1993). Based on

these early findings, the design guidelines such as CGS (2006) recommend the following design criterion: IPB mode is valid when *S*/*D* is greater than 3 otherwise the CS mode is applied, regardless of the soil properties. This design criterion has remained unchanged for over twenty years. According to these two FM's, the total axial resistance of helical piles (Figure 2-4) is assumed to be the summation of the shaft friction/adhesion and: 1) for IPB, the individual plate bearing/uplift resistance; or 2) for CS, the shear resistance acting on the cylindrical surface of the soil cylinder plus the uplift resistance against the top helix (uplift) or the bearing resistance on the bottom helix (bearing).

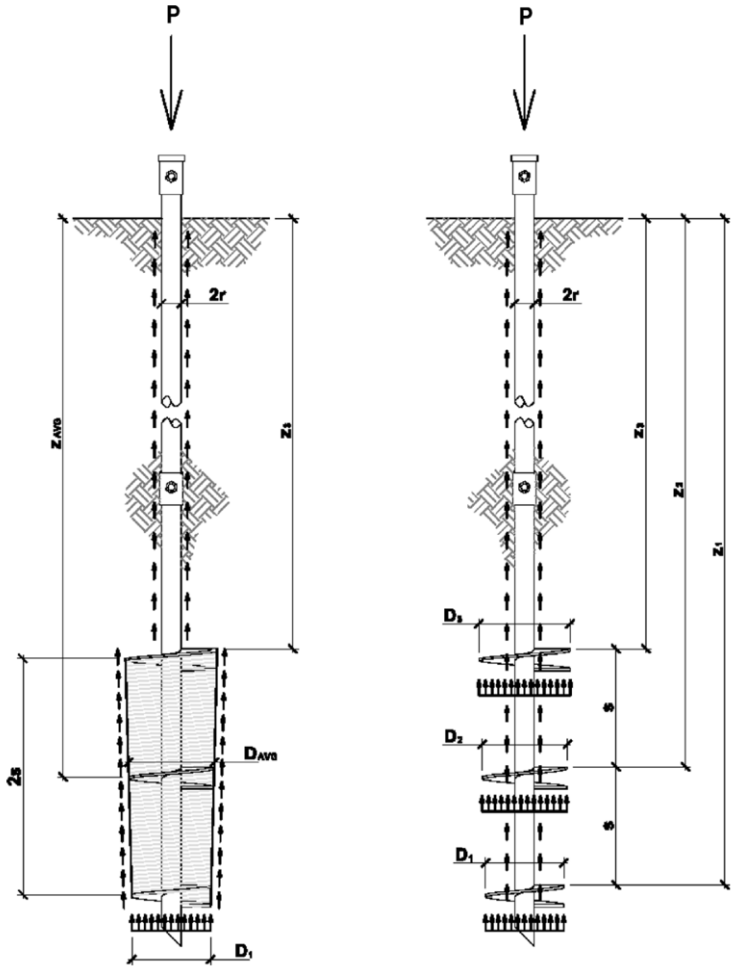

Figure 2-4: Failure Modes Suggested by Current Design Methods (Left) CS, and (Right) IP (Perko 2009)

2.4 Estimate Axial Capacity of Helical Pile

It is complicated to predict the mechanism of load transfer from the deep foundation to the surrounding soil. In this manner, full-scale load tests are needed to estimate the pile capacity and to decide the performance of piles. In general, the total capacity of the helical pile equals the combination of end-bearing resistance of the soil and the skin friction of the shaft. This is:

$$Q = Q_b + Q_f = q_b A_b + q_s A_s \quad [2.4]$$

where

Q_b = End bearing resistance in kN,

Q_f = Resistance along pile shaft in kN,

A_b = Total projected area of helical bearing plate,

A_s = Area of soil-shaft interface,

q_b = unit end bearing resistance in kPa, and

q_s = unit shaft resistance in kPa.

Most of the design methods require site investigation, e.g., SPT. The pile capacity can be predicted using in-situ testing results following two methods: indirect method and direct method. For the indirect method, in-situ investigation and (or) laboratory tests are conducted to evaluate the soil parameters and then applied to analytical formulas to produce the pile capacity; for direct method, the pile capacity is directly related to certain in-situ measurements without evaluating any intermediate soil parameters, which enables quicker design and less uncertainties (Zhang and Chen 2012). The following subsection will provide a summary of the theory and research related to indirect and direct methods to estimate the capacities of helical piles in sand.

2.4.1 Individual Plate Bearing Mode

The IPB mode describes the helical piles as a series of independent plates affixed along the shaft and embedded at different depths. Bearing failure is assumed to occur above each plate when the pile is loaded in tension and occur below each plate when loaded in compression (Tappenden 2007). The axial load applied to the head of a single-helix pile is transferred to the soil via soil-shaft shearing and soil-helix normal resistance. Thus, the failure mode of the single-helix pile can be treated as IPB mode as well.

The IPB mode is an extension of the analysis of shallow foundations or embedded plate anchors. Terzaghi (1943) proposed an important equation for analyzing the behaviour of a shallow foundation. With a few assumptions, the ultimate bearing pressure of soil may be determined using the familiar bearing capacity equation for circular bearing elements given by (Perko 2009):

$$q_b = 1.3cN_c + q'N_q + 0.3\gamma DN_\gamma \quad [2.5]$$

where

c = cohesion,

γ = unit weight of the soil,

D = diameter of the helical plate,

q' = effective overburden stress at the bearing depth, and

N_c, N_q, N_γ = bearing capacity factors.

Following Terzaghi's work, Meyerhof (1951) conducted a series of investigation on the bearing capacity factors. Meyerhof considered correction factors of eccentricity, load inclination, foundation roughness and depth. N_c, N_q and N_γ in Meyerhof equation are now known as general

bearing factors which depend on shape of the bearing element and depth. The modified equation took the form:

$$q_b = cN_c s_c d_c + q' N_q s_q d_q + 0.5\gamma D N_\gamma s_\gamma d_\gamma \quad [2.6]$$

where

s_c, s_q and s_γ = shape factors,

d_c, d_q and d_γ = depth factors,

$$N_c = (N_q - 1)\cot\phi \quad [2.7]$$

$$N_q = e^{\pi \tan\phi} \tan^2(45° + \phi/2) \quad [2.8]$$

$$N_\gamma = (N_q - 1)\tan(1.4\phi) \quad [2.9]$$

Hansen (1970) and Vesic (1973) refined the shape and depth factors. Vesic also included some extra factors for inclination of the bearing element and for sloping ground surface (Perko 2009). For shallow foundations, inclination and ground slope factors are important, but for deep foundations, they are typically irrelevant. When the above bearing capacity theory is applied to helical piles, many simplifications are feasible. For helical piles, the simplified bearing pressure equation is as follows:

$$q_b = cN'_c + q'(N'_q - 1) + 0.5\gamma D N'_\gamma \quad [2.10]$$

where

$$N'_c = N_c s_c d_c \quad [2.11]$$

$$N'_q = N_q s_q d_q \quad [2.12]$$

$$N'_\gamma = N_\gamma s_\gamma d_\gamma \quad [2.13]$$

The shape and depth factors can be grouped together with bearing capacity factors and plotted with respect to angel of internal friction ϕ shown in Figure 2-5.

The first component in Equation [2.10] becomes zero for coarse-grain soil when $c = 0$. Because the third term is relatively small for deep foundations, it is usually neglected. The ultimate bearing pressure for coarse-grain soils is derived by using these simplifications as Equation [2.14]:

$$q_b = q'(N'_q - 1) \quad [2.14]$$

When Equation [2.14] is used, however, the predicted ultimate bearing pressure increases without bounds as q' increases gradually with depth. In many situations, this results in an overestimation of bearing capacity. At a critical depth, it has been proposed that the bearing pressure at the base of a deep foundation hits a maximum bound (Meyerhof, 1951, 1976). Based on a series of load tests conducted by Perko (2009), the critical depth for straight shaft piles was determined. Perko performed 54 full-scale load tests in coarse-grain soils on helical piles with different shaft sizes and helical sizes. Based on a regression study, it was established that setting the critical depth to two times the average diameter of the helical bearing plates provides the greatest match to the load test data for helical piles. The relationship that best intersects the average of the helical pile load test data is the combined bearing capacity factor, N'_q, using Hansen and Vesic shape and depth factors.

In summary, Perko (2009) proposed that the ultimate bearing pressure for helical piles in coarse-grain soils may be computed using traditional bearing capacity theory by replacing the effective overburden stress, q', in Equation [2.14] with the product of soil unit weight, γ, and two times the average helix diameter, D_{avg}, as shown in Equation [2.15]:

$$q_b = 2D_{avg}\gamma(N'_q - 1) \quad [2.15]$$

The bearing factor N'_q is shown in Figure 2-5. Perko also suggested that it would be conservative to omit skin friction along the shaft. In addition, Perko reported that the axial capacity measured in field is 1.16 times the predicted axial capacity using Equation [2.15].

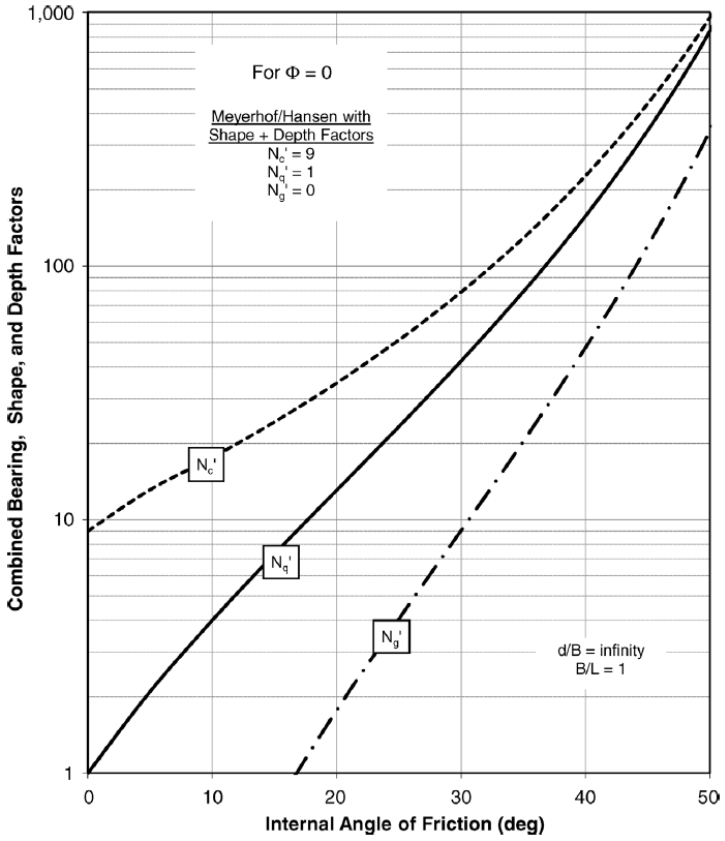

Figure 2-5: Combined Bearing, Shape, and Depth Factors (Perko 2009)

2.4.2 Capacity Due to Skin Friction

The capacity due to skin friction can be calculated as the sum of friction between soil and pile. Skin friction is hard to estimate accurately, especially for foundations in stiff, fissured clays where installation of the foundation can reduce soil shear resistance to much lower value due to remolding of sensitive clay (Zhang 1999). The capacity due to skin friction can be calculated as follows (CGS 2006):

$$Q_f = \sum (\pi d \Delta L_f q_s) \qquad [2.16]$$

where ΔL_f is the increment of embedment length in m (to allow for pile shaft variations and soil stratification). In addition, the area of shaft, expressed as $\pi d \Delta L_f$, does not include the contacted area from the bottom of helix to pile tip and shaft area exposed to air.

CGS (2006) suggested a β method to estimate shaft resistance for deep foundations installed in cohesionless soil at any depth z. This is:

$$q_s = \beta \sigma'_v = \sigma'_v K_s \tan\delta \qquad [2.17]$$

where

β = a combined shaft resistance factor,

K_s = coefficient of lateral earth pressure,

σ'_v = vertical effective stress adjacent to the pile at depth z, and

δ = the angle of friction between the pile and the soil.

The combined shaft resistance factor β as indicated in Table 2-1. The angle of shearing resistance, the technique of installation, the compressibility, degree of overconsolidation, and original state of stress in the ground, as well as the material, size, and shape of the pile, all impact the value of K_s (CGS 2006). It increases in proportion to the soil's in-situ density and angle of shearing resistance, as well as the amount of displacement. It is higher for displacement-type piles than low-displacement-type piles such as H-piles. K_s is typically considered to be equal to the coefficient of earth pressure at rest, K_o, for drilled piles. K_s is usually considered to be double the value of K_o for driven displacement-type piles. The value of δ is determined by the surface roughness of the pile, which depends on the pile material (steel, concrete, wood), the mean particle size of the soil, the normal pressure at the pile-soil interface and method of installation (CGS 2006). It ranges from 0.5 to 1.0ϕ. According to the rule of thumb, δ is equal to three-quarter of friction angle ϕ.

Table 2-1: Range of Combined Shaft Resistance Factor β (CGS 2006)

Soil Type	Cast-in Place Piles	Driven Piles
Silt	0.2 - 0.30	0.3 - 0.5
Loose sand	0.2 - 0.4	0.3 - 0.8
Medium sand	0.3 - 0.5	0.6 – 1.0
Dense sand	0.4 - 0.6	0.8 – 1.2
Gravel	0.4 - 0.7	0.8 – 1.5

2.4.3 Cylindrical Shear Method

Mooney et al. (1985) were among the first to recommend the use of a cylindrical failure model for the prediction of a helical pile's axial capacity when multiple helical bearing plates are present. Ultimate bearing capacity of a helical pile based on the cylindrical shear method is found by taking the sum of shear stress along the cylinder, adhesion along the shaft, and bearing capacity of the bottom helix given by:

$$Q_u = q_b A_1 + \tau(n - 1)s\pi D_{avg} + \alpha H(\pi d) \quad [2.18]$$

where

A_1 = the area of the bottom helix in m^2,

τ = soil shear strength in kPa,

H = the length of shaft above the top helix in m,

$(n - 1)s$ = the length of soil between the helices in m, and

α is the shaft adhesion, $\alpha = 2/3\,\tau$, the factor 2/3 is used to account for the reduced friction of soil on bare or galvanized steel.

2.4.4 Direct Method

Direct methods allow the geotechnical engineers to use in-situ test results directly into a design without the intermediate step of determining soil parameters. Direct methods can avoid the misrepresentations which possibly occur in laboratory testing when determining soil parameters. Certain soil properties can also prove very difficult to determine, whether in the laboratory or in-situ and therefore, direct methods provide an advantage in foregoing the need for intermediate calculation of representative soil parameters.

2.4.4.1 Torque Method

The relationship between helical pile capacity and installation torque have been used in industry for many years. It was first published by Hoyt and Clemence (1989). During the installation, final installation torque was recorded for each testing pile. The ultimate pile capacity is defined as:

$$Q_u = K_T T \quad [2.19]$$

where

K_T = empirical factor in m^{-1}, and

T = final installation torque (kN-m), which adopted from the records of field installer.

Hoyt and Clemence (1989) analyzed 91 load tests on helical piles at 24 different sites with various soil types to test the relationship between torque and capacity (Perko 2009). Hoyt and Clemence established a relationship between the ultimate helical pile capacities and K_T equal to 33 m^{-1} for square shafts helical piles, 23 m^{-1} for round shafts and 10 m^{-1} for large diameter tubular helical piles. However, the correlation came up from Hoyt and Clemence only applies to a few specific pile geometries, such as square shaft of 38-mm, 44-mm, and 51-mm and round

shafts with diameter of 89-mm diameter. It was stated that the correlation was not as strong (Perko 2009).

Ghaly and Hanna (1991) derived a more detailed relationship between the measured uplift capacity of screw piles installed in sand and the final installation torque achieved. The relationship is based on a rigorous theoretical analysis of the forces involved in resisting the insertion of the screw pile into the sand, thus determining the torque required for installation. The theory proposed for torque determination was employed in combination with experimental uplift capacity results to develop a correlation between the installation torque and the ultimate capacity of screw piles in tension. A torque factor, F_t, similar to the well-known uplift capacity factor, N_u, was introduced in order to express the installation torque in a non-dimensional form. This torque factor incorporated three key parameters that were found to affect the installation torque magnitude: the pile geometry, the installation depth, and the unit weight of the sand (Ghaly and Hanna 1991). The torque factor, F_t, and uplift capacity factor, N_u, were defined by Equations [2.20] and [2.21]:

$$F_t = \frac{T}{\gamma A_b H p} \quad [2.20]$$

$$N_u = \frac{Q_u}{\gamma A_b H} \quad [2.21]$$

where

γ = unit weight of the sand in kN/m^3,

H = pile embedment depth in m, and

p = pitch of the helix in m.

Ghaly and Hanna (1991) found that for all types of single-helix screw piles installed to varying depths in a range of sand deposits, there existed a unique relationship between N_u and F_t, approximated by the logarithmic Equation [2.22].

$$N_u = 2\,F_t^{(1.1)} \quad [2.22]$$

Substituting Equations [2.20] and [2.21] into Equation [2.22], the resulting equation may be manipulated to explicitly solve for the ultimate uplift capacity in terms of the installation torque (Equation [2.23]).

$$Q_u = 2(\gamma A_b H)\left[\frac{T}{\gamma A_b H p}\right]^{(1.1)} \quad [2.23]$$

Equation [2.23] was developed based on the formulation of forces acting on a single-helix helical pile; however, the equation was equally applicable to the case of a multi-helix helical pile of constant diameter and pitch (Ghaly and Hanna 1991).

2.4.4.2 Current SPT-based Direct Methods

Direct method is most commonly used to estimate the axial capacities of piles in the industry because of the effectiveness and simplicity. Six direct methods i.e., Meyerhof (1976), Shioi and Fukui (1982), Aoki and Velloso (1975) and Aoki et al. (1978), Decourt (1995), Shariatmadari et al. (2008) and AIJ (2004) of conventional straight piles associated with N are shown in Table 2-2. Based on numerous full-scale load tests, these direct methods established simple correlations between the average N over the pile shaft length (N_{bar}) and the unit shaft resistance q_s, and between the average N around pile base (N_b) and the unit end bearing resistance q_b.

Table 2-2: Summary of SPT-based Direct Methods for Prediction of Pile Capacities

No.	Method	Pile Type	Soil Type	Pile unit shaft resistance (q_s)	Pile unit end bearing resistance (q_b)
1	Aoki and Velloso (1975) and Aoki et al. (1978)	Driven pile	Sandy/silty Sandy ground	q_s(kPa) = $n_s N_{bar}$ n_s = 3.3 (sand), 3.8 (silty sand)	q_b(MPa) = $n_b N_b$ n_b = 0.48 (sand), 0.38 (silty sand)
2	Meyerhof (1976)	Driven pile	Sandy/Clayey ground	q_s(kPa) = $n_s N_{bar}$ n_s = 2	q_b(MPa) = $n_b N_b$ n_b = 0.4
3	Shioi and Fukui (1982)	Driven pile	Sandy/Clayey ground	q_s(kPa) = $n_s N_{bar}$ n_s = 2 (sand), 10 (clay)	q_b(MPa) = $n_b N_b$ n_b = 0.3 (sand) and 0.2 (silt)
4	Decourt (1995)	Displacement pile	Sandy ground	q_s(kPa) = α (2.8N_{bar} + 10)	q_b(kPa) = $K_b N_b$ K_b = 325
5	AIJ (2004)	Driven pile	Sandy ground	q_s(kPa) = 2N_{bar}	q_b(kPa) = 300N_b
6	Shariatmadari et al. (2008)	Not applicable	Sandy ground	q_s(kPa) = 3.65N_{bar}	q_b(kPa) = 385N_{gb}
7	Parry (1977)	Helical pile	Sandy ground	Not applicable	q_b(kPa) = $n_b N_b$ n_b = 40.6
8	Perko (2009)	Helical Pile	Sandy ground	Not applicable	q_b(kPa) = $n_b N_b$ n_b = 63.8

Note: N_{gb} = the geometrical average of N values between 8D above and 4D below pile base.

Decourt (1995) developed a comprehensive correlation of the shaft and end bearing resistance of piles with N. This can be expressed as:

$$q_s(\text{kPa}) = \alpha\,(2.8N_{bar} + 10) \quad [2.24]$$

$$q_b(\text{kPa}) = K_b N_b \quad [2.25]$$

where α equals 1 for displacement piles in any soil, and K_b is a base factor proposed by Decourt shown in Table 2-3.

Table 2-3: Base factor, K_b (Decourt 1995)

Soil Type	Displacement Piles	Non-Displacement Piles
Sand	325	165
Sandy silt	205	115
Clayey silt	165	100
Clay	100	80

As for helical piles, Parry (1977) proposed computing ultimate bearing pressure of coarse-grain soils with a simple correlation to N given by:

$$q_b(\text{kPa}) = 5\lambda_{SPT}N_{55} = n_bN_b \quad [2.26]$$

where

λ_{SPT} = the SPT blow count correlation factor equal to 6.2 kPa/blows/30 cm defined by Terzaghi and Peck (1967),

N_{55} = the blow count at an energy ratio of 55, and

n_b = 40.6.

A correction was made for the hammer energy in order to change the energy ratio from 55 and 70 to 60. As can be seen, the correlation by Parry (1977), which was originally derived for shallow foundations, does not correlate well for helical piles even with the energy correction. Perko (2009) collected results from the 54 load tests on helical piles and compared with correlation by Parry in Figure 2-6. The measured axial capacity in each of the 54 helical pile tests was divided by the total area of the helical bearing plates to obtain measured ultimate bearing pressure. Perko (2009) proposed a direct method to estimate q_b of helical piles in sand using N from 54 load tests of helical piles. Notably, the shaft resistance was neglected in this correlation.

The estimation of q_b follows:

$$q_b(\text{kPa}) = 12\lambda_{SPT}N_{70} = n_b N_b \quad [2.27]$$

where n_b is a constant 63.8.

Perko (2009) used this correlation as a rule of thumb to estimate capacities of helical piles. However, the essence of SPT penetration is more of a soil-pile shearing behaviour rather than an end bearing behaviour. The estimation of skin friction of piles based on SPT interpretation is more reliable than end bearing resistance. From this point of view, it is important to separate the skin friction from the end bearing resistance in the analysis.

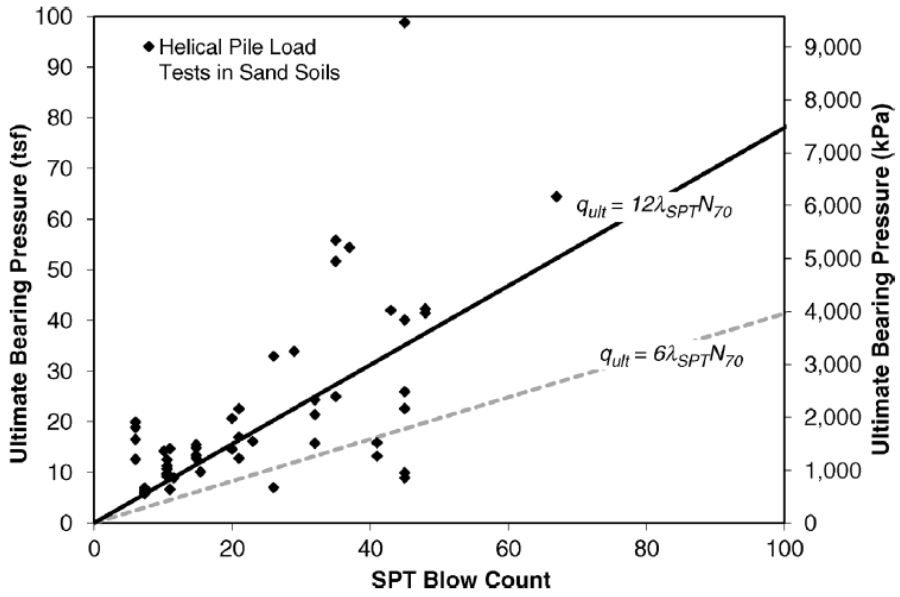

Figure 2-6: Correlation Between Bearing Pressure and Blow Counts (Perko 2009)

3 Field Axial Tests of Single-helix Piles in Sand

Twelve full-scale load tests of helical piles were installed and tested in a uniformly-graded sand site, including six axial compressive tests and six tensile tests. This chapter describes the site investigation program with laboratory testing and field load testing program specifically. The results of the test piles were presented as the axial load vs. displacement curves. Because not every pile was taken to a limit load, an ultimate load criterion is necessary. The ultimate pile capacity Q_u is defined as the pile resistance at the axial displacement of 10% of helix diameter D. Chin's (1970) method were introduced and used to some piles reached the loading frame capacity before the ultimate state. Chin's method also used to clarify and correct some abnormal observations in regard to curve segments. In this chapter, Chin's hyperbolic method was checked whether it's capable of estimating the axial limit capacity of helical piles installed in sandy soil. With laboratory testing results, the q_b and q_s values were back-calculated with indirect method proposed by CGS (2006) and Perko's (2009) to verify if indirect method is capable to predict capacity of helical piles.

3.1 Introduction

SPT is a popular and economical mean to obtain subsurface information. SPT has several advantages, such as simple operation in practice, low cost, and disturbed soil samples can also be obtained for laboratory testing. Numerous studies were conducted to correlate empirically the N values with geotechnical design parameters such as soil density, consistency, friction angles, undrained shear strength, young's modulus, shear modulus, settlement of shallow and deep foundations in sand, and bearing capacity values. Thus, estimating design parameters with N values can be cost-effective by reducing laboratory testing.

With those advantages, SPT were chosen to conduct to investigate the soil stratigraphy at Botanic Garden. However, one of the principal issues of the SPT is that the test equipment, drilling techniques, and test procedures have not been completely standardized on a worldwide premise (Robertson 2006). To eliminate the variability in equipment and test procedures encountered in practice, the N values need to be corrected with the ratio of the measured energy transferred to the rod to 60% of the theoretical potential energy. The corrected N-value's (N_{60}) was calculated by Equation [3.1]:

$$N_{60} = \frac{E_m C_B C_S C_R N}{0.60} \qquad [3.1]$$

where

E_m= hammer efficiency,

C_B= borehole diameter correction,

C_S= sample correction, and

C_R= rod length correction.

Note: E_m, C_B, C_S and C_R values are provided by the drilling operators.

As geotechnical engineers, we need to make sure that the piles will indeed perform adequately after installation. Static load tests on piles are often used to verify that the piles will support the designated load. The static load test is basically successive application of load increments to the pile and the measurement of the resulting settlement or lateral deflection (Salgado 2008). The most common pile load test is the axial compressive load test, followed by the tensile test.

The limit load Q_L, referred as the plunging load, is often very large and unattainable, particularly for the pile bearing in dense sand (Salgado 2008). The load reaction system often does not have the capacity to take a pile all the way to plunging, so a limit load often cannot be determined in situ. The pile load capacity is often defined in terms of ultimate load Q_u, and Q_u is

obtained based on load-displacement curves. Many ultimate load criteria were developed to interpret the pile load test results, such as the Davisson offset limit (Davisson 1972), the Brinch-Hansen 80% criterion (Hansen 1963) and the Chin-Kondner extrapolation (Chin 1978). Except for these three methods, the most common Q_u in industry convention is corresponding to an axial displacement equal to 10% of the pile diameter. It is necessary to apply a unique failure criterion in defining Q_u to make the load test results comparable.

3.2 Site Investigation

The test site at the University of Alberta Botanic Garden (Figure 3-1) is located 2 km to the east of Highway 60 in Devon, Alberta, Canada. The site was selected because it represents typical profiles of Albertan cohesionless soils, and the site stratigraphy is relatively homogenous. The soil at the test site was mainly sand dunes formed by meltwater rivers deposit (Godfrey 1993). Prior to advancing boreholes at the test location, the UAlberta group conducted the necessary underground utility clearances at the borehole location through Alberta One Call. The borehole location was cleared of any above or underground utilities before drilling commenced.

3.2.1 SPT Tests

The borehole elevation was measured and indicated on the borehole logs. The test site, at the time of investigation, was primarily covered with snow. The thickness of the frozen crust was approximately 30 cm. The area, at the time of investigation, was primarily covered with snow and frost. The drilling was conducted using a truck-mounted rig, equipped with 150 mm diameter continuous flight, solid stem augers. Two boreholes were drilled to the depth of 8.3 m, which was greater than the embedment of the longest piles (4.47 m) tested in situ. SPT's were conducted at 1.5 m depth intervals to determine the N at different depths. The depth to slough and groundwater levels within the borehole were measured upon drilling completion.

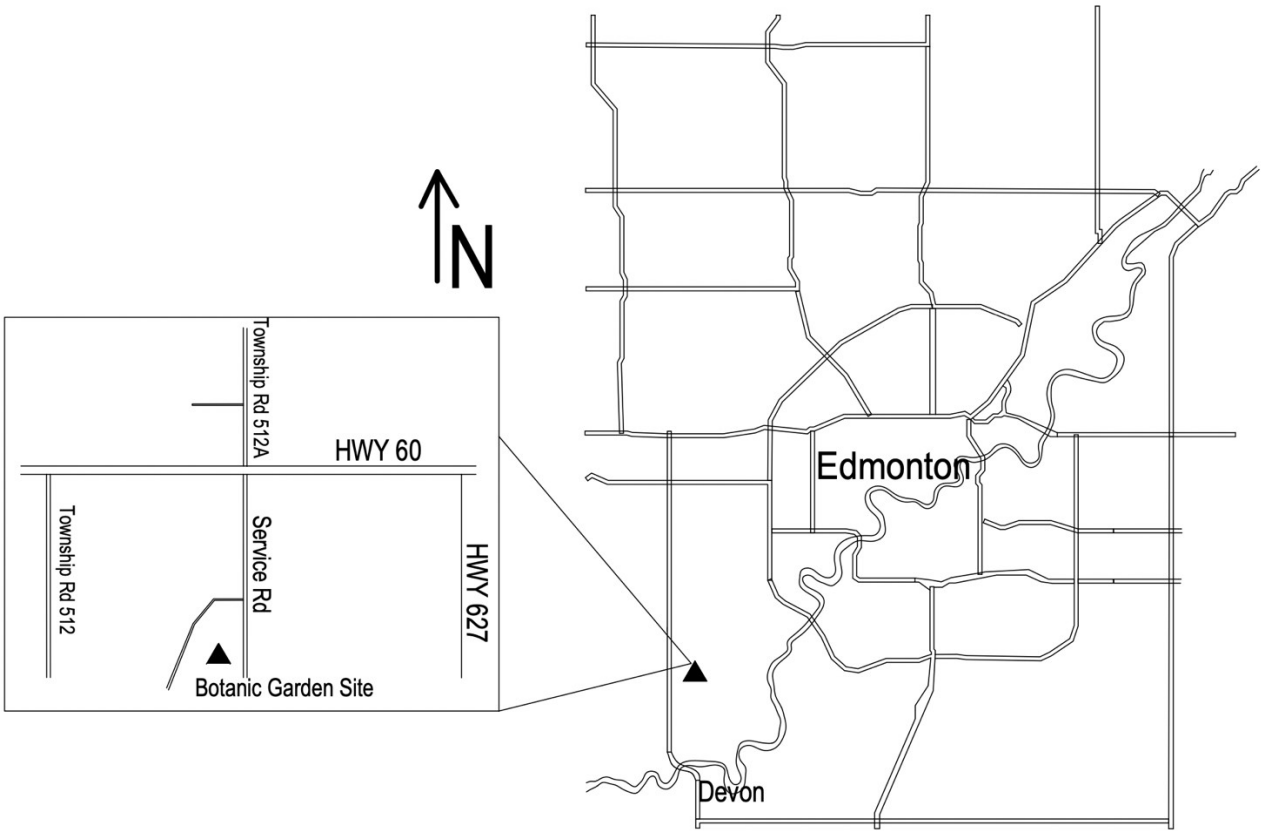

Figure 3-1: Location of Test Site at the University of Alberta Botanic Garden (53°24'08.7" N, 113°45'10.0" W).

The corrected N_{60} per Equation [3.1] of two boreholes are shown in Figure 3-2, which are important parameters in the SPT-based method. Provided by the drilling operator at Mobile Auger, the borehole diameter correction factor C_B is 1, sampling correction factor C_S is 1, and rod length factor C_R varies from 0.75 to 0.95. Those correction factors were used in Equation [3.1]. Figure 3-2 also shows the moisture content, in-situ relative densities and friction angles, and soil stratigraphy along the boreholes. After sampling, the boreholes were backfilled and sealed with bentonite at the top. Figure 3-3 shows a photo of a wet split-spoon sample taken in-situ. In Figure 3-4, the field crew were collecting grab samples. All samples collected from the

drilling program were immediately stored in plastic bags and stored in humidity conditioned room until further testing. All soil samples, including SPT samples and grab samples, were tested for moisture content immediately, but only a few of results were shown in Figure 3-2.

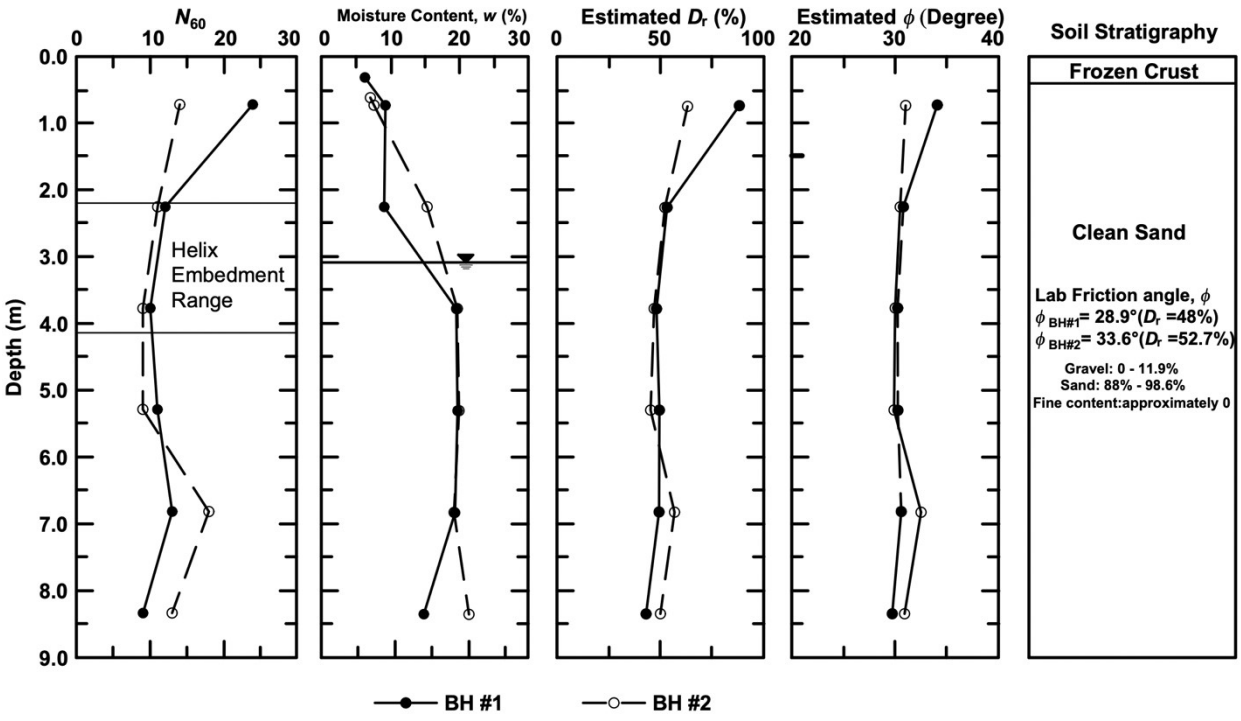

Figure 3-2: Soil Characterization from SPT Blow Count Index and Derived Soil Parameters

Figure 3-3: Split Spoon Sample (Wet Fine Sand) Collection.

Figure 3-4: Grab Sample Collection

Since high-quality samples of granular materials are difficult to sample in situ, the evaluation of the in-situ void ratio from laboratory measurements is rare. Under this circumstance, in-situ

relative density is often estimated with empirical relationships from SPT blow count. The N values provide a guide to the in-situ properties and indicate of the relative density and friction angle of the soil. Deriving from the work by Meyerhof (1956) and Skempton (1986), the relative density can be expressed as:

$$D_r = \sqrt{\frac{(N_1)_{60}}{C_d}} \quad [3.2]$$

where $(N_1)_{60}$ is the N value corrected and normalized for energy ratio of 60% and normalized for effective overburden pressure of 1.0 tsf or 96 kPa and C_d is a fitting parameter. A value of C_d is 41 from the original observations proposed by Meyerhof (1957). Then, Skempton (1986) suggested that C_d values for normally consolidated natural sand deposits were about 55 for fine sands and 65 for coarse sands. Cubrinovski and Ishihara (1999) concluded that average C_d values of about 51 for clean sand samples, about 26 for silty sand samples, and about 39 for all samples. All the samples were high-quality undisturbed samples and obtained by in-situ freezing conditions. The value of C_d was chosen as 51 according to experiments of Cubrinovski and Ishihara (1999) due to soil stratigraphy at the test site Botanic Garden.

N values are corrected to the equivalent value that would have been obtained in the identical sand if the vertical effective stress had been 1 tsf (96 kPa). This corrected value, denoted as $(N_1)_{60}$, following by Equation [3.3] (CGS 2006):

$$(N_1)_{60} = N_{60} C_N \quad [3.3]$$

where C_N is the overburden correction factor. A simple correction factor was summarized by Liao and Whitman (1986) as:

$$C_N = 0.77 \log_{10}\left(\frac{1920}{\sigma_v'}\right) \quad [3.4]$$

where σ_v' is the effective overburden stress at the level of N in kPa.

The equation is not valid for σ_v' less than about 24 kPa since the equation for C_N leads to unreasonably large correction factors at low overburden pressures. Thus, Peck et al. (1974) proposed a chart given as Figure 3-5 to solve this problem. Although the maximum value of C_N at zero effective overburden pressure was suggested, it is probably not to use values larger than about 1.5 in practice (CGS 2006). The in-situ D_r values shown in Figure 3-2 were obtained from Equations [3.2], [3.3] and [3.4]. In situ relative densities D_r were used as a reference for laboratory direct shear tests, where D_r values in laboratory testing were controlled approximately in the range of in-situ D_r determined from the SPT empirical relationship about 1.5 in practice (CGS 2006).

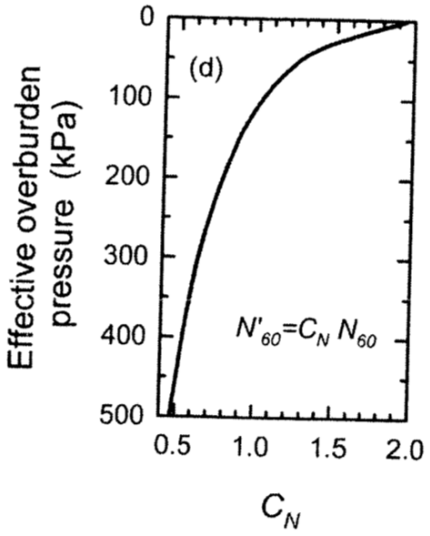

Figure 3-5: SPT N-Value from Field to be Modified by Factor C_N (CGS 2006).

There was a widely used correlation on estimating friction angle ϕ from N_{60} for sand proposed by Meyerhof (1956) and Peck et al. (1974). A graphical representation by Peck et al. (1974) was shown in Figure 3-6, then Wolff (1989) approximated the graph with Equation [3.5]:

$$\phi = 27.1 + 0.3N_{60} - 0.00054(N_{60})^2 \qquad [3.5]$$

The estimated ϕ values are shown in Figure 3-2.

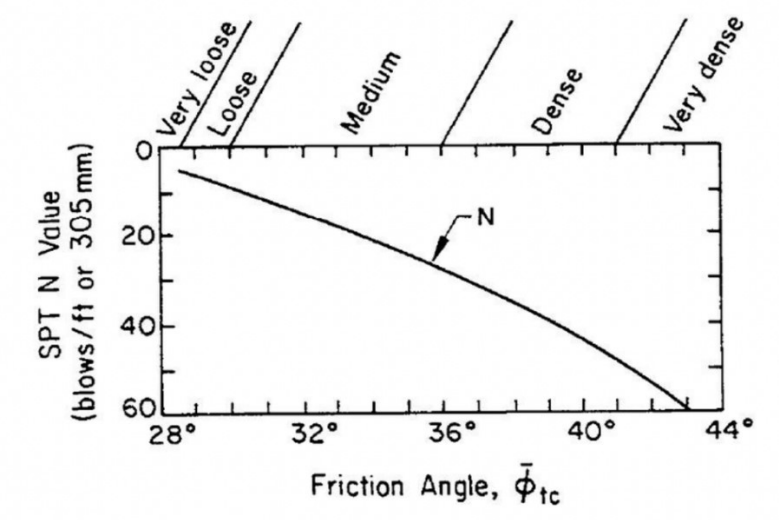

Figure 3-6: Relation of *N* and friction angles by Peck et al. (1974).

3.2.2 Laboratory Testing

Following the completion of the field drilling program, a detailed laboratory testing program was conducted on selected soil samples obtained from the borehole. The tests conducted consist of the following:

- Moisture content – ASTM D2216 (ASTM 2019)
- Sieve analysis – ASTM D6913 (ASTM 2008c)
- Atterberg limits – ASTM D4318 (ASTM 2008b)
- Specific gravity – ASTM D854 (ASTM 2010)
- Minimum index density and unit weight of soils – ASTM D4254 -16 (ASTM 2016)
- Direct shear test – ASTM D3080 (ASTM 2012)

A detailed borehole log that summarizes the soil sampling, field testing, laboratory test results, groundwater and subsurface conditions encountered at the borehole location is presented in

Figures 3-2. The groundwater levels were estimated by experienced driller as 3.1 m following drilling completion. Accumulations of collapsed soils (slough) were observed during the drilling.

Grain size analysis was performed on retrieved grab samples and SPT samples from BH #1 and BH #2. The grain-size distribution curves are plotted on a semi-log scale as percent finer than versus particle sizes. Figure 3-7 is an example of grain-size distribution curves of BH #1 at depth 0.30 m, 0.71 m, 2.24 m, 3.76 m, 5.28 m and 6.81 m, while Figure 3-8 is an example of grain-size distribution curves of BH #2. From the grain size distribution curves, the particles sizes on a percent finer level can be obtained. Also, the distribution curves were described by two properties: coefficient of uniformity (C_u) and coefficient of curvature (C_c). As per Unified Soil Classification System (USCS), all samples were classified as sand because more than 50% of soil has passed the #4 sieve. When less than 5% of soil passing the #200 sieve, the soil can be classified as SW or SP. According to C_u and C_c parameters, most of the samples can be classified as poorly graded sand (SP). At the bottom of some boreholes, a few soil samples with more than 5% but less than 12% passing through the #200 sieve. Additional Atterberg limit tests were conducted to determine USCS as dual symbol SP-SM.

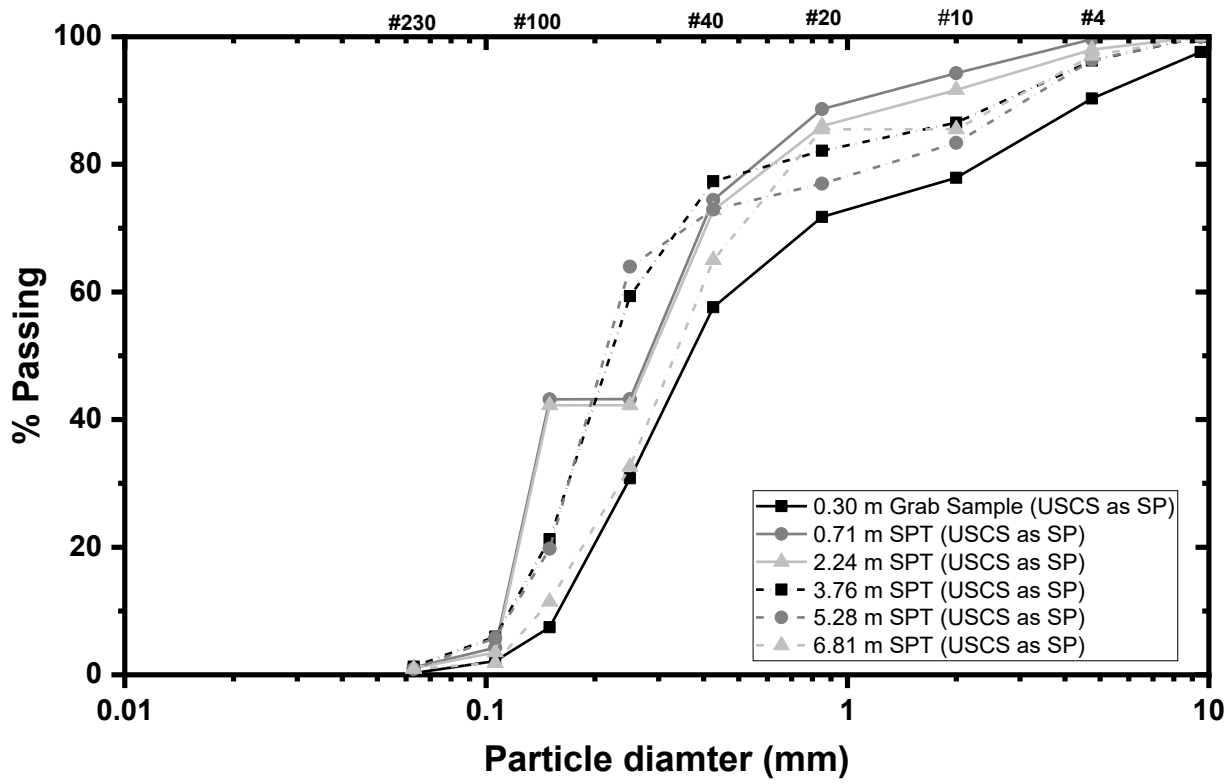

Figure 3-7: Grain-size Distribution Curve of BH #1

The specific gravity G_s is used in geotechnical engineering to compute the void ratio and the density of soil and is used for hydrometer analysis. In this experiment, the volume of a known mass of soil particles were obtained using a container of known volume by applying the Archimedes principle. Figure 3-9 shows that G_s varied with depths of BH #1 and BH #2.

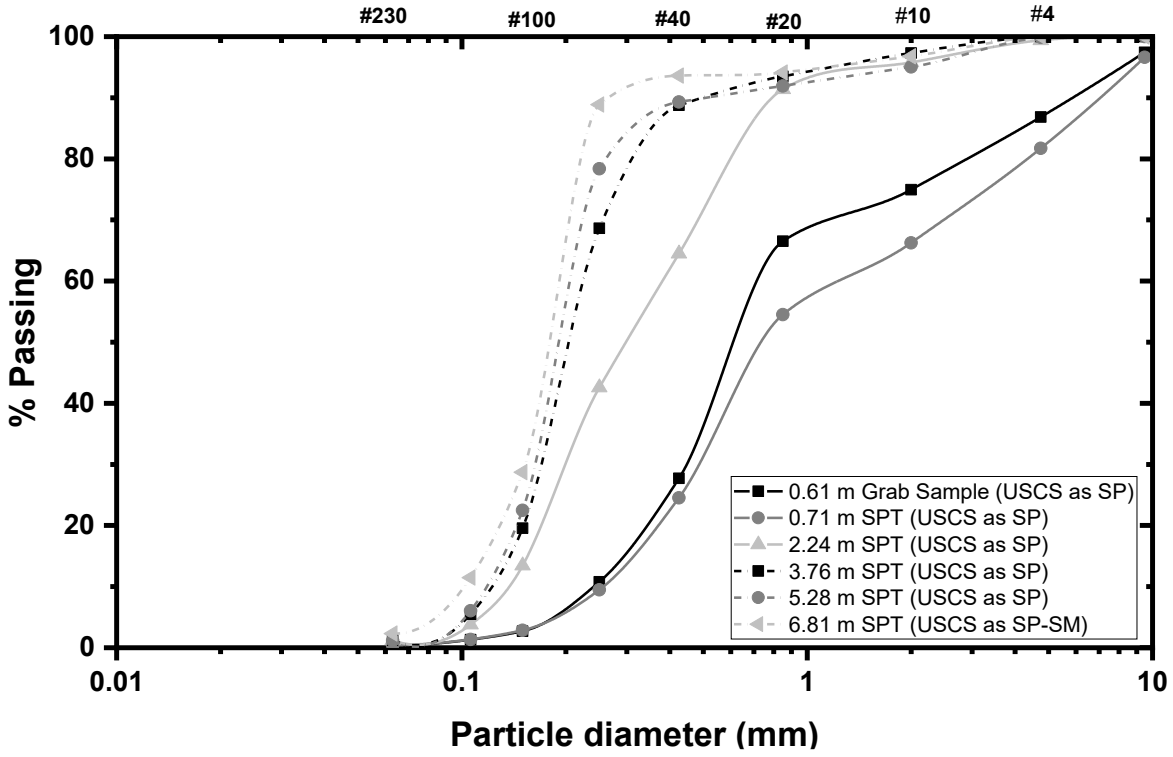

Figure 3-8: Grain-size Distribution Curve of BH #2

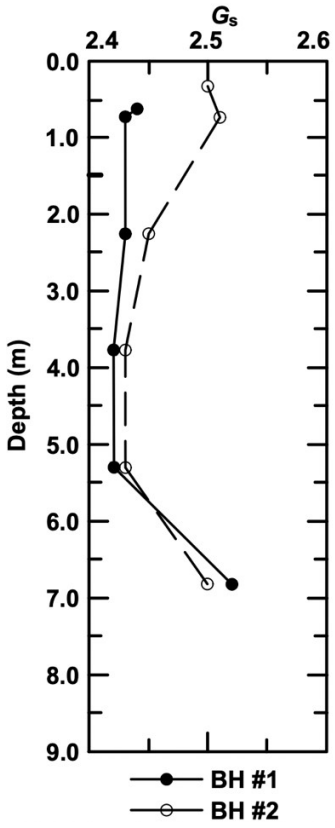

Figure 3-9: G_s versus Depth of Two Boreholes.

In the direct shear test, the specimen was confined in a metal shear box of circular cross-section. The shear box is split horizontally at mid-height, and a small clearance is maintained between the two halves of the box. A vertical load was applied to the specimens via a loading plate and lever/hanger mechanism. Shear stress was applied on a horizontal plane by causing the bottom half of the box to move relative to the top half at a constant rate of displacement. The curves shown in Figure 3-10 are recorded by the datalogger under different vertical loads. The values of D_r in direct shear tests were chosen so that they were approximately in the range of in-situ D_r, which were determined from the SPT empirical relationship. The tests were conducted with medium D_r, which approximately equals in-situ D_r, and additional tests with dense D_r. Depending on the D_r, different behaviors in terms of shear strength-shear strain were presented. Dense sand specimens tend to obtain maximum shear stress that subsequently drops, reaching a fixed value known as critical state strength shown in Figure 3-10 (b). The peak strength coincides with the residual strength for medium sand specimens. The friction angles from peak state and residual state were collected separately in Table 3-1.

The soil samples used in direct shear tests were mixed by four SPT test samples at depths of 0.71 m, 2.24 m, 3.76 m, and 5.28 m. Each borehole just uses a mixed sample because the soil stratigraphy is very homogeneous along the depth.

Table 3-1: Direct Shear Results

	e_{max}	e_{min}	Medium D_r (%)	Friction angle, ϕ		Dense D_r (%)	Friction angle, ϕ	
				Peak	Critical		Peak	Critical
BH 1	0.9	0.56	48	28.9	28.9	68.8	42.6	35.7
BH 2	0.88	0.55	52.7	33.6	33.6	75	39.5	35.5

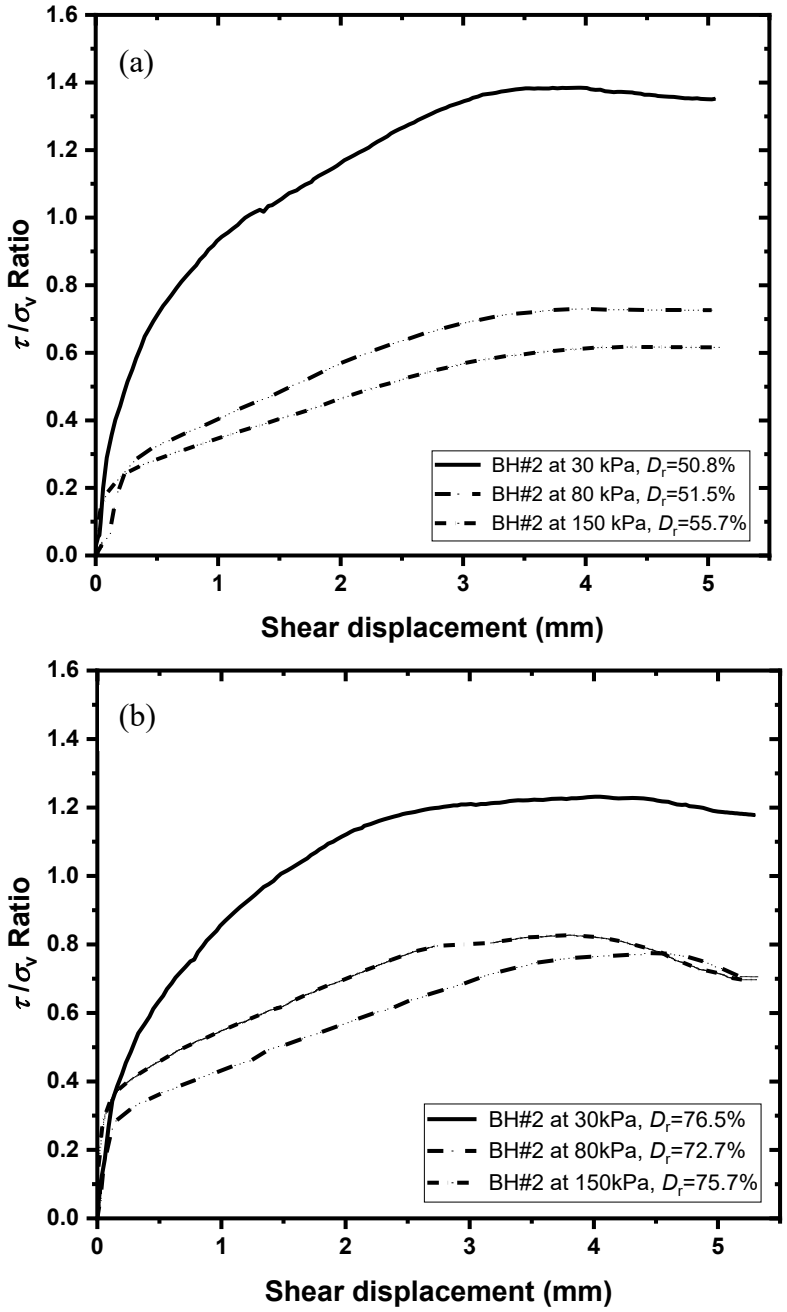

Figure 3-10: Direct Shear Tests of (a) Medium Specimens and (b) Dense Specimens of BH #2

3.3 Field Load Test Program

Helical pile installation is usually accomplished by two operators within 30 minutes per pile. The pile is screwed into the ground by the hydraulic torque head carried by a forklift or skid-steer

loader. Figure 3-11 shows the configuration of a single-helix pile. The reason for selecting single-helix piles is to avoid the complexities of cylindrical failure mode for multi-helix piles. The shaft diameter *d* of the tested piles varies from 73 mm to 114 mm, the helix diameter *D* from 305 mm to 406 mm, and the pile length *L* from 3.05 m to 4.57 m. These small-diameter piles were most commonly used in practice. The helix is designed to be vertically welded to the shaft so that the soil disturbance during installation is minimized. Each pile test was assigned with a code as shown in Table 3-2: the first letter denotes the term "Pile," and the following number denotes the pile type. Specifically, "1" means the pile with 73 mm (2.875") of *d*, "2" means 89 mm (3.5"), and "3" means 114 mm (4.5"). The second letter tells the loading directions, e.g., compression (C) or tension (T). The last number represents the pile length: "10" for 3.05 m (10') and "15" for 4.57 m (15'). To allow sufficient space for apparatus setup, the pile heads were set about 30 cm above the ground surface.

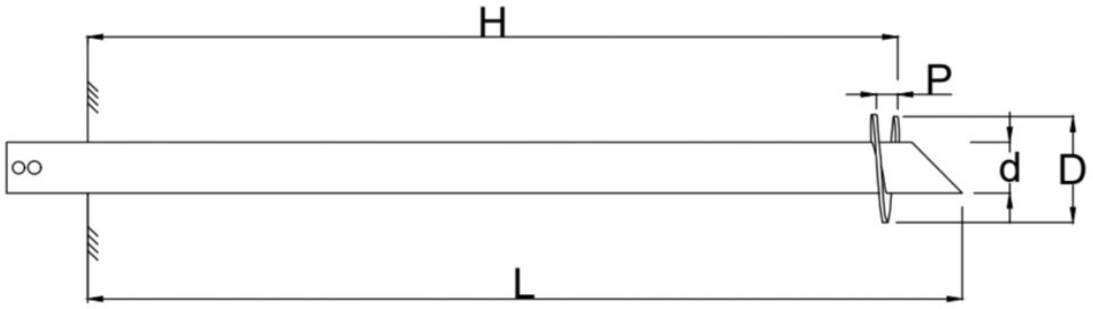

Figure 3-11: Sketch of a Typical Single-helix Pile and the Terminology

Figure 3-12 shows the layout of the test piles, reaction piles and SPT boreholes. In order to minimize the pile-to-pile interaction, the center-to-center spacing of every two adjacent piles was set to be 2.59 m, which was greater than 5 times of the helix diameter of the larger pile (if applicable) (ASTM 2013a and 2013b).

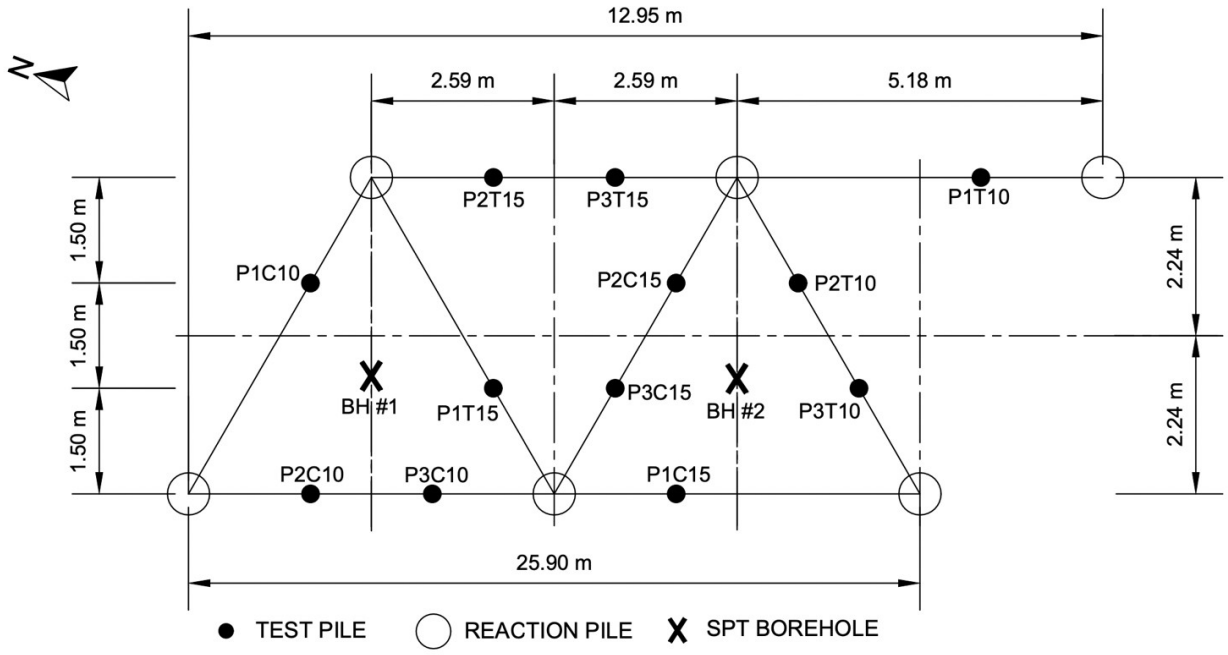

Figure 3-12: Layout of Test piles, Reaction Piles, and SPT Boreholes

The reaction system consists of an I-shaped beam and two double-helix reaction piles installed to the depth of 4.27 m. The dimensions of the reaction piles are presented in Table 3-2. The reaction beam was fixed to the top of the reaction piles as shown in Figure 3-13. Figure 3-14 (a) shows a photo of the test setup, and Figure 3-14 (b) shows the detail of the axial test arrangement. The hydraulic jack was connected with the load cell by the internal threads, and they worked as one unit throughout the load tests. The axial load applied to the test pile was measured by the load cell. The vertical pile movement was recorded using linear potentiometers (LP) attached to two steel reference beams as shown in Figure 3-14 (b). The probes of LPs were placed on the levelled reference beams, and the bodies of the LPs were attached to the pile cap using magnetic bases. The average readings of the LPs were used as the pile displacement to eliminate errors caused by potential inclination. A cylindrical load cell with a capacity of 900 kN was selected; it

can measure both tensile and compressive load. All instruments were calibrated prior to the field tests.

Table 3-2: Configurations of Test Piles

Pile code	Test type	Shaft diameter, *d* (mm)	Helix diam, *D* (mm)	Helix embedment, *H* (m)
P1C10	C	73	305	2.56
P1C15	C	73	305	4.21
P1T10	T	73	305	2.47
P1T15	T	73	305	4.11
P2C10	C	89	356	2.68
P2C15	C	89	356	4.01
P2T10	T	89	356	2.31
P2T15	T	89	356	3.99
P3C10	C	114	406	2.58
P3C15	C	114	406	4.19
P3T10	T	114	406	2.65
P3T15	T	114	406	4.26
Reaction piles	N/A	114	508 (Double-helix)	4.27

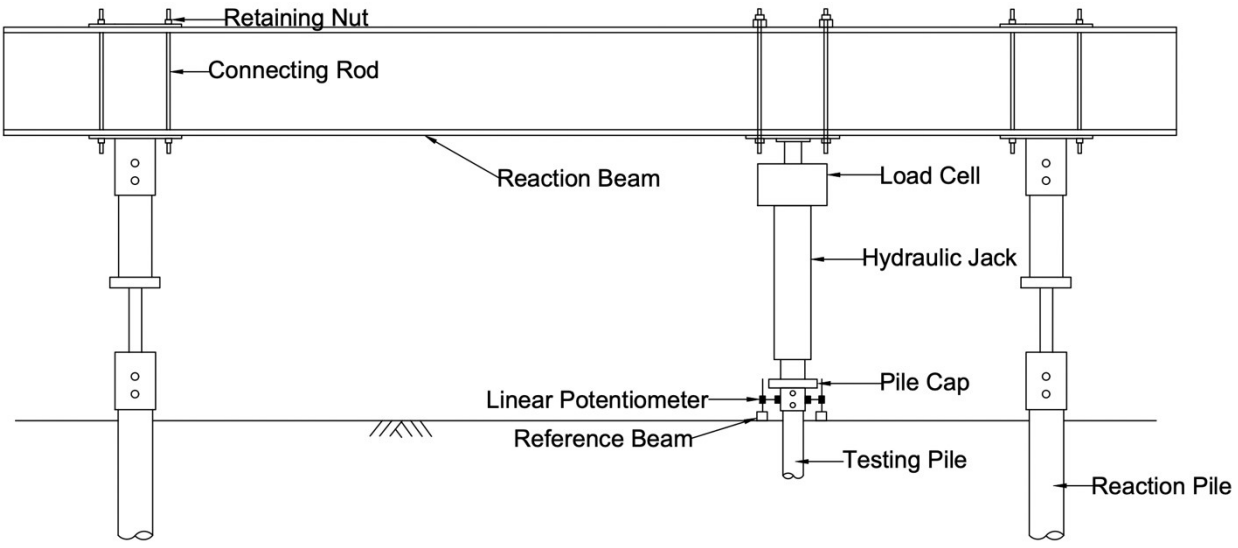

Figure 3-13: Schematic of Test Setup

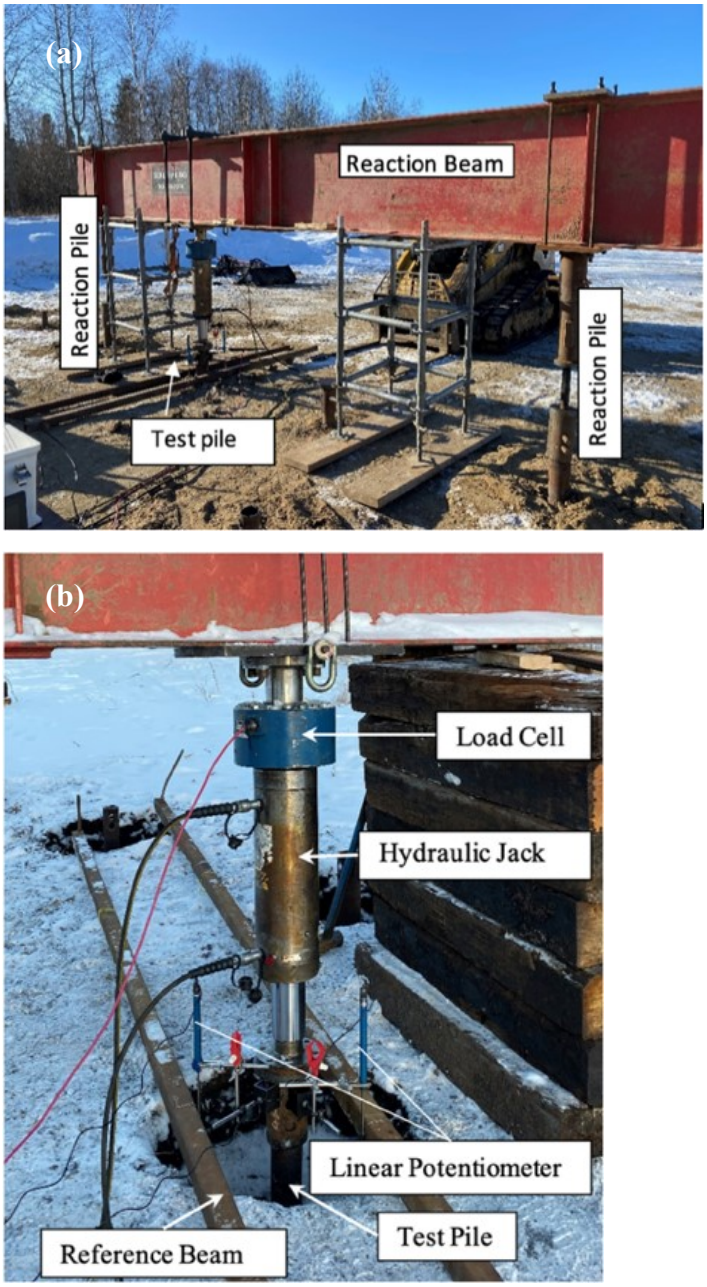

Figure 3-14: Setup of Axial Compression Tests: (a) Overview of Loading Frame, and (b) Hydraulic Jack Loading and Measurement System

Incremental loads of 5% of predicted capacity were applied to each test pile. The predicted capacities of test piles were generated by the torque-factor method and measured final installation torques. A constant time interval of 5 minutes was maintained at each load increment

to allow adequate time for pile settlement per D1143M-07 (ASTM 2013a) and D3689M-07 (ASTM 2013b). The applied loads were increased until the limit state was reached. However, in the present study, some piles whose helices were embedded in the deep dense sand, exceeded the capability of the loading frame. Therefore, these piles were loaded to the capacity of the loading frame or the limit capacity of test pile whichever reached first. The load at the "failure" state was held for 10 minutes, and then the unloading was started. The unloading stage adopted a load decrement of 20% of the previously achieved maximum load. The constant time interval was also 5 minutes.

3.4 Field Test Results

The axial load vs. displacement (Q-w) curves of all tested piles are presented in Figure 3-15 and 3-18. Most of Q-w curves consist of an initial linear segment, a transitioning segment, a plateau, and an approximately linear or bilinear unloading segment; however, some of the curves (Figure 3-14: P1C10, P1C15 and P2C15) behaved abnormal at the beginning of tests. In engineering practice, the ultimate capacity Q_u is more commonly used than the limit capacity Q_L. There are several recognized definitions of Q_u and herein this study, Q_u is defined as the pile resistance at the axial displacement of 10% of D, which is the diameter of helix in this context. Chin's hyperbolic method (Chin 1970) assesses whether the Q-w curves of helical piles follow the hyperbolic assumption and extrapolate the test curves to obtain Q_L for test piles. There are two reasons for using Chin's method: (1) Some piles reached the loading frame capacity before the ultimate state; thus, Q_u need to be extrapolated to the load at 10% of D using Chin's method; (2) abnormal observations in regard to curve segments must be clarified and corrected. Chin's method is based on the assumption that the pile load-displacement (Q-w) curve is hyperbolic:

$$Q=\frac{w}{C_1 w+C_2} \qquad [3.6]$$

where C_1 is the inverse of Q_L and C_2 is the inverse of initial slope of the Q-w curve. Equation [3.6] can be rewritten as:

$$\frac{w}{Q}=C_1 w+C_2 \qquad [3.7]$$

By plotting w/Q versus w curves in the loading phase, the limit capacity can be determined as:

$$Q_L=\frac{1}{C_1} \qquad [3.8]$$

The plunging failure was not observed in Figure 3-15 and 3-18, which indicated that the limit state was not reached. The load-displacement curves in Figures 3-15 and 3-18 were sketched by a series of points in order to simplify the results. The soil collapsed in the vicinity of the helix (localized) and the soil in the front of helix became densified as piles proceeded. The reduction in depth of the helix plate results in an associated reduction in capacity. Before the load was applied, there might be unsettled gaps between the LP's and reference beams or between the reaction beam and load adaptor; therefore, the initial slopes of some Q-w curves (Figure 3-14: P1C15 and P2C15) were significantly smaller than expected.

In order to obtain Q_L values, Chin's method was used. The w/Q versus w curves of the loading segment shown in Figures 3-15 and 3-18 are plotted in Figure 3-16 (a) and Figure 3-19 (a) according to Equation [3.2]. The linearly regressed curves and several w/Q versus w equations are also shown in Figure 3-16 (a) and Figure 3-19 (a). Because of LP measurement errors previously described, some curves P1C10, P1C15 and P2C15 in Figure 3-16 (a) and P1T10, P1T15 and P2T10 in Figure 3-19 (a) did not behave linearly in w/Q versus w plot and need to be corrected. Thus, the points at the beginning of curves and not following the regressed line were

back-calculated with regression equations. These points are denoted as 'hollow points' with different colours in Figure 3-16 and Figure 3-19. Some linearly regressed curves have significant intersections with the *w/Q*-axis, which needs to be eliminated. These linearly regressed curves were translated to get corrected *w/Q* versus *w* curves in Figure 3-16 (b) and Figure 3-19 (b).

Most of the compressive tests, except P2C15, did not reached the loading frame capacity before the ultimate state, thus, Q_u was extrapolated to the load at 10% of *D* using Chin's method. The modified *Q*-*w* curves with Chin's hyperbolic method were plotted in Figure 3-17 and Figure 3-20 for comparison with simplified *Q*-*w* curves. As shown in Figure 3-17 and Figure 3-20, the hyperbolic assumption works well, although not perfectly, for most of the *Q*-*w* curves. Generally, it is indicated that Chin's hyperbolic assumption proposed for straight-shaft piles is capable of estimating the axial limit capacity of helical piles installed in sandy soil.

The values of Q_L were obtained for all testing piles according to Equation [3.8] and summarized in Table 3-3. The coefficients of determination R^2 of the linear regression are also presented in Table 3-3. It shows that the most of R^2 values are close to 1.0 after the correction. The high R^2 confirms that Chin's hyperbolic assumption offers a good approach to predicting the *Q*-*w* curves of helical piles with a reasonable accuracy.

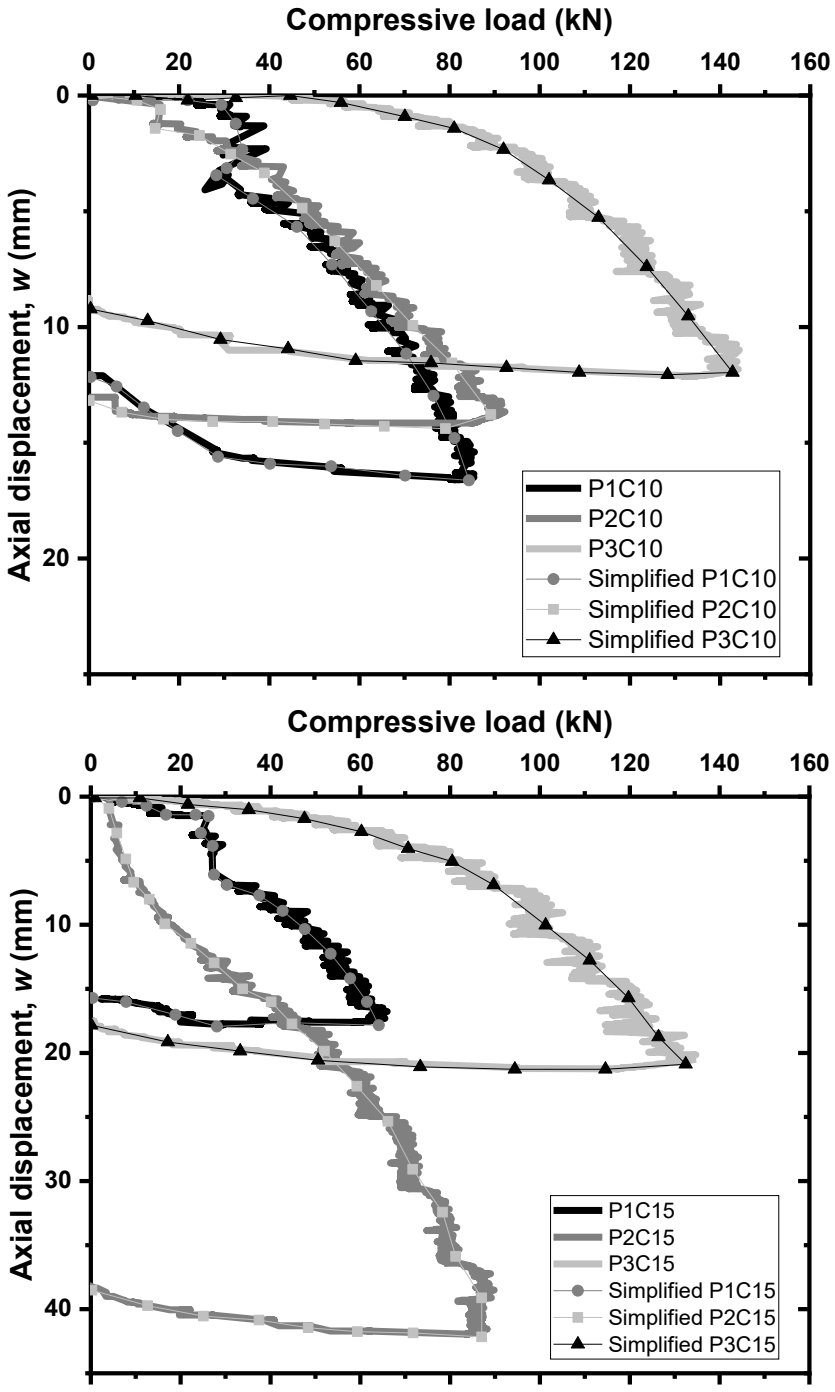

Figure 3-15: Original and Simplified Compressive Load *Q* versus Displacement *w* Curves

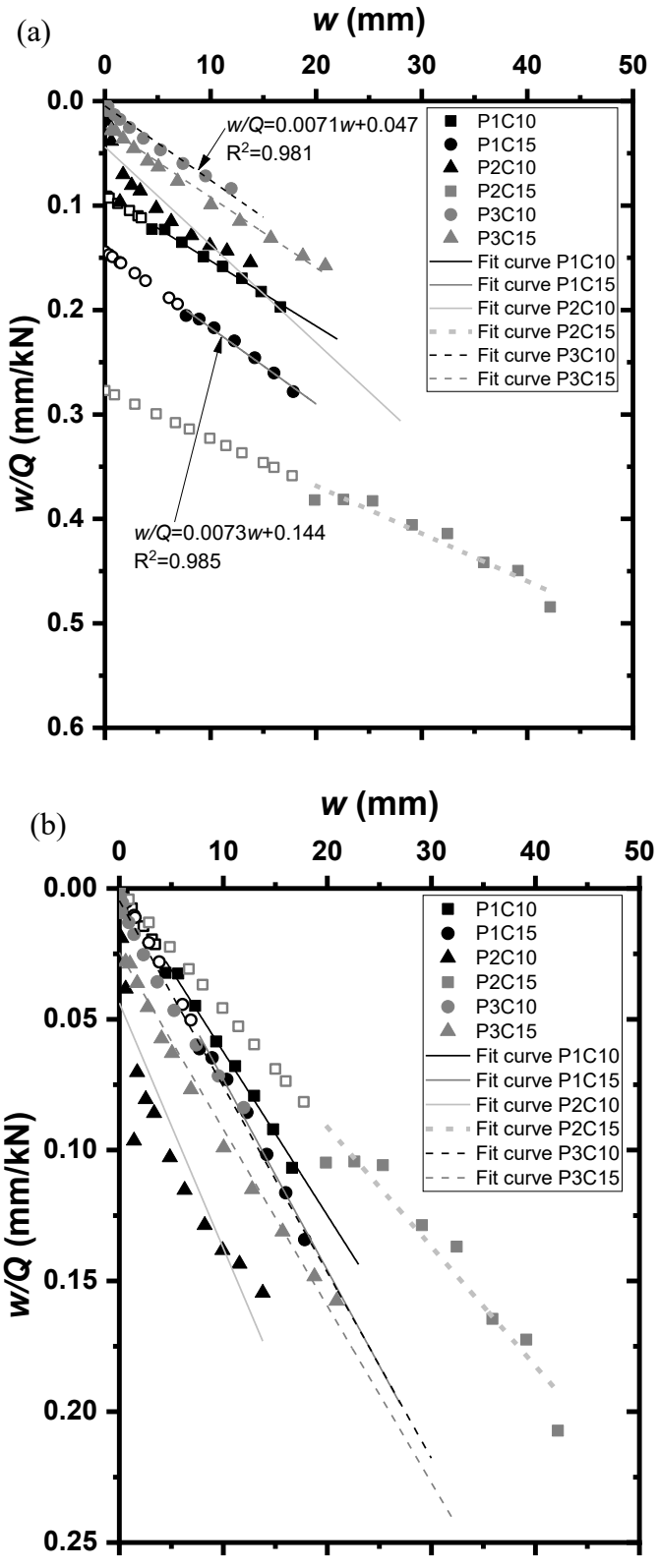

Figure 3-16: (a) Original and (b) Corrected *w/Q* versus *w* Curves of Compressive Test Results at the Loading Stage

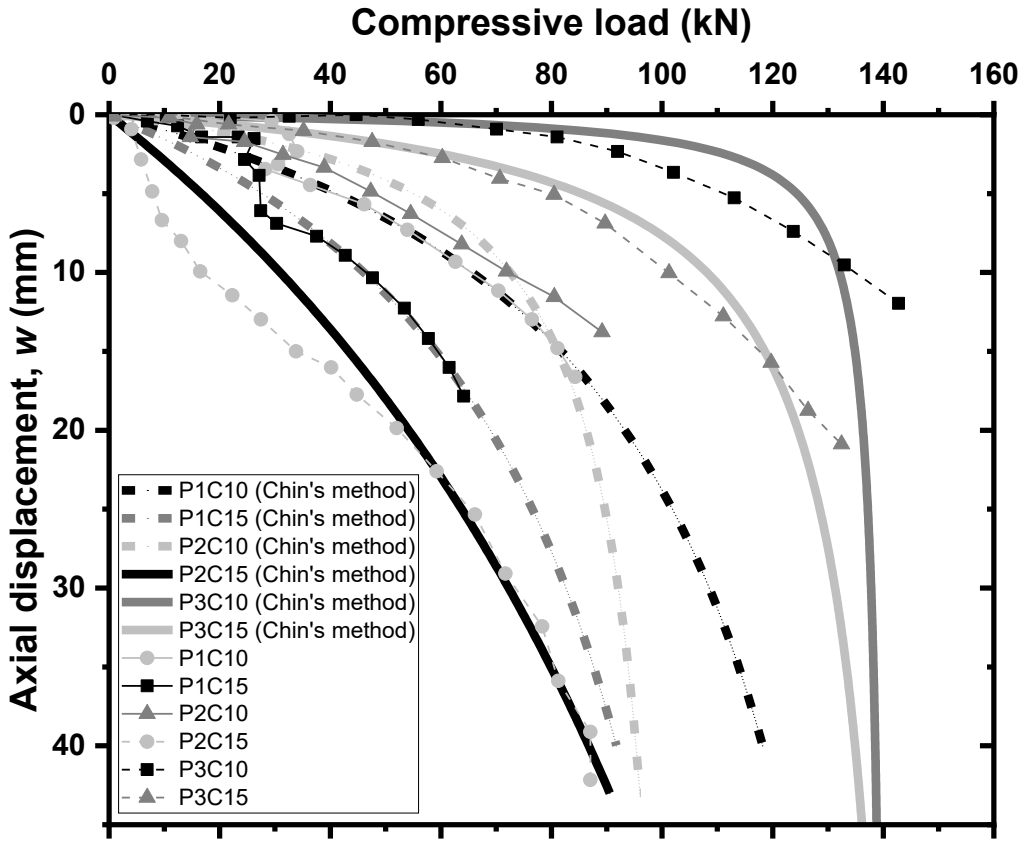

Figure 3-17: Modified Compressive Load *Q* versus Displacement *w* Curves with Chin's Hyperbolic Method

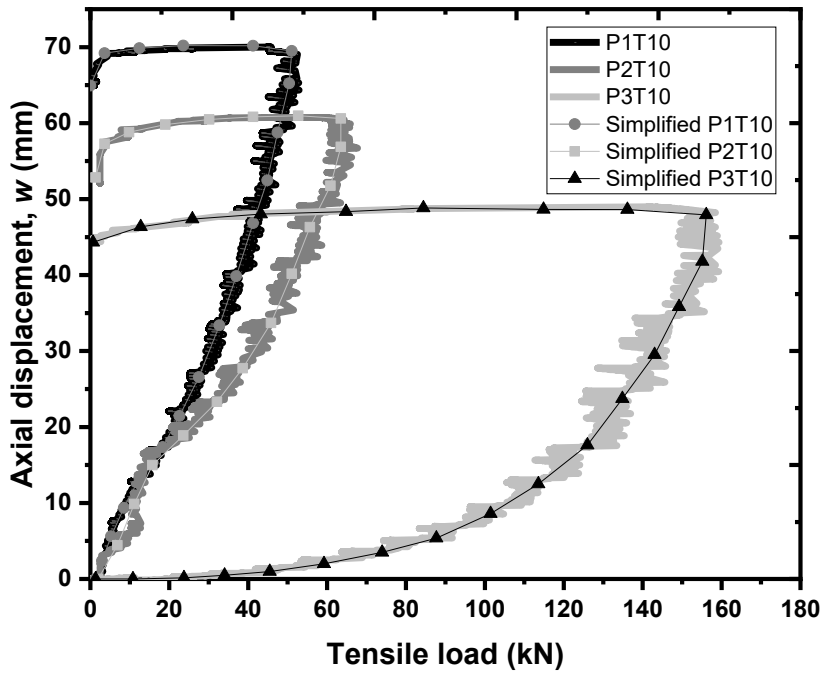

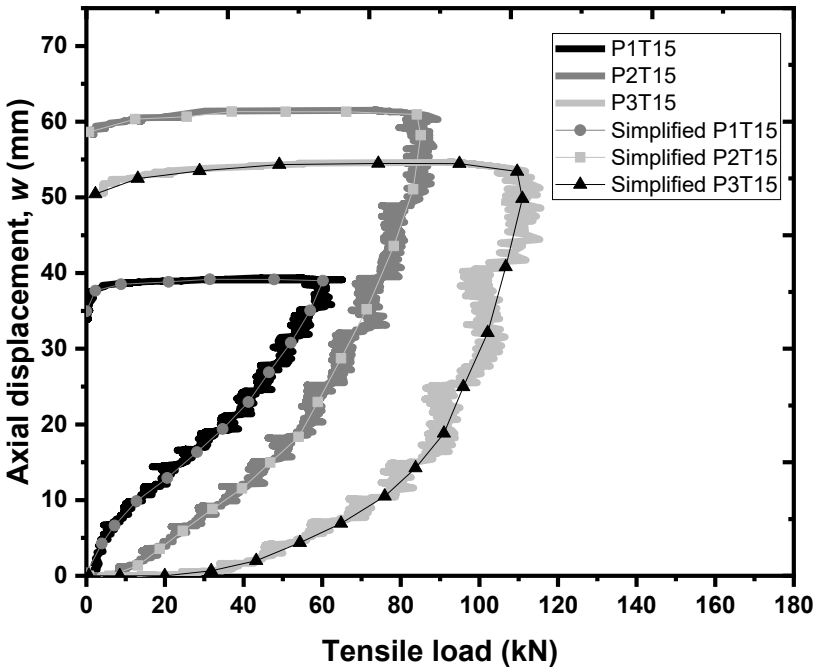

Figure 3-18: Original and Simplified Tensile Load *Q* versus Displacement *w* Curves

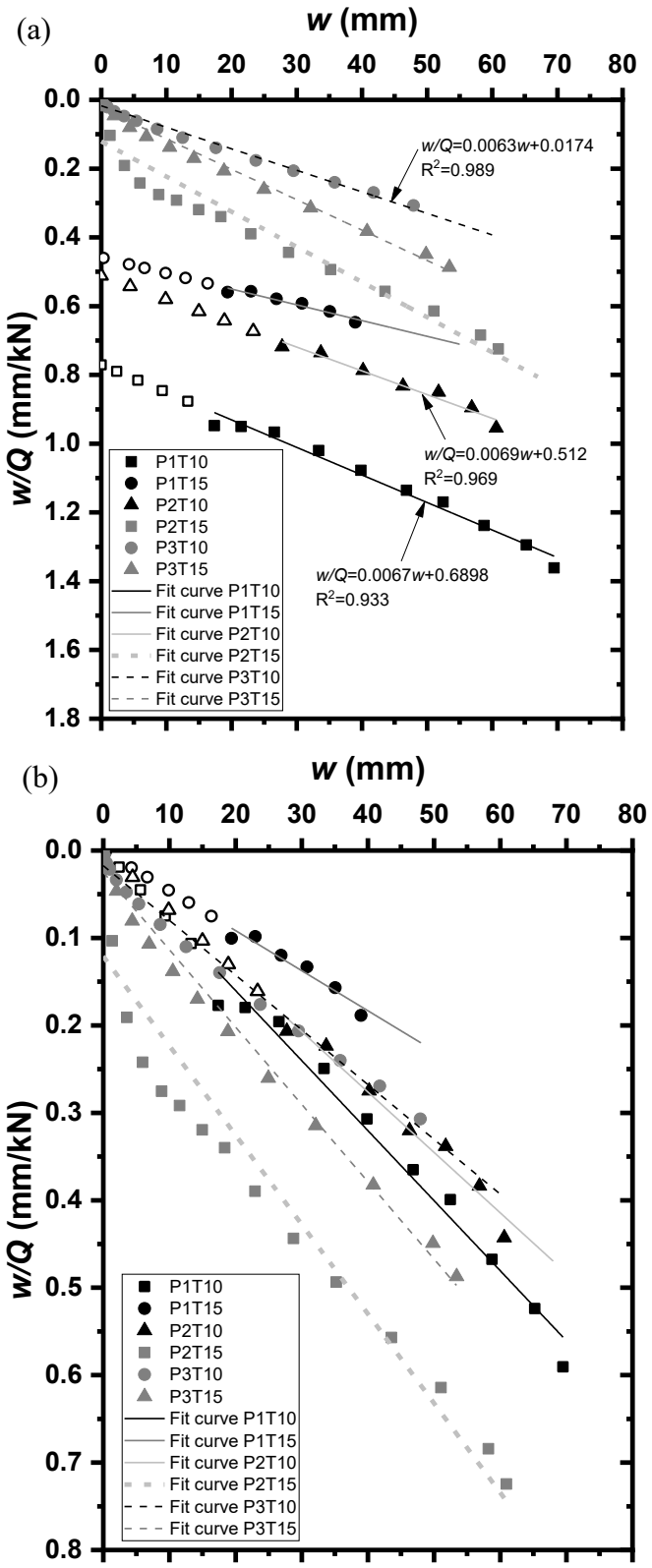

Figure 3-19: (a) Original and (b) Corrected *w/Q* versus *w* Curves of Tensile Test Results at the Loading Stage

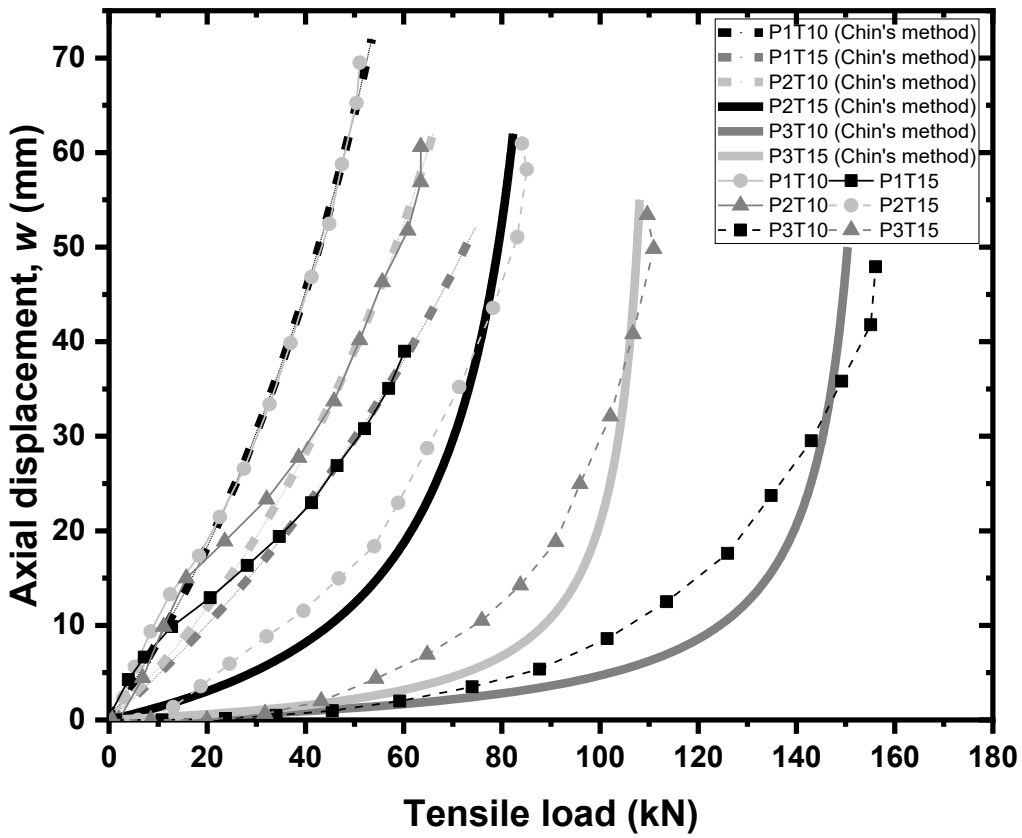

Figure 3-20: Modified Tensile Load Q versus Displacement w Curves with Chin's Hyperbolic Method

Table 3-3: Summary of Test Results

Pile	Pile ID	Test type	Q_u (kN)	Q_L (kN)	C_1	C_2	R^2
P1	P1C10	C	104.5	161.3	0.0062	0.0904	0.992
	P1C15	C	87.2	137	0.0073	0	0.985
	P1T10	T	32	125	0.008	0	0.980
	P1T15	T	50	217.4	0.0046	0	0.940
P2	P2C10	C	104.8	106.4	0.0094	0.0438	0.803
	P2C15	C	81	217.4	0.0046	0	0.930
	P2T10	T	48	144.9	0.0069	0	0.969
	P2T15	T	73	98	0.0102	0.121	0.934
P3	P3C10	C	164.4	140.8	0.0071	0.0047	0.981
	P3C15	C	136.2	147.1	0.0068	0.0245	0.983
	P3T10	T	155	158.7	0.0063	0.0174	0.989
	P3T15	T	104	113.6	0.0088	0.025	0.989

3.5 Back-calculation of q_s, q_b and Q_u

The helical pile capacity is the sum of the bearing capacity of individual helical plates and the skin friction of the shaft. The capacity due to skin friction can be calculated as the sum of friction between soil and pile.

The shaft resistance for deep foundations installed in cohesionless soil suggested by CGS (2006) as:

$$q_s = \beta\sigma'_v = \sigma'_v K_s \tan\delta \quad [3.9]$$

As a driven displacement-type piles, K_s is normally assumed to be twice the value of K_o. The value δ depends on the surface roughness of the pile and ranges from 0.5 to 1.0ϕ. According to the rule of thumb, δ is three-quarter of friction angle ϕ. The ϕ values in the present study were tested in the laboratory with direct shear apparatus, and the ϕ values from peak state and critical state were shown in Table 3-1. The q_s values along the pile shaft were back-calculated using Equation [3.9] and the results were presented in Table 3-4. The q_s values along the pile shaft are essential to estimate the helical pile capacities.

Terzaghi (1943) proposed an equation for analyzing the behaviour of a shallow foundation. Following Terzaghi's work, Meyerhof (1951) conducted a series of investigations on the bearing capacity factors. Meyerhof considered correction factors of eccentricity, load inclination, foundation roughness and depth. The factors N_c, N_q and N_γ in Meyerhof equations are now known as general bearing factors, which depend on the shape of the bearing element and depth. Then, Shape and depth factors were refined by Hansen (1970) and Vesic (1973). Vesic (1973) also had additional factors for the inclination of the bearing element and for the sloping ground surface. With several simplifications presented in Chapter 2, the ultimate bearing pressure for coarse-grain soils is given by

$$q_b = q'(N'_q - 1) \quad [3.10]$$

where q' is the effective overburden stress at the bearing depth in kPa and N'_q is obtained from Figure 2-5.

As described in Chapter 2, the use of Equation [3.10] would cause the calculated ultimate bearing pressure increasing without bound as q' increases steadily with depth. This leads to an overprediction of bearing capacity in many cases. Perko (2009) proposed that the ultimate bearing pressure for helical piles in coarse-grain soils may be computed using traditional bearing capacity theory by replacing the effective overburden stress q' in Equation [3.10] with the product of soil unit weight, γ, and two times the average helix diameter, D_{avg}, as shown in Equation [3.11]:

$$q_b = 2D_{avg}\gamma(N'_q - 1) \quad [3.11]$$

where γ is the unit weight of soil.

Table 3-4: Results of q_s, q_b, N_t, and Calculated Q_u

Pile ID	Field Q_u (kN)	Calculated q_s (kPa)	Calculated q_b (kPa)	Bearing capacity factor N_t	Calculated Q_u (kN)
P1C10	104.5	27.4	952.9	26.2	83.7
P1C15	87.2	24.8	1099.5	17.9	102.4
P1T10	32	27.4	1026.2	29.3	88.5
P1T15	50	24.8	952.9	15.9	91.2
P2C10	104.8	27.4	952.9	24.9	112.4
P2C15	81	24.8	1099.5	18.9	134.5
P2T10	48	27.4	1026.2	31.5	116.8
P2T15	73	24.8	952.9	16.4	119.8
P3C10	164.4	27.4	952.9	25.9	145.0
P3C15	136.2	24.8	1099.5	18	176.3
P3T10	155	27.4	1026.2	27.1	155.2
P3T15	104	24.8	952.9	15.3	157.9

Note: Average critical-state friction angle ϕ from BH #1 and BH#2 at medium D_r was used.

The values of q_b were back-calculated using Equation [3.11] and the results were presented in Table 3-4. To compare the bearing factor from Equation [3.11] with the factors in classic equations, the end bearing factor N_t was calculated with Equation [3.12] as proposed by CGS (2006):

$$N_t = q_b/q' \quad [3.12]$$

where N_t is the bearing capacity factor. The typical range of values for N_t are listed in Table 3-5 and values of N_t depend on soil composition in terms of grain size distribution, natural soil density, and other factors (CGS 2006). The values of N_t were calculated using Equation [3.12] using q_b based on Equation [3.11]. The range of N_t values is between 15.3 and 29.3, which is smaller than the value range 30 to 80 indicated in Table 3-5 by CGS (2006).

The total capacity of the helical pile equals the combination of end-bearing resistance of the soil and the skin friction of the shaft. This is:

$$Q = Q_b + Q_f = q_b A_b + q_s A_s \quad [3.13]$$

The predicted capacities of helical piles are shown in Table 3-4. Most values of predicted Q_u are larger than Q_u tested in field, as shown in Figure 3-21. The regression line shows that Q_u (predicted) = 1.18Q_u (field), which indicates using the indirect method to calculate helical piles' capacities will result in overestimating the values of Q_u. The coefficient of determination R^2 is 0.92 close to 1, which indicate the indirect method in statistical point of view is reliable. In Figure 3-21, the best-fit linear regression was derived from only 12 points, which can be considered as a truly small number. The strength of scatter plot Figure 3-21 is described as weak since the points spread out. The relationship Q_u (predicted) = 1.18Q_u (field) deriving from scatter plot cannot be used in design. There are uncertainties when reaching the range of the plot.

Another observation is that the bearing capacity factor N_t from CGS (2006) will further overestimate the end bearing capacity of helical piles. Hence, values of N_t from CGS (2006) for helical piles in sand should be carefully selected.

Table 3-5: Range of N_t factors (CGS 2006)

Soil Type	Cast-in-Place piles	Driven Piles
Silt	10 – 30	20 – 40
Loose sand	20 – 30	30 – 80
Medium sand	30 – 60	50 – 120
Dense sand	50 – 100	100 – 120
Gravel	80 – 150	150 – 300

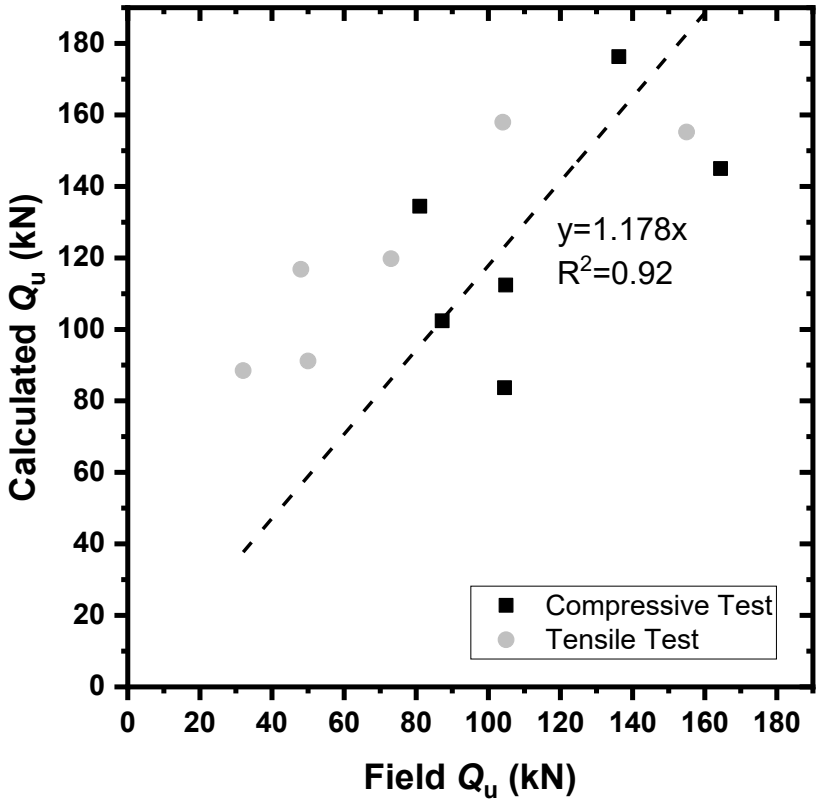

Figure 3-21: Comparison of Q_u Calculated with Indirect Method (Perko 2009, CGS 2006) to Q_u Tested in Field.

3.6 Conclusions

Twelve full-scale load tests of single-helical piles were conducted in field at sandy site, including six axial compressive tests and six tensile tests. Before conducting the load tests, two SPT tests were carried out at test site to investigate soil stratigraphy. The soil at Botanic Garden consists of uniformly-graded sand. The samples were obtained to proceed laboratory testing. The results from load testing were plotted on load-displacement curves and Q_u was defined as 10% of the D according to the industry convention. The following conclusions may be drawn:

1. In the cohesionless soils, the limit state has not been reached at an axial displacement of 10% of D. Q_L of all the test piles are generally greater than Q_u. The compression capacity was greater than the tension capacity for each type of tested pile. The axial capacity is dependent on the pile dimension, soil properties, and loading direction.
2. Chin's method was used to interpret the axial limit capacity $Q_{L,}$ and ultimate capacity Q_u of helical piles installed in sandy soil. The results show that, with the assumption of a hyperbolic backbone, Chin's method offers a valid analytical continuation of the Q-w curves of axially loaded helical piles in sand. Generally, Chin's hyperbolic assumption offers an acceptable approach to predicting the Q-w curves of helical piles with a reasonable accuracy.
3. The values of q_s and q_b were separately calculated by the indirect method proposed by CGS (2006) and Perko's (2009). The indirect method slightly overestimates Q_u following this equation: Q_u (predicted) = 1.18Q_u (field). The result suggests an acceptable agreement between the measured the estimated capacities when Perko's method for end bearing pressure was used. Perko (2009) proposed that the ultimate bearing pressure for helical piles in coarse-grain soils may be computed using traditional bearing capacity theory by

replacing the effective overburden stress q' with the product of soil unit weight, γ, and two times the average helix diameter, D_{avg}. The back-calculated bearing capacity factors N_t of the single-helix pile are significantly less than the range of N_t for piles suggested by CGS (2006). This suggests that the CGS (2006) method for estimating the end bearing pressure will overpredict the bearing pressure of helical piles.

There are some limitations in back-analysis. The best-fit linear regression in Figure 3-21 was derived from only 12 points, which can be considered as a truly small number. The relationship Q_u (predicted) = 1.18Q_u (field) deriving from scatter plot cannot be used in design. There are uncertainties when reaching the range of the plot.

4 SPT-based Method for Estimating Axial Capacities of Single-Helix Piles in Sand

In this chapter, results from the present study, including six axial compressive tests and six tensile tests, and the literature were compiled to construct a helical pile load-test database. The database includes the test results of 47 single-helix piles with various dimensions in sandy soils. From this database, a direct method based on SPT blow count N for estimating the axial capacity of single-helix piles was proposed. The proposed SPT-based method established simple correlations between the average N over the pile shaft length (N_{bar}) and the unit shaft resistance q_s, and between the average N around pile base (N_b) and the unit end bearing resistance q_b. In contrast to Perko's (2009) equation, the shaft resistance was taken into account. This modification is critical for a long pile whose shaft carries a considerable amount of load. In order to check the reliability of the proposed SPT-based method, the values of Q_u were back-calculated with indirect method (Perko 2009, CGS 2006) and direct torque method.

4.1 Introduction

Helical piles are broadly used across Canada in various engineering applications. Estimating the axial capacity is crucial to the helical piling industry. Most of the design methods require site investigation, e.g., SPT and cone penetration tests (CPT). The pile capacity can be predicted using in-situ testing results following two methods: indirect method and direct method. For the indirect method, in-situ investigation and (or) laboratory tests are conducted to evaluate the soil mechanical parameters and then empirical formulas are applied to produce the pile capacity; for the direct method, the pile capacity is directly related to certain in-situ measurements without evaluating any intermediate soil parameters, which enables quicker design and less uncertainties (Zhang and Chen 2012). A common direct torque method estimates the capacity from the

installation torque values using an empirical linear correlation, which may change with soil types and pile dimensions.

Direct methods are more common than indirect methods in small to intermediate-sized projects because laboratory tests of soil mechanical properties are not always available. The SPT-based direct method is one of the direct methods commonly used to predict the capacity of piles, since SPT is widely adopted in geotechnical investigation. The pile shaft friction and end bearing resistance are often empirically correlated with the results of SPT for conventional straight piles. Six direct methods, including Meyerhof (1976), Shioi and Fukui (1982), Decourt (1995), Aoki and Velloso (1975) and Aoki et al. (1978), AIJ (2004) and Shariatmadari et al. (2008) for conventional straight piles associated with N are shown in Table 2-2. These direct methods established simple correlations between the average N_{60} over the pile shaft length (termed N_{bar} herein) and the unit shaft resistance q_s, and between the average N_{60} around pile base (N_b) and the unit end bearing resistance q_b.

The direct methods for conventional straight piles mentioned above may be unsuitable for helical piles, because installation methods have a significant effect on the pile behaviour. Particularly, the reasons for proposing a new direct method instead of using direct methods for conventional straight piles are: 1) the soil below the lowermost helix is far less densified than conventional toe bearing piles during the helical pile installation; 2) when uplift force applies, the upper side helix provides bearing capacity rather than lower side. The industry of helical piles needs a direct method that can estimate the pile capacities in order to effectively select appropriate pile types based on SPT.

Perko (2009) proposed an empirical correlation for estimating the unit end bearing resistance q_b of helical piles. The correlation was derived from 54 load tests of helical piles. The estimation of q_b is as follows:

$$q_b\,(\text{kPa}) = n_b N_b \qquad [4.1]$$

where n_b is 63.8 and N_b is the average N_{60} around pile base.

Notably, Perko did not distinguish the end bearing and shaft friction; Perko attempted to correlate the bulk pile capacities with the SPT blow counts. The problem with this method is that it will mask the mechanisms of bearing and shaft friction, which is not suitable for piles with varying lengths. A number of studies indicate that the shaft resistance contributes a significant share (up to 30%) to the total axial capacity, e.g., Elsherbiny and El Naggar (2013), Li et al. (2018), and Lanyi-Bennett and Deng (2019). In cases where long piles are adopted, Perko's correlation will tend to underestimate the pile capacities. In addition, the essence of SPT is more of a soil-pile shearing behaviour rather than an end bearing behaviour. Estimation of skin friction of piles based on SPT interpretation may be more reliable than end bearing resistance. For these reasons, it is important to separate the skin friction from the end bearing resistance in the analysis. Therefore, Perko's (2009) correlation may need to be modified with an evaluation of shaft resistance and improved with the expanded database. Separation of the end bearing resistance from the shaft resistance may be a difficult task because a majority of pile tests available in the literature did not measure either component. However, back-analysis of helical bearing resistance and shaft friction may be performed using existing methods based on available soil properties in the adopted literature.

4.2 Database Collection

In this study, 12 axial load tests of single-helix piles were conducted in a sandy soil site. The present test results and available results from the literature were compiled to construct a load-test database of helical piles. The corrected N values (N_{60}) derived from the site investigation were correlated with the measured axial capacities via a calibrated equation.

Because the results in the present research and published literature did not differentiate the shaft friction and end bearing, it is necessary to estimate the values of these two terms so that the SPT-based direct method can be properly developed for both shaft friction and end bearing. The database includes the test results of 47 single-helix piles with various dimensions in sandy soils, as shown in Table 4-1. Except for 12 pile tests in the present testing program described in the prior chapter, 35 full-scale pile load tests of single-helix piles from Perko (2009), Elshebiny and El Naggar (2013), Fahmy and El Naggar (2017), and Li and Deng (2019) were compiled into the database. These 35 full-scale tests of single-helix piles were selected because they are tested in sand and SPT N values and other soil properties are available from site investigation.

Table 4-1: Database of Single-helix Piles Tested in Sand.

Reference	Q_u (kN)	Shaft Diameter, d (mm)	Helix Diameter, D (mm)	Helix embedment (m)	N_b	N_{bar}	Soil type
Present study at Alberta	104.5	73	305	2.56	13	18	SP
	87.2	73	305	4.21	15	16.3	
	32	73	305	2.47	14	18	
	50	73	305	4.11	13	16.3	
	104.8	89	356	2.68	13	18	
	81	89	356	4.01	15	16.3	
	48	89	356	2.31	14	18	
	73	89	356	3.99	13	16.3	

	164.4	114	406	2.58	13	18	
	136.2	114	406	4.19	15	16.3	
	155	114	406	2.65	14	18	
	104	114	406	4.26	13	16.3	
Elsherbiny and El Naggar (2013) at Northern Alberta	210	273	610	5.2	21	19.3	Sand
	210	219	508	5.3	21	19.3	
Fahmy and El Naggar (2017)	435	200	390	2.55	17	23.3	Medium sand with silt
	375	200	390	2.55	17	23.3	
Perko (2009) Tensile tests at various sites	293.6	76	305	4.88	42	42	SP/GP
	290.0	76	305	5.49	48	48	SP/GP
	280.2	76	305	5.18	45	45	SP/GP
	131.2	73	203	5.49	48	48	SP/GP
	173.5	73	203	3.96	34	34	SP/GP
	322.5	73	356	3.35	27	27	SP/GP
	48.9	89	203	3.05	4	4	SP
	271.3	89	356	6.1	34	34	GP
	19.1	73	203	2.74	4	4	SP
	40.0	73	203	3.05	4	4	SP
	106.8	73	356	4.57	9	9	SP
Perko (2009) Compressive tests at various sites	102.3	73	203	3.05	24	24	SP/GP
	169.0	73	203	4.27	37	37	SP/GP
	66.7	73	356	3.05	24	24	SP/GP
	231.3	73	356	3.66	31	31	SP/GP
	62.3	89	203	3.66	7	7	SP
Reaction Piling, Alberta	258.0	114	406	7.01	20	28.3	In sandy layer
	187.5	114	457	4.15	16	12.5	Sand (some silt)
	158.8	114	406	4.72	12	9.3	In sandy layer (sand: 78.7%)
Li and Deng (2019) at Alberta	104	73	305	1.83	13	13.1	Sand, some gravel, loose
	96	73	305	1.83	13	13.1	
	79	73	305	1.83	13	13.1	
	73	73	305	1.83	13	13.1	
	126	89	356	2.44	6.5	10.9	
	134	89	356	2.44	6.5	10.9	
	108	89	356	2.44	13	10.9	

93	89	356	2.44	13	10.9
128	114	406	3.96	9	9.6
114	114	406	3.96	9	9.6
178	114	406	3.96	6	9.6
164	114	406	3.96	6	9.6

Note: N_b = the average N around pile base, and N_{bar} = the average N over the pile shaft length. Corrected N_{60} values are used in the calculation unless specified.

Salgado (2008) suggested the N_b obtained from 1B above to 1.5B below the base of conventional straight piles, where B is the pile diameter. For helical piles in Table 4-1, the values of N_b were obtained 1D above to 1.5D below the helix.

4.3 Capacity of Single-Helix Piles in Sand

The ultimate capacity of the single-helix pile equals the summation of helical plate bearing resistance and the shaft friction as described in Equation [4.2]:

$$Q_u = Q_b + Q_f = q_b A_b + q_s A_s \quad [4.2]$$

The frictional resistance of the helical pile is estimated using Equation [4.3]:

$$Q_f = \pi d H_{eff} q_s \quad [4.3]$$

where d is the shaft diameter and $H_{eff} = L\text{-}D$ is the effective shaft length according to Narasimha Rao et al. (1993) and Zhang (1999).

Santos et al. (2013) indicated that CPT sleeve friction f_s was affected by the installation of helical pile in particular tropical clay. Santos et al. (2013) stated that the shear resistance above the helical plates decreased after helical pile installation and emphasized this finding should be considered for the prediction of helical pile capacity. Furthermore, Komatsu (2007) performed model tests on a small-scale helical pile in sand and founded after the installation of single-helix pile, the sand above the helix was loosened and rose upwards. Ghaly et al. (1991) conducted 56 small-scale helical pile tests in a U-masonry tank in dense, medium, and loose dry sand

respectively. The suggested, due to the soil disturbance caused by helical pile installation, the δ/ϕ ratios (δ is the friction angle of disturbed soil) were greatly affected. The ratio δ/ϕ is equal to 1 in loose sand (ϕ=30°), 0.8 in medium sand (ϕ=35°), and 0.65 in dense sand (ϕ=40°). Therefore, a modification factor α is herein applied to the correlation between q_s and N_{bar} with regard to different soil behaviour types as shown in Equation [4.4]:

$$\alpha=\begin{cases} 1 & \text{for loose sand} \\ \dfrac{\tan(0.8\phi)}{\tan\phi}=0.76 & \text{for medium sand} \\ \dfrac{\tan(0.65\phi)}{\tan\phi}=0.58 & \text{for dense sand} \end{cases} \quad [4.4]$$

Then, the modified correlation between q_s and N_{bar} can be written as:

$$q_s = \alpha(2N_{bar}) \quad [4.5]$$

where the coefficient of 2 was obtained from SPT-based direct methods to predict q_s of piles proposed by Meyerhof (1976), Shioi and Fukui (1982) and AIJ (2014) in Table 2-2. In Equation [4.5], it is assumed that the shaft friction of helical piles is similar to the friction of conventional straight piles. In addition, due to the soil disturbance caused by helical pile installation, a modification factor α is herein introduced to the correlation in Equation [4.5]. The values of α were calculated from Equation [4.4]. The motivation of applying modification factor was from Fakharian and Vafaei (2020). They found the sand–pile skin friction reducing with initial relative density increment from medium to dense and highly suggested that skin friction of piles requires modifications for dense sand conditions.

In Equation [4.4], the sand was classified as loose, medium, and dense sand. The relationship between sand types and N from Meyerhof (1956) was used: N from 4 to 10 stands for loose sand, 10 to 30 stands for medium sand and 30 to 50 stands for dense sand. The shaft frictional

resistance of all piles from the adopted references was thus calculated using Equations [4.4] and [4.5].

The shaft friction Q_s was then subtracted from Q_u to produce q_b. The unit end bearing capacities of the selected pile tests were plotted in Figure 4-1 against N_b. A best-fit linear regression suggested the following equation:

$$q_b = 73.3N_b \quad [4.6]$$

where the 95% prediction band is a band that contains 95% of future observable realizations if to repeat experiment many times.

Combining Equations [4.5] and [4.6], the equation of Q_u for single-helix pile in sand is suggested as:

$$Q_u = Q_b + Q_f = q_b A_b + q_s A_s = 73.3N_b A_b + 2\alpha N_{bar} A_s \quad [4.7]$$

Equation [4.6] offers a larger n_b value (73.3) than Perko's (63.8) and allows the consideration of shaft resistance. This modification is especially important for the design of relatively long helical piles. The installation effect in different soil behaviour type conditions is also handled by selecting α properly for a given soil type.

To verify the reliability of the SPT-based Equation [4.7], the values of q_s, q_b, Q_u, Q_b and Q_f of 47 piles in database are calculated in order to compare with other direct method and indirect methods presented in Chapter 2. The results of q_s, q_b, Q_u, Q_b and Q_f using Equation [4.7] are listed in Table 4-2 for further comparison.

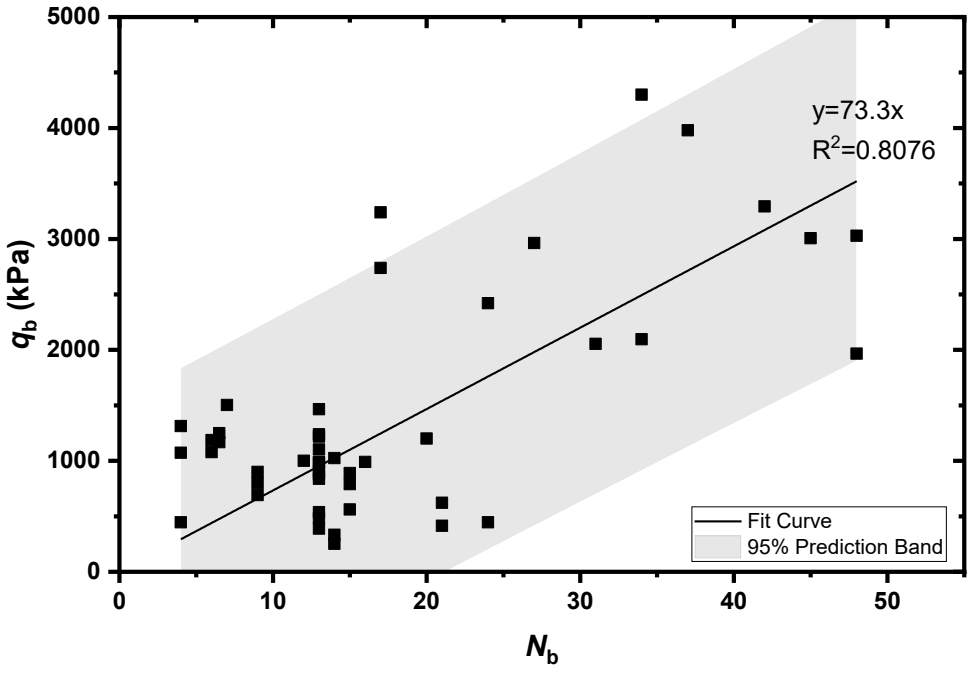

Figure 4-1: Correlation Between q_b and N_b.

Table 4-2: Results of q_s, q_b, Q_u, Q_b and Q_f using the Proposed SPT-based Method

Reference	ID	Field Q_u (kN)	Predicted Q_u (kN)	Predicted Q_f (kN)	Predicted Q_b (kN)	Predicted q_s (kPa)	Predicted q_b (kPa)
Present study	1	104.5	83.7	14.1	69.5	27.4	952.9
	2	87.2	102.4	22.2	80.2	24.8	1099.5
	3	32	88.4	13.6	74.9	27.4	1026.2
	4	50	91.2	21.7	69.5	24.8	952.9
	5	104.8	112.4	17.8	94.6	27.4	952.9
	6	81	134.5	25.3	109.2	24.8	1099.5
	7	48	116.8	14.9	101.9	27.4	1026.2
	8	73	119.8	25.2	94.6	24.8	952.9
	9	164.4	145.0	21.4	123.6	27.4	952.9
	10	136.2	176.3	33.7	142.6	24.8	1099.5
	11	155	155.2	22.0	133.1	27.4	1026.2
	12	104	158.0	34.4	123.6	24.8	952.9
Elsherbiny and El Naggar (2013)	13	210	565.0	115.2	449.9	29.3	1539.3
	14	210	408.5	96.5	312.0	29.3	1539.3
Fahmy and El Naggar (2017)	15	435	196.8	48.0	148.9	35.3	1246.1
	16	375	196.8	48.0	148.9	35.3	1246.1
Perko (2009)	17	293.6	278.0	53.3	224.6	48.7	3078.6

Tensile tests	18	290	325.8	69.1	256.7	55.7	3518.4
	19	280.2	301.6	60.9	240.7	52.2	3298.5
	20	131.2	181.6	67.5	114.1	55.7	3518.4
	21	173.5	114.8	34.0	80.8	39.4	2492.2
	22	322.5	224.8	28.2	196.6	41.0	1979.1
	23	48.9	15.9	6.4	9.5	8.0	293.2
	24	271.3	310.7	63.2	247.5	39.4	2492.2
	25	19.1	14.2	4.7	9.5	8.0	293.2
	26	40	14.7	5.2	9.5	8.0	293.2
	27	106.8	83.0	17.4	65.5	18.0	659.7
Perko (2009) Compressive tests	28	102.3	80.9	23.8	57.0	36.5	1759.2
	29	169	128.0	40.0	88.0	42.9	2712.1
	30	66.7	197.2	22.5	174.7	36.5	1759.2
	31	231.3	252.9	27.2	225.7	36.0	2272.3
	32	62.3	30.1	13.5	16.6	14.0	513.1
Reaction Piling, Alberta	33	258	292.3	102.1	190.2	43.1	1466
	34	187.5	217.6	25.2	192.4	19.0	1172.8
	35	158.8	143.0	28.9	114.1	18.7	879.6
Li and Deng (2019)	36	104	76.6	7.0	69.6	20.0	952.9
	37	96	76.6	7.0	69.6	20.0	952.9
	38	79	76.6	7.0	69.6	20.0	952.9
	39	73	76.6	7.0	69.6	20.0	952.9
	40	126	57.1	9.7	47.4	16.6	476.45
	41	134	57.1	9.7	47.4	16.6	476.45
	42	108	104.5	9.7	94.8	16.6	952.9
	43	93	104.5	9.7	94.8	16.6	952.9
	44	128	109.8	24.4	85.4	19.2	659.7
	45	114	109.8	24.4	85.4	19.2	659.7
	46	178	81.4	24.4	56.9	19.2	439.8
	47	164	81.4	24.4	56.9	19.2	439.8

4.4 Back-Analysis with Indirect Methods

4.4.1 Q_b with Modified Terzaghi Method

As mentioned in Chapter 3, the ultimate bearing pressure for coarse-grain soils is given by

$$q_b = q'(N'_q - 1) \quad [4.7]$$

The accuracy of Equations [4.7] and [4.1] was examined by comparing the estimated end bearing capacities Q_b of 47 pile load tests based on SPT N_b with the indirect modified Terzaghi method based on bearing factor N'_q and effective overburden stress q'. The results of the comparison are shown in Figure 4-2. On average, the value of Q_b using the modified Terzaghi method is 8.49 times the SPT-based predicted Q_b. According to Perko (2009), Equation [4.7] leads to an overprediction of bearing capacity in many situations, since the predicted ultimate bearing pressure increases without bound as q' increases steadily with depth. This statement was verified here in Figure 4-2.

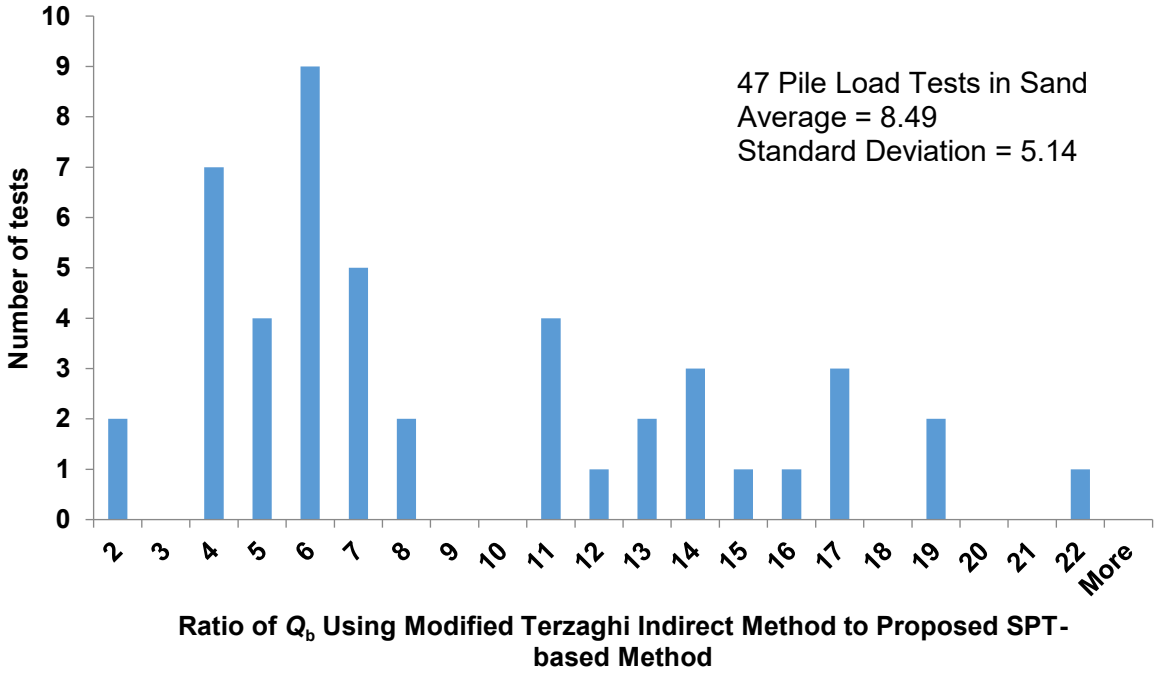

Figure 4-2: Ratio of Q_b Estimated from the Modified Terzaghi Indirect Method and the Proposed SPT-based Method.

4.4.2 Q_b with Perko's indirect method

Perko (2009) proposed that the ultimate bearing pressure for helical piles in coarse-grain soils:

$$q_b = 2D_{avg}\gamma(N'_q - 1) \qquad [4.8]$$

The accuracy of using Equations [4.8] and [4.1] was examined by comparing predicted unit end bearing resistance Q_b of 47 pile load tests based on SPT N_b with the indirect Perko's method based on bearing factor N'_q, helix diameter D and unit weight of soil γ. The results of the comparison are shown in Figure 4-3. On average, the value of Q_b calculated from Perko's method is 1.54 times the SPT-based predicted Q_b, and the standard deviation of data is 0.81, indicating reasonably good correlation.

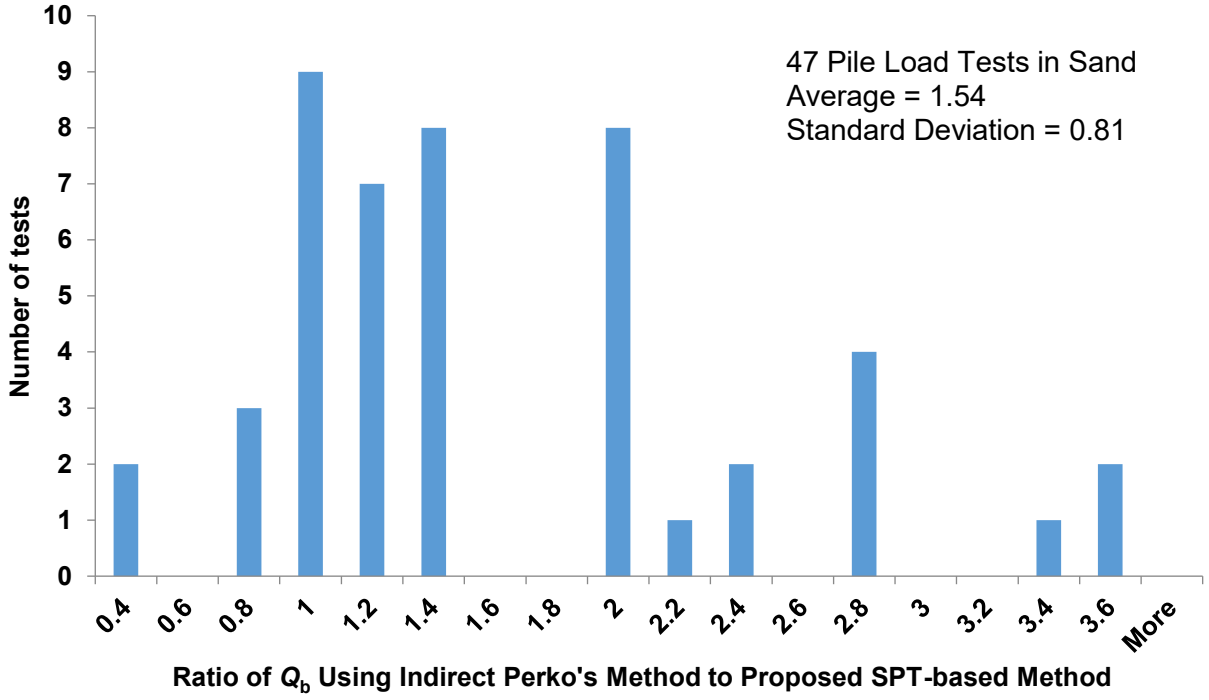

Figure 4-3: Comparison of Q_b Estimated from the Indirect Perko's Method and the Proposed SPT-based Method.

4.4.3 Q_s with β method

CGS (2006) suggested a β method to estimate shaft resistance for deep foundations installed in cohesionless soil at any depth z. This is:

$$q_s = \beta\sigma'_v = \sigma'_v K_s \tan\delta \qquad [4.9]$$

For helical piles, K_s is normally assumed to be twice the value of K_o and δ is three quarter of friction angle ϕ. The accuracy of using Equations [4.9] and [4.5] was examined by comparing predicted the unit shaft resistance Q_s of 47 pile load tests based on SPT N_{bar} with the indirect β method. The results of the comparison are shown in Figure 4-4. On average, the Q_s calculating using indirect β method is 0.52 times the SPT-based predicted Q_s, and the standard deviation of data is 0.27.

Per subsection 4.4.2 and 4.4.3, Q_u using indirect method can be calculated as summation of Q_b with Perko's indirect method and Q_s with β method.

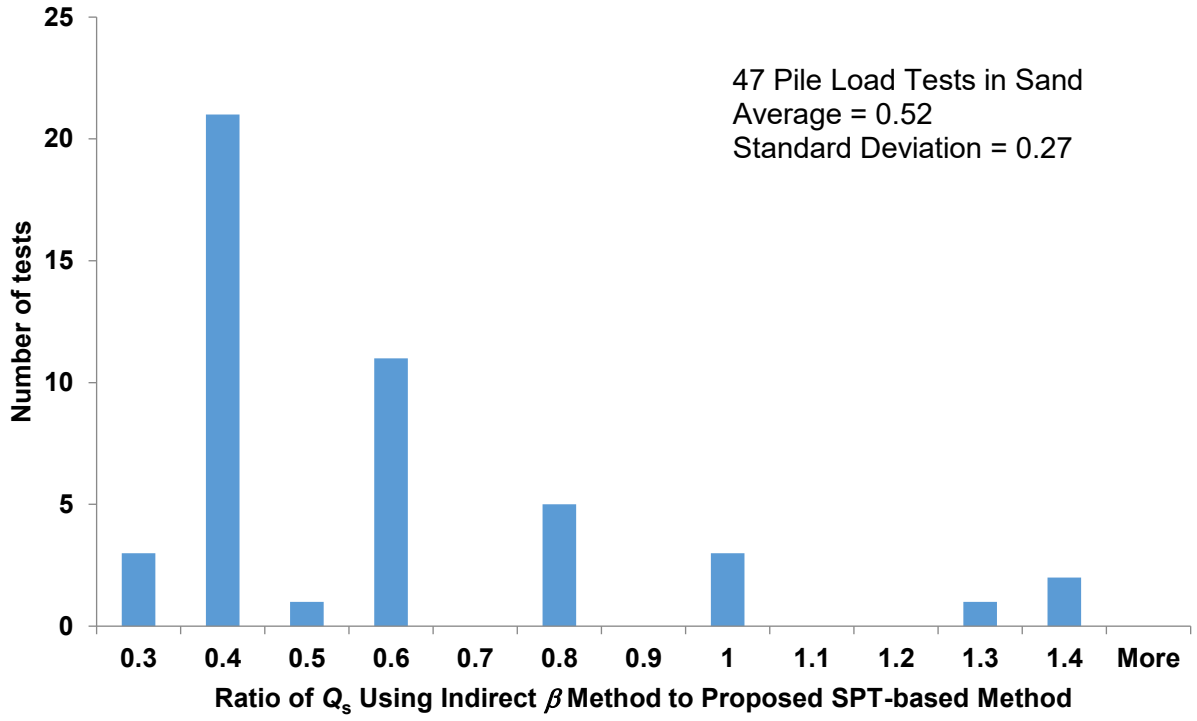

Figure 4-4: Comparison of Q_s Estimated from the Indirect β Method and the Proposed SPT-based Method.

4.5 Back-Analysis Q_u with Torque Method

During the installation, final installation torque was recorded for each testing pile. The ultimate pile capacity is defined as:

$$Q_u = K_T T \quad [4.10]$$

Torque factors K_T were predicted from the literature, for example, 33 m^{-1} for single-helix pile of d = 73 mm, 25 m^{-1} for d = 89 mm and 20 m^{-1} for d = 114 mm (Li and Deng 2019). Li and Deng (2019) found a simple tendency that K_T decreases when d increases as shown in Figure 4-5. From Figure 4-5, the K_T of each pile in database can be determined, and Q_u can be calculated following Equation [4.10].

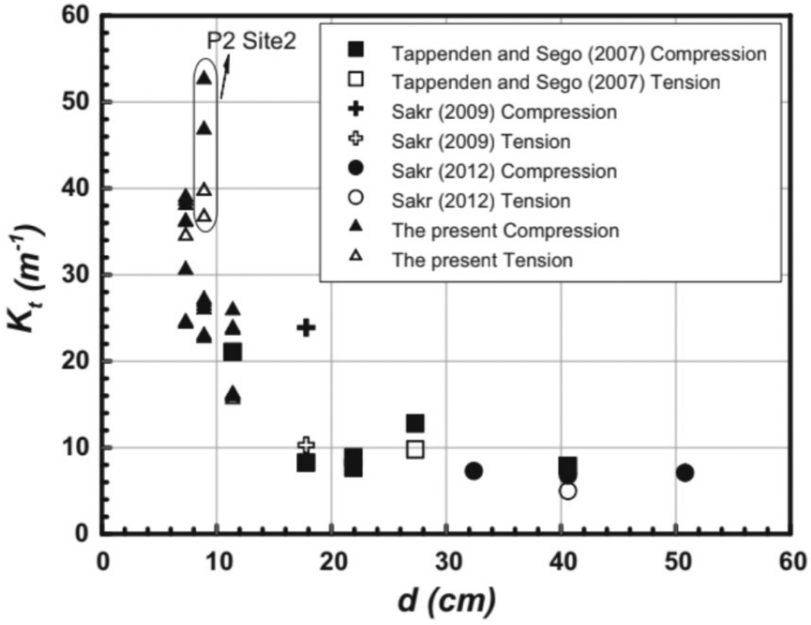

Figure 4-5: Summary of Torque Factors of Single-helix Piles (Li and Deng 2019)

4.6 Comparison of Different Methods

The value of Q_u was calculated using three different methods, including the proposed SPT-based method, indirect method, and direct torque method. Plot the values of Q_u from field tests versus

the value of Q_u calculated from the other three methods in Figure 4-6. The regression fitting lines and the coefficients of determination R^2 for each method versus field testing results:

SPT-based method (present proposal): y = 0.94 x; R^2 = 0.79

Indirect method (Perko 2009, CGS 2006): y = 1.23 x; R^2 = 0.75

Torque method (Hoyt and Clemence 1989, Li and Deng 2019): y = 1.24 x; R^2 = 0.76

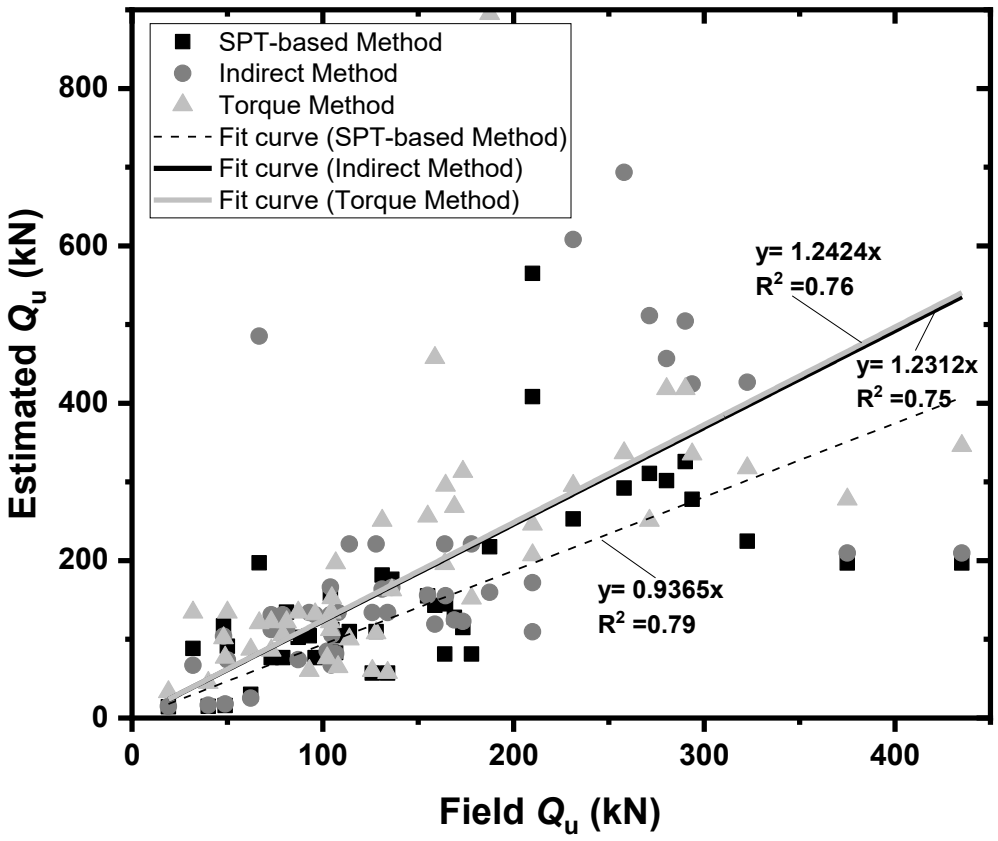

Figure 4-6: Comparison of Q_u from Different Methods.

The regression lines of Q_u estimated with indirect method (Perko 2009, CGS 2006) and direct torque method is pretty close in slope and R^2. These two methods overestimated the capacity of single-helix piles as 1.2 times of tested capacity in the field on average. For SPT-based method

proposed in this thesis, the slope of regression line is 0.94, which is close to 1 with a little bit underestimation, can indicate the new proposed method is reliable.

4.7 Conclusions

A direct method based on SPT blow count for estimating the axial capacity of single-helix piles was proposed. The equation was calibrated using a database implemented with 35 field load tests available in the literature and 12 field load tests accomplished in the present research. The following conclusions may be drawn.

- The axial capacity of a single-helix pile in sand may be estimated with the following equation: $Q_u = Q_b + Q_f = 73.3 N_b A_b + 2\alpha N_{bar} A_s$, where N_b is the average N around pile base, and N_{bar} is the average N over the pile shaft length. In contrast to Perko's (2009) equation, the shaft resistance is taken into account. This modification is critical for a long pile whose shaft carries a considerable amount of load. In addition, the installation-induced soil disturbance is properly handled with the factor α.
- In order to check the reliability of the proposed SPT-based method, back-analysis with indirect methods proposed by Perko and CGS (2006) and direct torque method were conducted in this chapter. From the best-fit of linear regression, the slope of regression line for the proposed SPT-based method is 0.94 and R^2 is 0.79, which indicated that the proposed SPT-based method is reliable, but slightly underestimated Q_u. Furthermore, the indirect method and direct torque method overestimated single-helix pile capacity by 1.2 times the capacity tested in the field.

5 Conclusions, Limitations, and Recommendations

Helical piles have been used for a wide range of applications, such as solar farm, power transmission tower, and buildings in North America. Estimating the axial capacity is crucial to the helical piling industry. Direct methods are more common than indirect methods in small to intermediate-sized projects. SPT-based direct method is one of the direct methods commonly used to predict the capacity of piles, since SPT is a popular and economical mean in subsurface exploration. The pile shaft friction and end bearing resistance are empirically correlated with the results of SPT for conventional driven and cast-in-place piles, based on case histories of piles with varying sizes. Motivated by the methods of conventional piles, the industry of helical piles also needs a direct method that can estimate the helical pile capacities with the results of SPT to effectively select appropriate pile types.

Full-scale axial load tests were conducted on twelve steel single-helix piles at a cohesionless soil site located at the University of Alberta Botanic Garden. Comprehensive site investigation and laboratory tests were carried out to obtain the soil stratigraphy. The soil stratigraphy at Botanic Garden is relatively homogenous and consists of uniformly-graded sand. Results from the present tests and the literature were compiled to construct a helical pile load-test database. From this database, a direct method based on SPT blow count N for estimating the axial capacity of single-helix piles is proposed. To check the reliability of the proposed SPT-based method, the values of Q_u were back-calculated with existing methods.

5.1 Conclusions

Following conclusions may be drawn.

1. The present studies presented a series of field axial loading tests of single-helix piles in sand. The soil stratigraphy was characterized by in-situ SPT and laboratory soil testing.

The test results were then used to develop a database of axial loading tests of single-helix piles in sand.

2. A direct method based on SPT for estimating the axial capacity of single-helix piles is proposed. The equation was calibrated using a database implemented with 35 field load tests available in the literature and 12 field load tests accomplished in the present research.
3. The axial capacity of a single-helix pile in sand may be estimated with the following equation:

   $Q_u = Q_b + Q_f = 73.3 N_b A_b + 2\alpha N_{bar} A_s$.

   where N_b is the average N around pile base, N_{bar} is the average N over the pile shaft length, A_b is total projected area of helical bearing plate, A_s is area of soil-shaft interface, and α is a modification factor due to soil disturbance.

   In contrast to Perko's (2009) equation, the shaft resistance is taken into account. This modification is critical for a long pile whose shaft carries a considerable amount of load. In addition, the installation-induced soil disturbance is properly handled with the factor α.
4. In order to check the reliability of the proposed SPT-based method, back-analysis with indirect method proposed by Perko and CGS, and direct torque method were conducted. These two methods overestimated the capacity of single-helix piles as 1.2 times of tested capacity in the field on average. For SPT-based method proposed, the slope of regression line is 0.94, which is close to 1 with a little bit underestimation, can indicate the new proposed method is reliable.

5.2 Limitations and Recommendations

Owing to the limited scope of test results available in the literature, the present study contains several limitations as follows:

- The proposed SPT-based method is only valid in sand.
- The proposed SPT-based method is only valid for single-helix piles that fail in the IPB mode; hence cautions should be taken if it is used in multi-helix piles. For multi-helix piles, the S/D ratio, where S is the spacing between helical plates and D is the diameter of the helical plates, and the soil stress history are expected to affect the failure modes of piles in sand.
- The proposed SPT-based method only considered the best-fit from a linear regression. The compiled load-test database only includes 47 helical piles, which can be considered a slightly small number. Perko (2009) also used the best-fit from a linear regression to draw a conclusion, and his database contained 54 helical pile results in sand. Expanding the database will definitely increase the reliability of the proposed methods.
- Because a majority of pile tests available did not directly measure either component, the end bearing resistance was separated from the shaft resistance when analyzing the pile test database. However, the methods of separation, which were largely based on existing methods, may be not sufficiently accurate. The shaft resistance was obtained from SPT-based direct methods for conventional straight piles from other publications, which assumed that shaft friction of helical piles is similar to the friction of conventional straight piles; then, a modification factor α was applied in equation of estimating q_s due to soil disturbance. The shaft friction Q_s was then subtracted from Q_u to produce unit end bearing resistance q_b.

Considering the limitation of present research, further recommendations are presented as follows:

- The development of a SPT-based direct method for estimating the capacities of helical piles in cohesive soil is suggested for further research.

- In practice, multi-helix piles are commonly used; thus, the SPT-based method needs to consider CS mode and extend it to multi-helix piles.
- In order to increase the reliability of linear fitting, the load-test database needs to be expanded.
- In order to separate the end resistance and the shaft resistance, results from axial loading tests of instrumented test piles would be warranted.

References

Architectural Institute of Japan (AIJ). 2004. Recommendations for Design of Building Foundation. Architectural Institute of Japan: Tokyo, Japan.

American Society for Testing and Materials (ASTM). 2008a. ASTM D1586 Standard Test Method for Standard Penetration Test (SPT) and Split-Barrel Sampling of Soils. Annual Book of Standards. West Conshohocken, PA.

American Society for Testing and Materials (ASTM). 2008b. ASTM D4318 Standard Test Methods for Liquid Limit, Plastic Limit, and Plasticity Index of Soils. Annual Book of Standards. West Conshohocken, PA.

American Society for Testing and Materials (ASTM). 2008c. ASTM D6913 Standard Test Method for Particle-Size Distribution (Gradation) of Soils Using Sieve Analysis. Annual Book of ASTM Standards. American Society for Testing and Materials, West Conshohocken, PA.

American Society for Testing and Materials (ASTM). 2010. ASTM D854 Standard Test Methods for Specific Gravity of Soil Solids by Water Pycnometer. Annual Book of ASTM Standards. American Society for Testing and Materials, West Conshohocken, PA.

American Society for Testing and Materials (ASTM). 2012. ASTM D3080 Standard test method for Direct Shear Test of Soil Under Consolidated Drained Conditions. Annual Book of ASTM Standards. American Society for Testing and Materials, West Conshohocken, PA.

American Society for Testing and Materials (ASTM). 2013a. ASTM D1143/D1143M Standard test methods for deep foundations under static axial compressive loads. Annual Book of ASTM Standards. American Society for Testing and Materials, West Conshohocken, PA.

American Society for Testing and Materials (ASTM). 2013b. ASTM D3689/D3689M Standard test methods for deep foundations under static axial tensile loads. Annual Book of ASTM Standards. American Society for Testing and Materials, West Conshohocken, PA.

American Society for Testing and Materials (ASTM). 2016. ASTM D4254 Standard test methods for minimum index density and unit weight of soils and calculation of relative density. Annual Book of ASTM Standards. American Society for Testing and Materials, West Conshohocken, PA.

American Society for Testing and Materials (ASTM). 2019. ASTM Standard D2216-19 Standard Test Methods for Laboratory Determination of Water (Moisture) Content of Soil and Rock by Mass. Annual Book of ASTM Standards. American Society for Testing and Materials, West Conshohocken, PA.

Aoki, N., and Velloso, D. A. 1975. An approximate method to estimate the bearing capacity of piles. Procs. Proc. 5th Pan-American Conference of Soil Mechanics and Foundation Engineering, Buenos Aires, Vol. 1, pp. 367–376.

Aoki, N., Velloso, D. A., and Salamoni, J.A. 1978. Fundações para o Silo Vertical de 100000 t no Porto de Paranaguá. 6th Brazilian Conference of Soil Mechanics and Foundation Engineering, Vol. 3, pp. 125-132.

Bowles, J. E. 1988. Foundation Analysis and Design. 4th ed. New York: McGraw-Hill.

Canadian Geotechnical Society (CGS). 2006. Canadian Foundation Engineering Manual. 4th ed. BiTech Publisher Ltd., Canada.

Chin, F. K. 1970. Estimation of the ultimate load of piles not carried to failure. In: Proceedings of the 2nd Southeast Asian conference on soil engineering, Singapore, 11–15 June 1970, pp. 81–90.

Cubrinovski, M. and Ishihara, K. 1999. Empirical correlation between SPT N-value and relative density for sandy soils. Soils and Foundations, 39(5), pp. 61–71.

Davisson, M. T. 1972. High-capacity piles. Proc. Lecture Series on Innovations in Foundation Construction, ASCE, University of California, Berkeley, CA.

Decourt, L. 1995. Prediction of load-settlement relationships for foundations on the basis of the SPT. Ciclo de Conferencias Internationale, Leonardo Zeevaert, UNAM, Mexico, pp. 85-104.

Elsherbiny, Z. and El Naggar, M. H. 2013. Axial compressive capacity of helical piles from field tests and numerical study. Canadian Geotechnical Journal, 50(12): 1191–1203.

Fahmy, A. and El Naggar, M. H. 2017. Axial performance of helical tapered piles in sand, Geotechnical and Geological Engineering, 35: 1549-1576.

Fakharian, K. and Vafaei, N. 2020. Effect of density on skin friction response of piles embedded in sand by simple shear interface tests. Canadian Geotechnical Journal, 58(5), 619-636.

Ghaly, A. M. and Hanna, A. M. 1991. Experimental and Theoretical Studies on Installation Torque of Screw Anchors, Canadian Geotechnical Journal, 28, No. 3, pp. 353–364.

Ghaly, A., Hanna, A., and Hanna, M. 1991. Uplift behavior of screw anchors in sand. I: dry sand. Journal of Geotechnical Engineering, 117(5), pp. 773-793.

Godfrey, J. D. 1993. Edmonton beneath our feet: a guide to the geology of the Edmonton region, Edmonton Geological Society, Edmonton, AB.

Hansen, J. B. 1963. Discussion on hyperbolic stress-strain response: cohesive soils, American Society of Civil Engineers, Journal for Soil Mechanics and Foundation Engineering, 89, (SM4), pp. 241–242.

Hansen, J. B. 1970. A revised and extended formula for bearing capacity. Danish Geotechnical Institute, Bull No 28, pp. 5-11.

Hoyt, R. M., and Clemence, S. P. 1989. Uplift capacity of helical anchors in soil. Proceedings of the 12th International Conference on Soil Mechanics and Foundation Engineering, Rio de Janeiro, Brazil, 2: 1019-1022.

Komatsu, A. 2007. Development on battered pile with screw pile method (NS-ECO pile). In Proceedings of the International Workshop on Recent Advances of Deep Foundations (IWDPF07), Yokosuka, Japan. Edited by Yoshiaki Kikuchi. Taylor & Francis. pp. 253–257.

Lanyi-Bennett, S.A. and Deng, L. 2018. Axial load testing of helical pile groups in glaciolacustrine clay. Canadian Geotechnical Journal, 56: 187–197.

Lutenegger, A.J. 2003. Helical screw piles and screw anchors—an historical prospective and introduction. In Proceedings of the Helical Foundations and Tie-Backs Seminar, Deep Foundation Institute, Cincinnati, OH.

Li, W. and Deng, L. 2019. Axial load tests and numerical modeling of single-helix piles in cohesive and cohesionless soils, Acta Geotechnica, 14: 461-475.

Li, W., Zhang, D., Sego, D.C. and Deng, L. 2018. Field testing of axial performance of large-diameter helical piles at two soil sites. ASCE Journal of Geotech Geoenvironmental Engineering, 144(3): 06017021-1-06017021-5.

Liao, S. and Whitman, R. V. 1986. Overburden correction factors for SPT in sand. ASCE Journal of Geotech Geoenvironmental Engineering, 112(3), pp. 373–377.

Mayne, P.W., Christopher, B.R. and DeJong, J. 2001. Manual on subsurface investigation. National Highway Institute Publication, No. FHWA NHI-01-031, Federal Highway Administration, Washington, DC.

Meyerhof, G.G. 1951. The Ultimate bearing capacity of foundations. Geotechnique, Vol. 2, No. 4, pp. 301–331.

Meyerhof, G. G. 1957. The ultimate bearing capacity of foundations on slopes. In Proceedings of 4th International Conference on Soil Mechanics and Foundation Engineering, Vol. 1, pp. 384-386.

Meyerhof, G. G. 1976. Bearing capacity and settlement of pile foundations. Journal of the Geotechnical Engineering Division, ASCE, 102(3): 195-228.

Mooney, J. S., Adamczak, S., and Clemence, S.P. 1985. Uplift capacity of helix anchors in clay and silt. Uplift Behavior of Anchor Foundations in Soil, ASCE, pp. 48–72.

Narasimha Rao, S., Prasad, Y.V.S.N, and Dinakara Shetty, M. 1991. The behavior of model screw piles in cohesive soils. Soils and Foundations, 31: 35–50.

Narasimha Rao, S., Prasad, Y.V.S.N., and Veeresh, C. 1993. Behaviour of embedded model screw anchors in soft clays. Geotechnique, 43: 605-614.

Parry, R.H.G. 1977. Estimating Bearing Capacity of Sand from SPT Values. Journal of Geotechnical Engineering Division, Vol. 103, No. GT 9, pp. 1014–1019.

Perko, H.A. 2009. Helical piles: a practice guide to design and installation. John Wiley & Sons, Hoboken, NJ: Wiley.

Peck, R. B., Hanson, W. E., and Thornburn, T. H. 1974. Foundation engineering 2nd Ed. Wiley, New York.

Robertson, P.K. 2006. Guide to in-situ testing. Gregg Drilling & Testing, Inc., Signal Hill, CA.

Salgado, R. 2008. The engineering of foundations. McGraw Hill, New York, NY.

Sakr, M. 2009. Performance of helical piles in oil sand. Canadian Geotechnical Journal, 46(9): 1046–1061.

Santos, T. C., Tsuha, C. H. C., and Giacheti, H. L. 2013. The use of CPT to evaluate the effect of helical pile installation in tropical soils. In Geotechnical and Geophysical Site Characterization: Proceedings of the 4th International Conference on Site Characterization ISC-4 Vol. 1, pp. 1079-1084.

Shariatmadari, N., Eslami, A. and Karimpour-fard, M. 2008. Bearing capacity of driven piles in sands from SPT– applied to 60 case histories. Iranian Journal of Science & Technology, vol .32, pp.125-140

Shioi, Y. and Fukui, J. 1982. Application of N-Value to design of foundations in Japan. In Proceeding of the Second European Symposium on Penetration Testing 1 (1982): 159–116.

Skempton, A. W. 1986. Standard penetration test procedures and the effects in sands of overburden pressure, relative density, particle size, ageing and overconsolidation. Geotechnique, Vol. 36, No. 3, pp. 425-447.

Tappenden, K. M. 2007. Predicting the axial capacity of screw piles installed in Western Canadian soils. M.Sc. thesis, Department of Civil and Environmental Engineering, University of Alberta, Edmonton, Alberta.

Terzaghi, K. 1943. Theoretical soil mechanics. New York: John Wiley and Sons.

Terzaghi, K. and Peck, R.B. 1967. Soil mechanics in engineering practice. John Wiley and Sons, NY.

Weikart, A.M. and Clemence, S.P. 1987. Helix anchor foundations —Two case histories. Foundations for transmission line towers (GSP 8), ASCE, New York, pp. 72–80.

Wolff, T.F. 1989. Pile capacity prediction using parameter functions. ASCE Geotechnical Special Publication No. 23, pp. 96-107.

Vesic, A.S. 1973. Analysis of ultimate loads of shallow foundations. Journal of Soil Mechanics and Foundation Design, Vol. 99, No. SM 1, pp. 45–73.

Zhang, L.Z. and Chen, J.C. 2012. Effect of spatial correlation of standard penetration test (SPT) data on bearing capacity of driven piles in sand. Canadian Geotechnical Journal, 49: 394-402.

Zhang, D.J. 1999. Predicting capacity of helical screw piles in Alberta soils. MSc thesis, Department of Civil and Environmental Engineering, University of Alberta, Edmonton, Alberta.

Appendix A – Pile Load Tests in Clay

The author conducted a series of field load tests of helical piles at two sites located in Alberta. These two sites were chosen because they represent typical soil profiles in Alberta with cohesionless or cohesive soils. This thesis focuses on field tests and the SPT-based method in sand. However, the test results at the University Farm can be useful in further research. The present appendix is used for elaborating the tests and results of load tests in cohesive soil.

Four helical piles were designed by the industrial partner and tested at University Farm (Site 2). Clay Site at the University Farm shown in Figure A-1 is located in central Edmonton, Alberta, Canada. The surficial deposits are glaciolacustrine sediments as a part of the Glacial Lake Edmonton deposits formed 10,000 years approximately before the present. The general composition of the deposits includes varved silts and clays, with pockets of till, sand, or sandy gravel (Godfrey 1993). Cone penetration tests (CPT) were performed to a depth of 10.0 m to develop the soil profile. The CPT results (Figure A-2) show that at University Farm, the top 5.5 m layer consists of uniform clay, underlain by interbedded silty sand or silty sand from 7 m to 10 m. Deeper than 10 m is the overconsolidated glacial till. The groundwater table is about 5 m deep obtained the CPT u_2 records and the dissipation tests during CPT sounding.

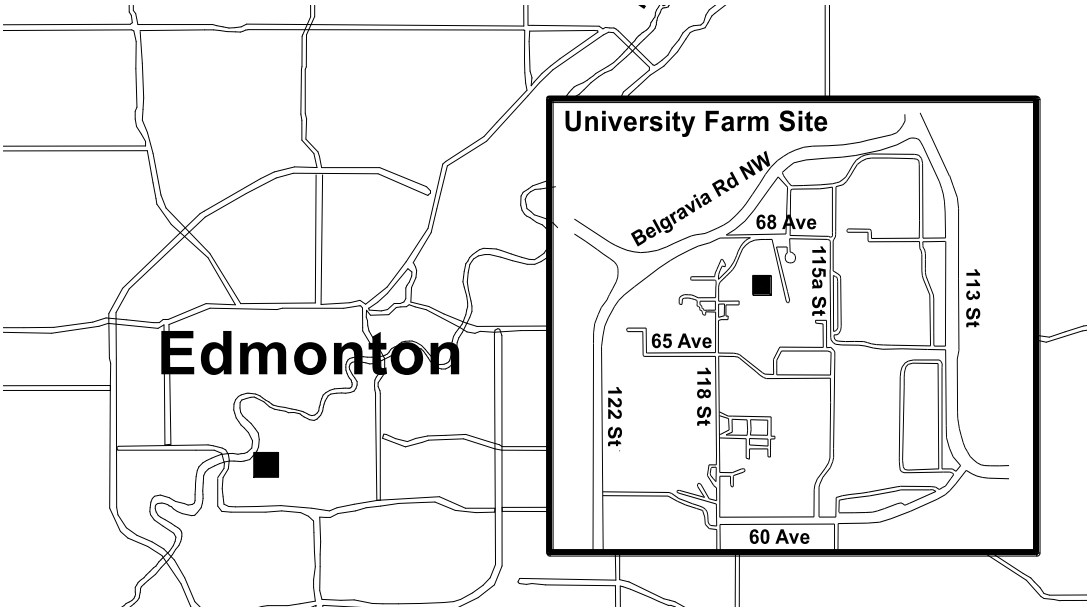

Figure A-1: Location of Cohesive Soil Test Site on the University of Alberta Farm.

Three single-helix and one double-helix pile types developed by Reaction Piling were tested on the University Farm. The helical piles consist of a steel tubular shaft and a single or double circular helix affixed to the shaft. Figure A-3 shows a sketch of the helical pile configuration with a single and double helix and defines the symbols for dimensions: depth from the ground surface to top helix H, shaft diameter d, helix diameter D, pile length L, and spacing of helix S (for double helix types). The dimensions of each type of pile are presented in Table A-1. After conducting the field testing at University Farm cohesive site, all testing piles were uninstalled and reused at Botanic Garden cohesionless site.

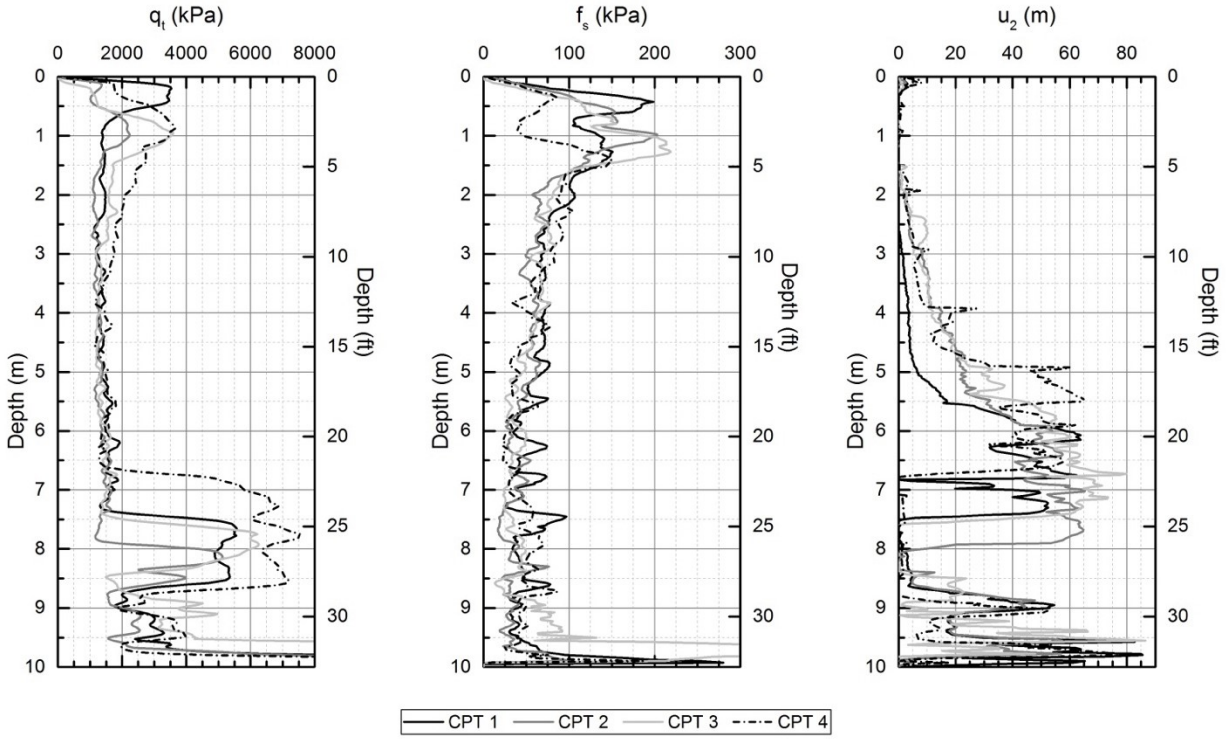

Figure A-2: CPT Profile at the University Farm

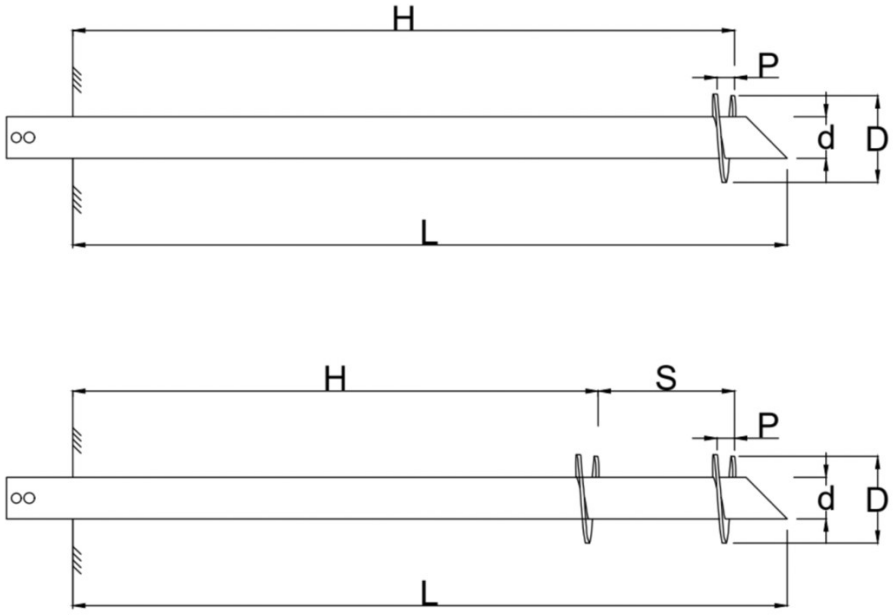

Figure A-3: Sketch of a Helical Pile: (up) Single Helix, and (down) Double Helices

Each test pile is assigned a pile code. As shown in Table A-1, the first letter denotes the term "Pile" and the following number denotes the pile size. “1” means single-helix 73 mm shaft diameter, “2” means single-helix 89 mm shaft diameter, “3” stands for single-helix 114 mm shaft diameter and “4” for double-helix 89 mm shaft diameter. The second letter tells us tension or compression test proceed on this pile. The last number represents the pile length, “10” for 10 ft (3.05 m) and “15” for 15 ft (4.57 m). To allow sufficient space for apparatus setup, the pile heads were set about 30 cm above the ground surface.

Figure A-4 shows the layout of the test piles. In order to minimize the pile-to-pile interaction, the center-to-center spacing of every two adjacent piles was set to be 2.59 m, which was greater than 5 times of the helix diameter of the larger pile (if applicable) (ASTM 2013a and 2013b). The reaction system consists of an I-shaped beam and two double-helix reaction piles installed to the depth of 4.27 m.

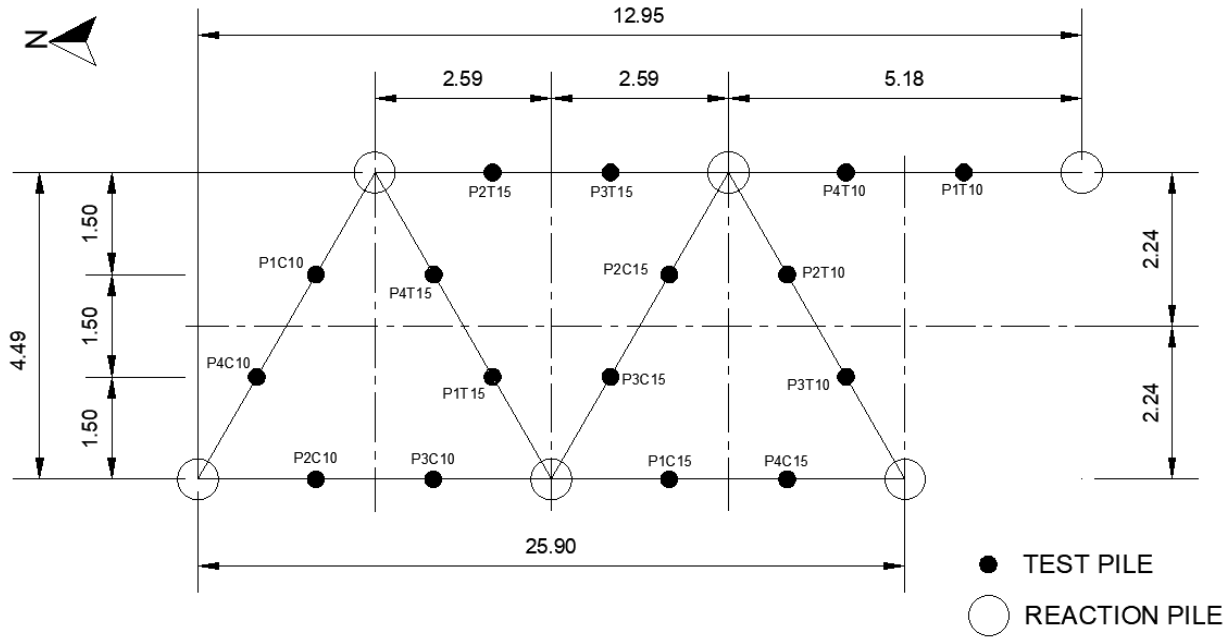

Figure A-4: Pile Layout at the University Farm. Unit in meters (CPT is out of Pile Layout map)

Incremental loads of 5% of predicted capacity were applied to each test pile. The predicted capacities of test piles were generated by the torque-factor method and measured final installation torques. A constant time interval of 5 minutes was maintained at each load increment to allow adequate time for pile settlement per D1143M-07 (ASTM 2013a) and D3689M-07 (ASTM 2013b). Test piles were loaded to the capacity of the loading frame or the limit capacity of test pile whichever reached first. The load at the "failure" state was held for 10 minutes, and then the unloading was started. The unloading stage adopted a load decrement of 20% of the previously achieved maximum load. The constant time interval was also 5 minutes.

The capacity of Q_u is defined as the pile resistance at the axial displacement of 10% of D according to Salgado (2008). Load vs. displacement curves for each pile are presented in Figure A-5 and A-6. Test results are summarized in Table A-2. According to the 10% criterion, the axial

compressive and tensile capacity of each pile were obtained. It was observed that axial compression capacities generally are not equal to the axial tension capacity.

Table A-1: Dimension of Test Piles

Pile code	Test type	Shaft diameter, *d* (mm)	Helix diam, *D* (mm)	Helix embedment, *H* (m)	Helix spacing, *S* (m)
P1C10	C	73	305	2.44	N/A
P1C15	C	73	305	3.89	N/A
P1T10	T	73	305	2.45	N/A
P1T15	T	73	305	4.00	N/A
P2C10	C	89	356	2.64	N/A
P2C15	C	89	356	3.74	N/A
P2T10	T	89	356	2.14	N/A
P2T15	T	89	356	3.86	N/A
P3C10	C	114	406	2.60	N/A
P3C15	C	114	406	4.11	N/A
P3T10	T	114	406	2.47	N/A
P3T15	T	114	406	4.05	N/A
P4C10	C	89	406	2.34	1.22
P4C15	C	89	406	2.98	1.22
P4T10	T	89	406	2.33	1.22
P4T15	T	89	406	4.10	1.22
Reaction piles	N/A	114	508 (Double-helix)	4.27	N/A

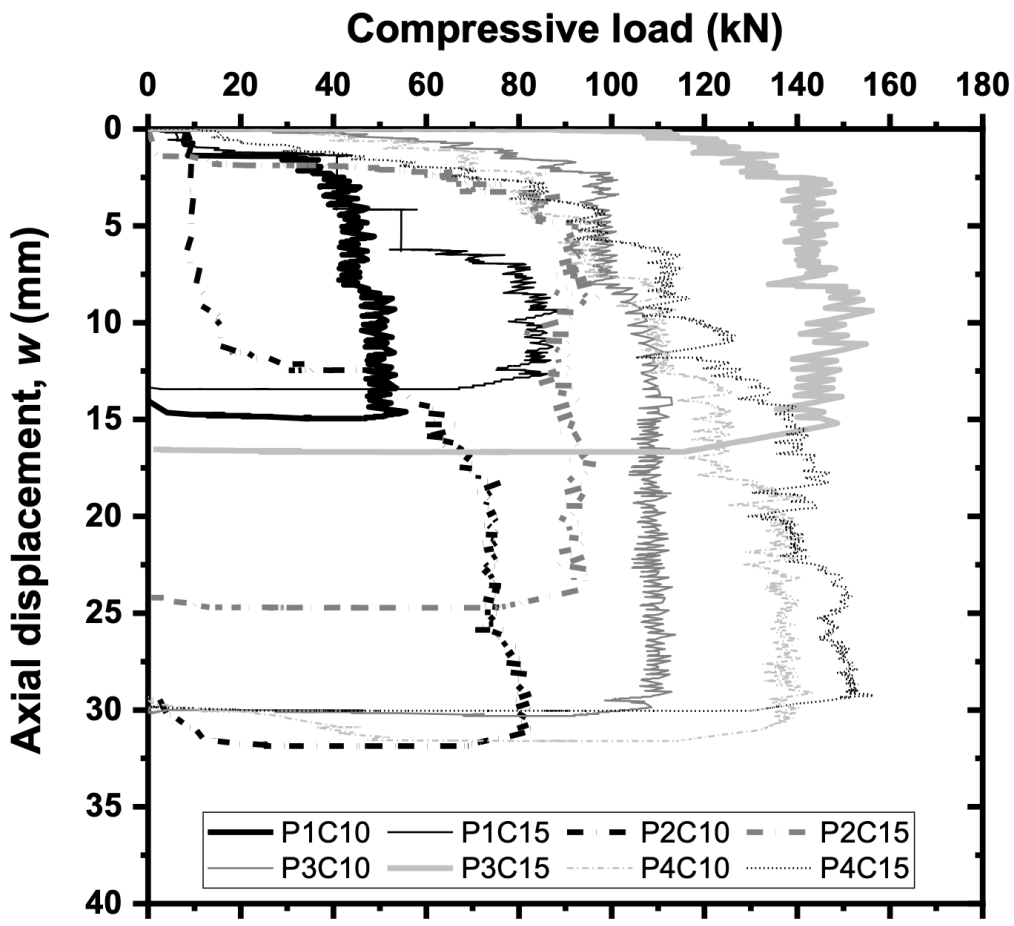

Figure A-5: Compressive Load *Q* versus Displacement *w* Curves

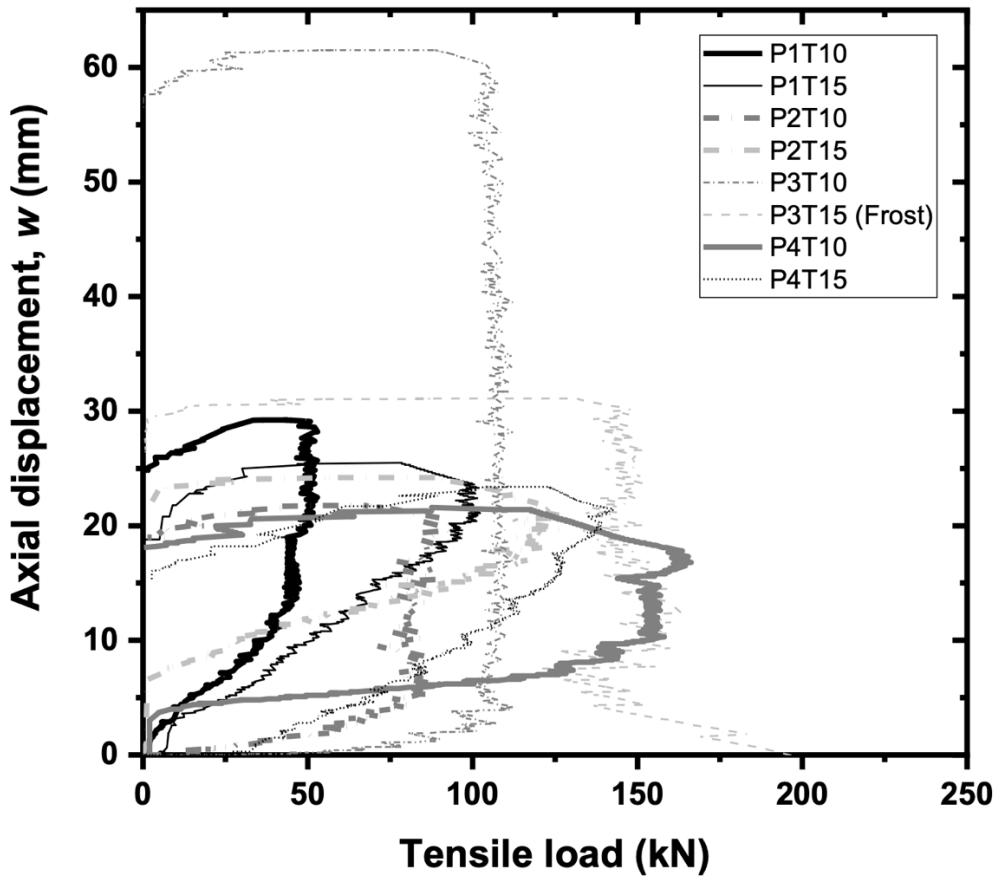

Figure A-6: Tensile Load *Q* versus Displacement *w* Curves

Table A-2: Summary of Test Results

Pile ID	Test type	Length, L (m)	T (kN-m)	Q_u (kN)	w at Q_u (mm)
P1C10	C	2.57	2.03	55.6	30.5
P1C15	C	4.04	2.44	86.1	30.5
P1T10	T	2.79	2.24	53.0	30.5
P1T15	T	4.13	2.44	101.6	30.5
P2C10	C	2.81	3.25	83.3	35.6
P2C15	C	4.20	4.88	97.1	35.6
P2T10	T	2.25	3.66	93	35.6
P2T15	T	4.00	3.66	127.2	35.6
P3C10	C	2.84	4.07	112.9	40.6
P3C15	C	4.24	4.88	148.7	40.6
P3T10	T	2.59	3.66	109.1	40.6
P3T15	T	4.20	5.69	Frost	40.6
P4C10	C	2.40	4.88	140.5	40.6
P4C15	C	3.13	5.28	156.5	40.6
P4T10	T	2.47	4.47	166.3	40.6
P4T15	T	4.41	5.28	142.8	40.6

Appendix B – Structural Design of Reaction System

The present appendix is to describe the structural design of reaction system including dimensions of some important components of reaction system and structural failure check of selected part.

The reaction system consisted of a reaction beam and two reaction piles on the end of the beam. The reaction system was provided and designed by Reaction Piling who is the industrial collaborator. For the testing apparatus, the hydraulic jack was connected with the load cell through the internal threads and was kept as one unit throughout the entire project as shown in Figure B-1. The top of the load cell was bolted on the mounting plate using an adaptor, while another side of adaptor was connected to load cell with internal threads. The detailed dimensions of mounting plate and adaptor are shown in Figure B-2 and Figure B-3.

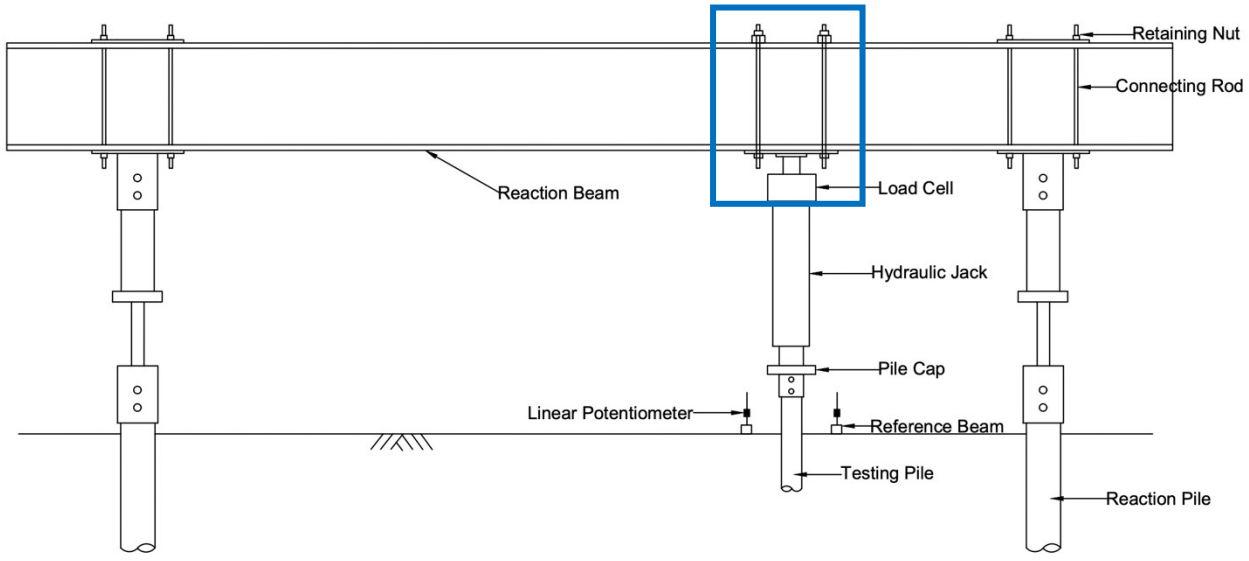

Figure B-1: Schematic of Setup.

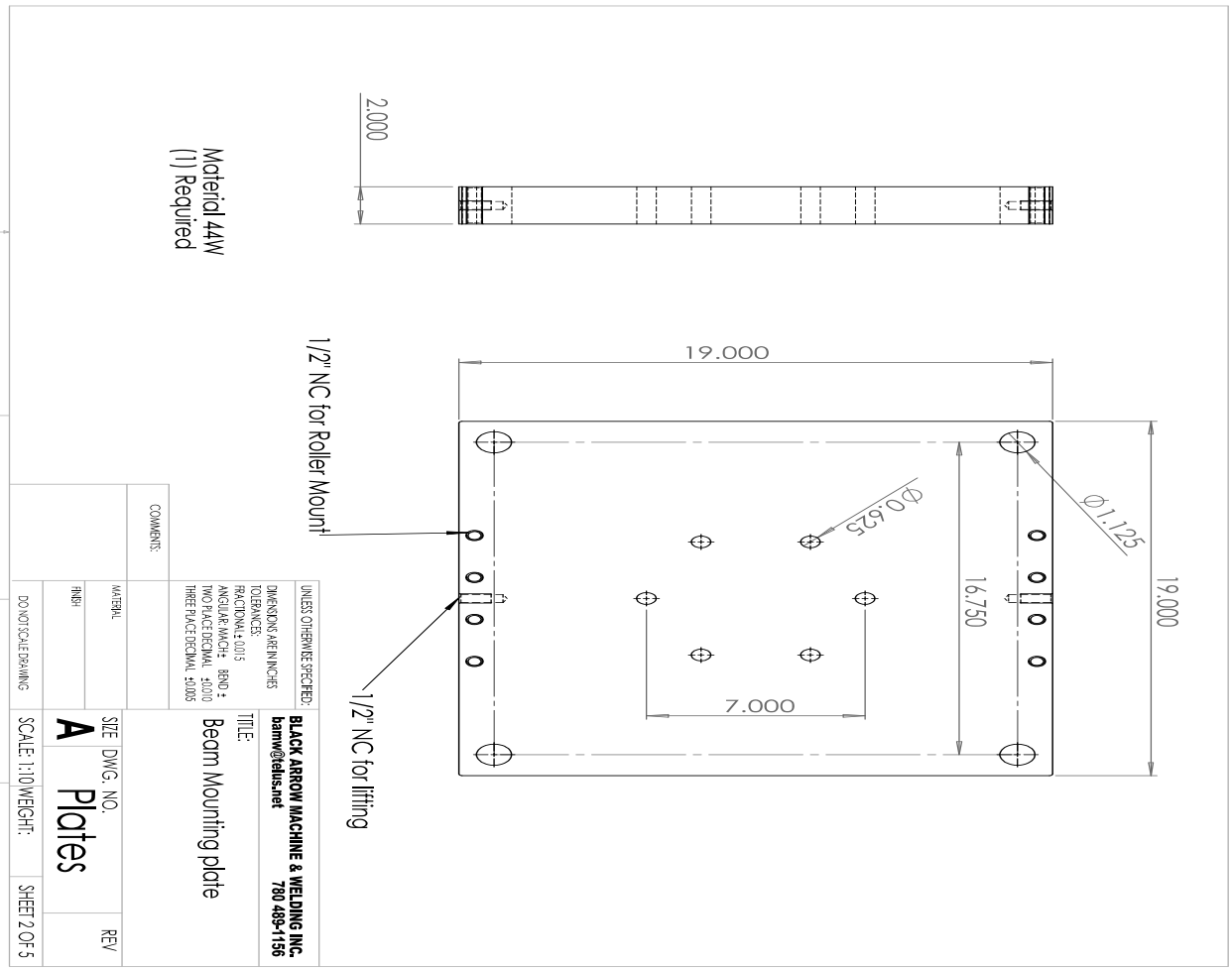

Figure B-2: Detailed Drawing of the Beam Mounting Plate

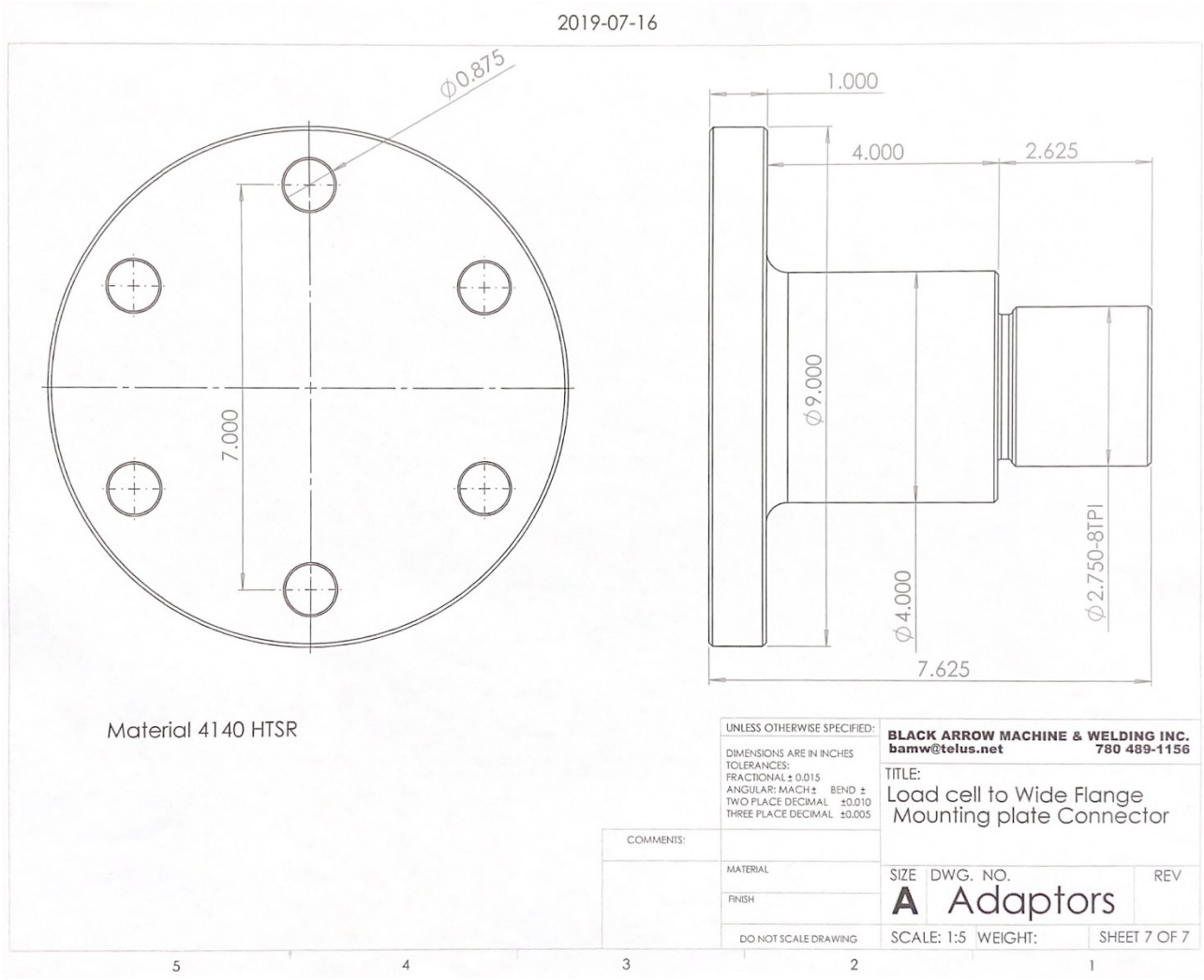

Figure B-3: Detailed Drawing of the Adaptor

The detailed calculation for design of connecting rods:

For design tensile members:

$T_r = \phi A_g F_y$

where

$\phi = 0.9$; $F_y = 350$ MPa; $d = 1$ inch $= 25.4$ mm; $A_g = (\pi/4)d^2 = 506.7$ mm^2

In Figure B-4 (a), there are 4 rods and each of them carries: 140 kN/4 = 35 kN

Considering the Factor of Safety: FS = 2.5

F = (0.9)(506.7 mm^2)(350 MPa)/(2.5) =63.84 kN > 35 kN => OK

4 additional 1-inch rods are sufficient for tensile loading test. The Figure B-4 (b) presents schematic of the cross section and shows the connection between each part.

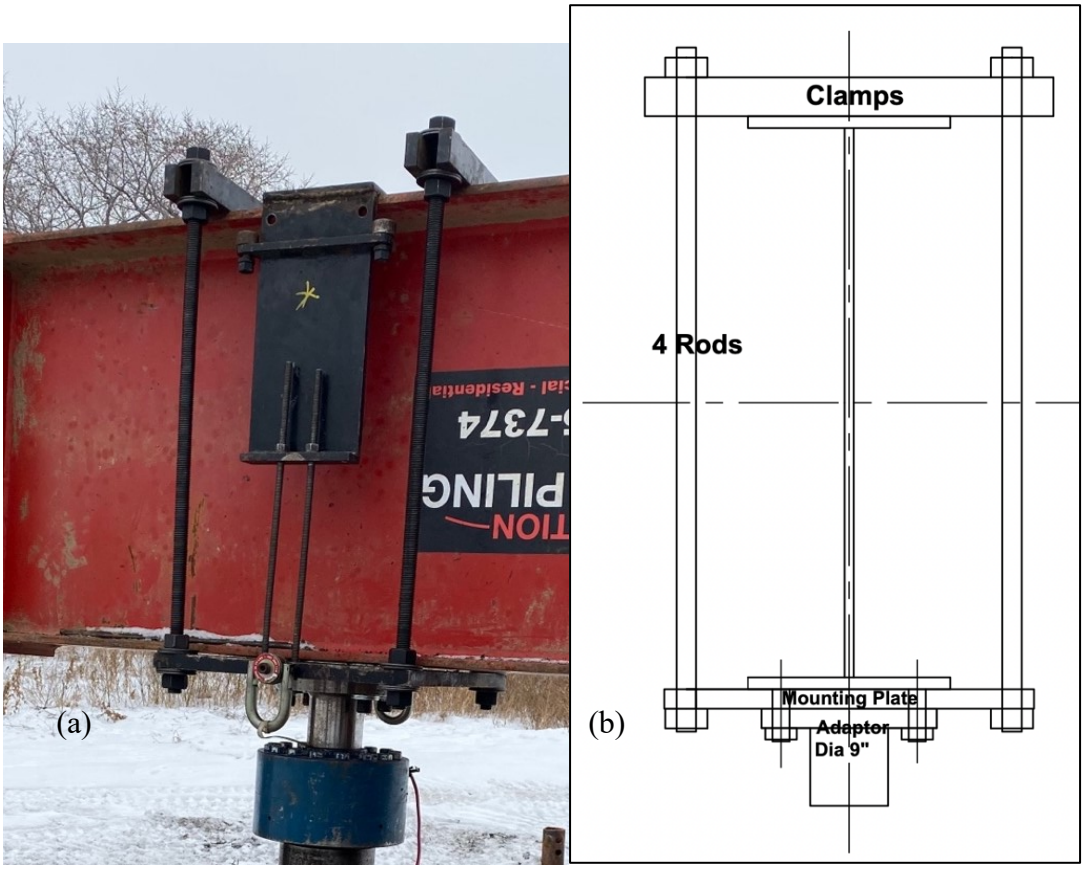

Figure B-4: (a) Photo and (b) Schematic of the Cross Section Highlighted in Figure B-1